Received: 22 February 2019 | Revised: 11 May 2020 | Accepted: 31 May 2020

DOI: 10.1002/nla.2318



RESEARCH ARTICLE

WILEY

# NURBS in isogeometric discretization methods: A spectral analysis

**Carlo Garoni**[1] | **Carla Manni**[1] | **Stefano Serra-Capizzano**[2,3] | **Hendrik Speleers**[1]

[1]Department of Mathematics, University of Rome Tor Vergata, Rome, Italy

[2]Department of Science and High Technology, University of Insubria, Como, Italy

[3]Department of Information Technology, Uppsala University, Uppsala, Sweden

**Correspondence**
Hendrik Speleers, Department of Mathematics, University of Rome Tor Vergata, Via della Ricerca Scientifica 1, Rome 00133, Italy.
Email: speleers@mat.uniroma2.it

**Funding information**
Istituto Nazionale di Alta Matematica; Knut och Alice Wallenbergs Stiftelse, Grant/Award Number: KAW 2013.0341; Ministero dell'Istruzione, dell'Università e della Ricerca, Grant/Award Number: CUP E83C18000100006; University of Rome Tor Vergata, Grant/Award Number: CUP E84I19002250005

**Summary**

Nonuniform rational B-splines (NURBS) are the most common representation form in isogeometric analysis. In this article, we study the spectral behavior of discretization matrices arising from isogeometric Galerkin and collocation methods based on $d$-variate NURBS of degrees $(p_1, \dots, p_d)$, and applied to general second-order partial differential equations defined on a $d$-dimensional domain. The spectrum of these matrices can be compactly and accurately described by means of a so-called symbol. We compute this symbol and show that it is the same as in the case of isogeometric discretization matrices based on $d$-variate polynomial B-splines of degrees $(p_1, \dots, p_d)$. The theoretical results are confirmed with a selection of numerical examples.

**KEYWORDS**

isogeometric methods, NURBS, spectral distribution, symbol

## 1 | INTRODUCTION

Isogeometric analysis (IgA) is a paradigm aiming to bridge the gap between classical finite element analysis (FEA) and computer aided design (CAD).[1,2] It has the potential of providing a true design-through-analysis process by exploiting a common representation model. In the traditional process, complex geometries are first modeled by means of CAD tools and then converted into a computational mesh needed for the numerical solution of the governing partial differential equations (PDEs). For decades, this process has presented a severe bottleneck in performing efficient simulations. On the other hand, the key concept in IgA is to use directly the CAD geometry and to approximate the PDE solution by the same type of functions. The so-called nonuniform rational B-splines (NURBS) are the dominant technology in CAD systems used in engineering, and thus also in IgA. The most interesting geometries in practical engineering applications contain conic sections, and NURBS allow for an exact representation of such geometries. Moreover, as it is well known, dealing with discretization spaces for the field variables containing the functions used to describe the geometry ensures that the approximation scheme passes some tests (for example, the patch test) which are reputed in engineering. IgA has been shown to be a viable alternative to existing FEA in various engineering fields, including structural mechanics, electromagnetics, and fluid-structure interaction.[1,3,4]

  

Like any discretization technique for PDEs, isogeometric (Galerkin and collocation) methods require to solve large linear systems. Unfortunately, the plain application of classical iterative fast (multigrid) solvers to the isogeometric case fails in practice. As illustrated and explained in the literature,[5,6] their performance worsens dramatically when the involved spline degrees increase. Hence, a complete and robust development of the IgA paradigm is in need of ad hoc fast solvers, and this begs for a profound knowledge of the spectral properties of the related matrices. Such knowledge is important for

- the convergence analysis of (preconditioned) Krylov methods;[7,8]
- the design and the theoretical analysis of effective preconditioners and fast multigrid solvers;[9,10]
- the performance analysis of isogeometric methods for approximating the spectrum of the underlying continuous differential operators.[4,11]

Several fundamental steps in the spectral analysis of isogeometric (Galerkin and collocation) matrices have already been made in the simplified case of polynomial B-spline discretizations. A full picture of the spectral distribution in this case has been sketched in a recent sequel of articles,[12-15] by exploiting the properties of the B-spline basis and generalized locally Toeplitz (GLT) sequences.[16] The related spectral distribution is compactly described by means of a so-called symbol, which may help in designing optimal and totally robust multigrid solvers.[5,17,18] Alternative solution strategies for B-spline discretizations have been proposed that make use of overlapping Schwarz preconditioning,[19] BPX-preconditioning,[20] preconditioning based on the solution of a Sylvester-like equation,[21] or multigrid based on a stable splitting of subspaces.[6,22]

In this article, we complete the above spectral analysis by considering NURBS-based IgA in its full generality. More precisely, we focus on general second-order elliptic PDEs, with variable coefficients and homogeneous Dirichlet boundary conditions:

$$\begin{cases} -\nabla \cdot K\nabla u + \boldsymbol{\alpha} \cdot \nabla u + \gamma u = \mathrm{f}, & \text{in } \Omega, \\ u = 0, & \text{on } \partial\Omega, \end{cases} \tag{1}$$

where $\Omega$ is a bounded open Lipschitz domain in $\mathbb{R}^d$, $K : \overline{\Omega} \to \mathbb{R}^{d\times d}$ is a symmetric matrix of functions $\kappa_{ij}$, $i,j = 1,\dots,d$, and $\boldsymbol{\alpha} : \overline{\Omega} \to \mathbb{R}^d$ is a vector of functions $\alpha_i$, $i = 1,\dots,d$. We consider isogeometric Galerkin and collocation discretizations of (1), using NURBS basis functions of arbitrary degrees $\boldsymbol{p} := (p_1,\dots,p_d)$ and a fixed geometry map $\mathbf{G} : [0,1]^d \to \overline{\Omega}$, which exactly describes the domain $\Omega$ in agreement with the IgA paradigm. We investigate the asymptotic spectral distribution of the corresponding matrices when the fineness parameters tend to zero (so that the matrix size tends to infinity). As the IgA paradigm requires to maintain the exact representation of the geometry along the entire refinement process, the choice of the considered NURBS weights is fixed by the given geometry.

The presented analysis reveals the asymptotic spectral behavior of the (sequences of) matrices arising from NURBS-based isogeometric methods. The results can be summarized as follows:

- a spectral distribution exists and is compactly described by a symbol which incorporates the discretization technique, the geometry (identified by the map $\mathbf{G}$) and the diffusion coefficients of the PDE;
- the symbol in the Galerkin case based on $\boldsymbol{p}$-degree NURBS is, up to a factor depending on the Jacobian of the geometry map, equivalent to the symbol in the collocation case based on $(2\boldsymbol{p}+\mathbf{1})$-degree NURBS;
- the NURBS symbol is the same as the symbol derived for B-spline discretizations of (1), both in the Galerkin and collocation case.

The existence of a spectral distribution and the formal structure of the symbol as described in the first item is intrinsic to the discretization of PDEs by any local method. In particular, this has been confirmed for finite differences and linear finite elements.[16] The second item shows that NURBS-based isogeometric Galerkin and collocation discretizations are equivalent from the spectral point of view, up to a proper scaling. The result stated in the third item might be surprising at first glance, but it is actually expected because of the structure (that is, the rational part) of a refined sequence of NURBS. According to the IgA paradigm, such a structure is determined by the geometry, which is fixed along the entire refinement process. As a consequence of that, there is asymptotically no difference between B-splines and NURBS of the same degrees in isogeometric discretizations. This insight suggests that the same type of symbol-based fast solvers developed for IgA discretizations using B-splines[5,17,18] may be also successfully applied in the context of NURBS-based IgA.

The remainder of the article is organized as follows. In Section 2, we introduce the notation and definitions used throughout the article and we also report some results on matrix analysis. In Section 3, we describe the general setting for isogeometric Galerkin and collocation discretizations of (1). The definition and some relevant properties of B-splines and NURBS are presented in Section 4. Section 5 contains our main results: the computation of the spectral distribution of the NURBS-based isogeometric Galerkin and collocation matrices, the identification of the corresponding symbols, and some related remarks. To improve the readability of the section, several technical results are deferred to appendices. Section 6 presents a selection of numerical examples illustrating the effectiveness of the derived asymptotic spectral analysis. We conclude the work in Section 7.

## 2 | PRELIMINARIES ON MATRIX ANALYSIS

In this section, we introduce the main notation, definitions, and results on matrix analysis used throughout the article.

For all $X \in \mathbb{C}^{m\times m}$, the eigenvalues of $X$ are denoted by $\lambda_i(X)$, $i = 1, \dots, m$. The $\infty$-norm and the spectral norm (2-norm) of both vectors and matrices are denoted by $\|\cdot\|_\infty$ and $\|\cdot\|$, respectively. We recall that $\|X\|_\infty$ is the maximum among the 1-norms of the rows of $X$, and $\|X\|$ equals the largest singular value of $X$. Moreover,

$$\|X\| \le \sqrt{\|X\|_\infty \|X^T\|_\infty}. \tag{2}$$

We denote by $\|X\|_1$ the trace-norm (or Schatten 1-norm) of $X$, that is, the sum of all the singular values of $X$. Since $\operatorname{rank}(X)$ is the number of nonzero singular values of $X$, we have

$$\|X\|_1 \le \operatorname{rank}(X)\|X\| \le m\|X\|. \tag{3}$$

If $X$,$Y$ are matrices of the same dimension, the componentwise (Hadamard) product of $X$ and $Y$ is denoted by $X \circ Y$. If $X \in \mathbb{C}^{m_1\times m_1}$ and $Y \in \mathbb{C}^{m_2\times m_2}$, the tensor (Kronecker) product $X \otimes Y$ is defined by

$$X \otimes Y := [x_{ij}Y]_{i,j=1}^{m_1} = \begin{bmatrix} x_{11}Y & \dots & x_{1m_1}Y \\ \vdots & & \vdots \\ x_{m_11}Y & \dots & x_{m_1m_1}Y \end{bmatrix} \in \mathbb{C}^{m_1m_2\times m_1m_2}.$$

Tensor products possess a lot of nice algebraic properties. One of them is the associativity, which allows us to omit parentheses in expressions like $X_1 \otimes \dots \otimes X_d$. The matrix $X_1 \otimes \dots \otimes X_d$ is Hermitian (respectively, symmetric) whenever all the matrices $X_1, \dots, X_d$ are Hermitian (respectively, symmetric). The spectral norm of tensor products can be computed through the following identity:

$$\|X_1 \otimes \dots \otimes X_d\| = \|X_1\| \dots \|X_d\|. \tag{4}$$

Let $X_1, \dots, X_d, Y_1, \dots, Y_d$ be matrices such that $X_k, Y_k \in \mathbb{C}^{m_k\times m_k}$, $k = 1, \dots, d$; then

$$\operatorname{rank}(X_1 \otimes \dots \otimes X_d - Y_1 \otimes \dots \otimes Y_d) \le \left(\prod_{k=1}^{d} m_k\right)\left(\sum_{k=1}^{d} \frac{\operatorname{rank}(X_k - Y_k)}{m_k}\right). \tag{5}$$

### 2.1 | Multiindex notation

A multiindex $\boldsymbol{m} \in \mathbb{Z}^d$, also called a $d$-index, is simply a (row) vector in $\mathbb{Z}^d$; its components are denoted by $m_1, m_2, \dots, m_d$. We denote by $\mathbf{0}$, $\mathbf{1}$, $\mathbf{2}$ the vectors consisting of all zeros, all ones, all twos, respectively (their size will be clear from the context). For any $d$-index $\boldsymbol{m}$, we set $N(\boldsymbol{m}) := m_1m_2 \dots m_d$. If $\boldsymbol{m} \in \mathbb{N}^d$ we write $\boldsymbol{m} \to \infty$ to indicate that $\min(\boldsymbol{m}) \to \infty$. Inequalities between multiindices must be interpreted in the componentwise sense. For example, $\boldsymbol{j} \le \boldsymbol{k}$ means that $j_i \le k_i$ for every $i$. If $\boldsymbol{j}$,$\boldsymbol{k}$ are $d$-indices such that $\boldsymbol{j} \le \boldsymbol{k}$, the multiindex range $\boldsymbol{j}, \dots, \boldsymbol{k}$ is the set $\{\boldsymbol{i} \in \mathbb{Z}^d : \boldsymbol{j} \le \boldsymbol{i} \le \boldsymbol{k}\}$. We assume for

this set the standard lexicographic ordering:

$$[\ \dots\ [\ [\ (i_1,\ \dots\ ,i_d)\ ]_{i_d=j_d,\dots,k_d}\ ]_{i_{d-1}=j_{d-1},\dots,k_{d-1}}\ \ \dots\ ]_{i_1=j_1,\dots,k_1}. \tag{6}$$

For example, in the case $d=2$, this ordering is

$$(j_1,j_2),\ (j_1,j_2+1),\ \dots\ ,(j_1,k_2),\ (j_1+1,j_2),\ (j_1+1,j_2+1),\ \dots\ ,(j_1+1,k_2),\ \dots\ ,(k_1,j_2),\ (k_1,j_2+1),\ \dots\ ,(k_1,k_2).$$

When writing $\boldsymbol{i}=\boldsymbol{j},\dots,\boldsymbol{k}$, we mean that the multiindex $\boldsymbol{i}$ varies from $\boldsymbol{j}$ to $\boldsymbol{k}$ following the ordering (6). If $\boldsymbol{m}\in\mathbb{N}^d$ and $\mathbf{x}=[x_{\boldsymbol{i}}]_{\boldsymbol{i}=\mathbf{1}}^{\boldsymbol{m}}$, then $\mathbf{x}$ is a vector of length $N(\boldsymbol{m})$ whose components $x_{\boldsymbol{i}}$, $\boldsymbol{i}=\mathbf{1},\dots,\boldsymbol{m}$, are ordered according to (6): the first component is $x_{\mathbf{1}}=x_{(1,\dots,1,1)}$, the second component is $x_{(1,\dots,1,2)}$, and so on until the last component, which is $x_{\boldsymbol{m}}=x_{(m_1,\dots,m_d)}$. Similarly, if

$$X=[x_{\boldsymbol{ij}}]_{\boldsymbol{i},\boldsymbol{j}=\mathbf{1}}^{\boldsymbol{m}}, \tag{7}$$

then $X$ is an $N(\boldsymbol{m})\times N(\boldsymbol{m})$ matrix whose entries are indexed by two $d$-indices $\boldsymbol{i},\boldsymbol{j}$, both varying from $\mathbf{1}$ to $\boldsymbol{m}$ according to (6). The symbol $\sum_{\boldsymbol{i}=\boldsymbol{j}}^{\boldsymbol{k}}$ denotes the summation over all multiindices $\boldsymbol{i}=\boldsymbol{j},\dots,\boldsymbol{k}$. Operations involving multiindices that do not have a meaning when considering multiindices like usual vectors must always be interpreted in the componentwise sense. For example, $\boldsymbol{jk}:=(j_1k_1,\dots,j_dk_d)$, $\boldsymbol{j}/\boldsymbol{k}:=(j_1/k_1,\dots,j_d/k_d)$, and so on. For any pair of $d$-indices $\boldsymbol{j},\boldsymbol{k}$, we define

$$\boldsymbol{j}\wedge\boldsymbol{k}:=\begin{cases}\boldsymbol{j}, & \text{if } \boldsymbol{j}\preccurlyeq\boldsymbol{k},\\ \boldsymbol{k}, & \text{otherwise,}\end{cases}$$

where $\boldsymbol{j}\preccurlyeq\boldsymbol{k}$ means that $\boldsymbol{j}$ precedes or equals $\boldsymbol{k}$ in the lexicographic ordering. Note that $\boldsymbol{j}\wedge\boldsymbol{k}$ is simply the minimum among $\boldsymbol{j}$ and $\boldsymbol{k}$ with respect to the lexicographic ordering. In particular, if $j$ and $k$ are standard scalar indices (that is, 1-indices), then $j\wedge k=\min(j,k)$.

Finally, we apply the multiindex notation to tensor products: if we have $d$ matrices $X_k\in\mathbb{C}^{m_k\times m_k}$, $k=1,\dots,d$, then the $(\boldsymbol{i},\boldsymbol{j})$th entry of $X_1\otimes\ \dots\ \otimes X_d$ is computed as

$$(X_1\otimes\ \dots\ \otimes X_d)_{\boldsymbol{ij}}=(X_1)_{i_1j_1}\ \dots\ (X_d)_{i_dj_d},\quad \boldsymbol{i},\boldsymbol{j}=\mathbf{1},\ \dots\ ,\boldsymbol{m}. \tag{8}$$

Note that (8) can be rewritten in the form (7) as

$$X_1\otimes\ \dots\ \otimes X_d=[(X_1)_{i_1j_1}\ \dots\ (X_d)_{i_dj_d}]_{\boldsymbol{i},\boldsymbol{j}=\mathbf{1}}^{\boldsymbol{m}}.$$

The simplicity of Equation (8) motivates the introduction of multiindices for indexing the entries of a matrix formed by (a sum of) tensor products.

## 2.2 | Toeplitz and diagonal sampling matrices

We now describe two important families of matrices, namely, multilevel Toeplitz matrices and multilevel diagonal sampling matrices.

**Definition 1** (Multilevel Toeplitz matrix). Given $\boldsymbol{m}\in\mathbb{N}^d$ and $f:[-\pi,\pi]^d\to\mathbb{C}$ belonging to $L^1([-\pi,\pi]^d)$, the multilevel Toeplitz matrix $T_{\boldsymbol{m}}(f)$ associated with $f$ is the $N(\boldsymbol{m})\times N(\boldsymbol{m})$ matrix defined by

$$T_{\boldsymbol{m}}(f):=[\hat{f}_{\boldsymbol{i}-\boldsymbol{j}}]_{\boldsymbol{i},\boldsymbol{j}=\mathbf{1}}^{\boldsymbol{m}},$$

where $\hat{f}_{\boldsymbol{\ell}}$ are the Fourier coefficients of $f$,

$$\hat{f}_{\boldsymbol{\ell}}:=\frac{1}{(2\pi)^d}\int_{[-\pi,\pi]^d}f(\boldsymbol{\theta})\,\mathrm{e}^{-\mathrm{i}\boldsymbol{\ell}\cdot\boldsymbol{\theta}}\mathrm{d}\boldsymbol{\theta},\quad \boldsymbol{\ell}\in\mathbb{Z}^d,$$

with i the imaginary unit and $\boldsymbol{\ell}\cdot\boldsymbol{\theta} := \sum_{k=1}^{d}\ell_k\theta_k$. The function $f$ is called the generating function of the Toeplitz family $\{T_{\boldsymbol{m}}(f)\}_{\boldsymbol{m}\in\mathbb{N}^d}$.

It is not difficult to see that the Toeplitz operator $T_{\boldsymbol{m}}(\cdot) : L^1([-\pi,\pi]^d) \to \mathbb{C}^{N(\boldsymbol{m})\times N(\boldsymbol{m})}$ is linear:

$$T_{\boldsymbol{m}}(af+bg) = a\,T_{\boldsymbol{m}}(f) + b\,T_{\boldsymbol{m}}(g), \quad a,b\in\mathbb{C}, \quad f,g\in L^1([-\pi,\pi]^d), \quad \boldsymbol{m}\in\mathbb{N}^d.$$

Moreover,

$$T_{\boldsymbol{m}}(\bar{f}) = (T_{\boldsymbol{m}}(f))^*, \quad f\in L^1([-\pi,\pi]^d), \quad \boldsymbol{m}\in\mathbb{N}^d, \tag{9}$$

where $\bar{f}$ is the conjugate of $f$. In particular, when $f$ is real-valued all the matrices $T_{\boldsymbol{m}}(f)$ are Hermitian. Whenever $f$ belongs to $L^\infty([-\pi,\pi]^d)$, the spectral norm of $T_{\boldsymbol{m}}(f)$ can be bounded as follows (see Corollary 4.2 in Reference 23):

$$\|T_{\boldsymbol{m}}(f)\| \le \|f\|_{L^\infty([-\pi,\pi]^d)}, \quad f\in L^\infty([-\pi,\pi]^d), \quad \boldsymbol{m}\in\mathbb{N}^d. \tag{10}$$

Given $f_k : E_k \to \mathbb{C}$, $k=1,\dots,d$, the tensor-product function $f_1\otimes\dots\otimes f_d : E_1\times\dots\times E_d\to\mathbb{C}$ is defined as

$$(f_1\otimes\dots\otimes f_d)(\xi_1,\dots,\xi_d) := f_1(\xi_1)\dots f_d(\xi_d), \quad (\xi_1,\dots,\xi_d)\in E_1\times\dots\times E_d.$$

If $f_1,\dots,f_d\in L^1([-\pi,\pi])$ and $\boldsymbol{m}\in\mathbb{N}^d$, then

$$T_{\boldsymbol{m}}(f_1\otimes\dots\otimes f_d) = T_{m_1}(f_1)\otimes\dots\otimes T_{m_d}(f_d). \tag{11}$$

**Definition 2** (Multilevel diagonal sampling matrix). Given $\boldsymbol{m}\in\mathbb{N}^d$ and $a : [0,1]^d\to\mathbb{C}$, the multilevel diagonal sampling matrix $D_{\boldsymbol{m}}(a)$ associated with $a$ is the $N(\boldsymbol{m})\times N(\boldsymbol{m})$ diagonal matrix defined by

$$D_{\boldsymbol{m}}(a) := \operatorname*{diag}_{\boldsymbol{j}=\boldsymbol{1},\dots,\boldsymbol{m}} a\left(\frac{\boldsymbol{j}}{\boldsymbol{m}}\right).$$

From $D_{\boldsymbol{m}}(a)$ we construct the $N(\boldsymbol{m})\times N(\boldsymbol{m})$ symmetric matrix $\tilde{D}_{\boldsymbol{m}}(a)$, whose $(\boldsymbol{i},\boldsymbol{j})$th entry is given by

$$(\tilde{D}_{\boldsymbol{m}}(a))_{\boldsymbol{ij}} := (D_{\boldsymbol{m}}(a))_{\boldsymbol{i}\wedge\boldsymbol{j},\boldsymbol{i}\wedge\boldsymbol{j}} = \begin{cases} (D_{\boldsymbol{m}}(a))_{\boldsymbol{ii}}, & \text{if } \boldsymbol{i}\preccurlyeq\boldsymbol{j},\\ (D_{\boldsymbol{m}}(a))_{\boldsymbol{jj}}, & \text{otherwise.}\end{cases} \tag{12}$$

Note that $\tilde{D}_{\boldsymbol{m}}(a)$ can be expressed in the form (7) as

$$\tilde{D}_{\boldsymbol{m}}(a) = \left[a\left(\frac{\boldsymbol{i}\wedge\boldsymbol{j}}{\boldsymbol{m}}\right)\right]_{\boldsymbol{i},\boldsymbol{j}=\boldsymbol{1}}^{\boldsymbol{m}}.$$

## 2.3 | Spectral distribution and symbol

By a sequence of matrices we mean a sequence of the form $\{X_{\boldsymbol{m}}\}_n$, where

- $n$ varies in some infinite subset of $\mathbb{N}$;
- $\boldsymbol{m}=\boldsymbol{m}(n)$ is a multiindex in $\mathbb{N}^d$ which depends on $n$, and $\boldsymbol{m}\to\infty$ as $n\to\infty$;
- $X_{\boldsymbol{m}}$ is a square matrix of size $N(\boldsymbol{m})$.

We denote by $\mu_d$ the Lebesgue measure in $\mathbb{R}^d$ and by $C_c(\mathbb{C})$ the space of continuous functions $F : \mathbb{C}\to\mathbb{C}$ with bounded support.

**Definition 3** (Spectral distribution). Let $\{X_{\boldsymbol{m}}\}_n$ be a sequence of matrices and let $f : D\to\mathbb{C}$ be a measurable function defined on a set $D\subset\mathbb{R}^q$ with $0<\mu_q(D)<\infty$. We say that $\{X_{\boldsymbol{m}}\}_n$ has a spectral (or eigenvalue) distribution described by

$f$ and we write $\{X_{\boldsymbol{m}}\}_n \sim_\lambda f$, if

$$\lim_{n\to\infty} \frac{1}{N(\boldsymbol{m})} \sum_{i=1}^{N(\boldsymbol{m})} F(\lambda_i(X_{\boldsymbol{m}})) = \frac{1}{\mu_q(D)} \int_D F(f(\mathbf{x}))\, \mathrm{d}\mathbf{x}, \quad \forall F \in C_c(\mathbb{C}). \tag{13}$$

A function $f$ satisfying (13) is called the (spectral) symbol of $\{X_{\boldsymbol{m}}\}_n$.

*Remark* 1. The informal meaning behind Definition 3 is the following. If $f$ is continuous and $\{\mathbf{x}_i,\ i = 1, \dots, N(\boldsymbol{m})\}$ is an equispaced grid on $D$, then the pairs $\{(\mathbf{x}_i, \lambda_i(X_{\boldsymbol{m}}))\}$ reconstruct approximately the surface $(\mathbf{x}, f(\mathbf{x}))$ for a suitable ordering of the eigenvalues of $X_{\boldsymbol{m}}$. For example, if $q = 1$, $m_1(n) = n$, and $D = [a, b]$, then the eigenvalues of $X_{m_1(n)}$ are approximately equal to $f(a + i(b-a)/n)$, $i = 1, \dots, n$, for $n$ large enough.

Two useful theorems for computing the spectral distribution are given below. We refer the reader to Theorem 3.4 of Reference 24 for a proof of the first theorem and to Corollary 2.6 of Reference 12 for the second one. It is worth mentioning that Theorem 2 can be seen as a corollary of the results summarized in items **GLT 1**, **GLT 3**, and **GLT 4** of Chapter 6 of Reference 16. These results are formulated in the more general framework known as the theory of GLT sequences, which is a powerful tool for computing spectral distributions of PDE discretization matrices.[16]

**Theorem 1.** *Let $\{X_{\boldsymbol{m}}\}_n, \{Y_{\boldsymbol{m}}\}_n$ be two sequences of matrices, and set $Z_{\boldsymbol{m}} := X_{\boldsymbol{m}} + Y_{\boldsymbol{m}}$. Assume that*

- *each $X_{\boldsymbol{m}}$ is Hermitian and $\{X_{\boldsymbol{m}}\}_n \sim_\lambda f$ as in Definition 3;*
- *there exists a constant $C$ such that $\|X_{\boldsymbol{m}}\|, \|Y_{\boldsymbol{m}}\| \le C$ for all $n$;*
- *$\|Y_{\boldsymbol{m}}\|_1 = o(N(\boldsymbol{m}))$ as $n \to \infty$, that is, $\lim_{n\to\infty} \|Y_{\boldsymbol{m}}\|_1 / N(\boldsymbol{m}) = 0$.*

*Then, $\{Z_{\boldsymbol{m}}\}_n \sim_\lambda f$.*

**Theorem 2.** *Let $f_i, i = 1, \dots, k$, be $d$-variate trigonometric polynomials and let $a_i, i = 1, \dots, k$, be Riemann-integrable functions defined on $[0, 1]^d$. Assume that all the $a_i$ and $f_i$ are real-valued. Then,*

$$\left\{ \sum_{i=1}^{k} \tilde{D}_{\boldsymbol{m}}(a_i) \circ T_{\boldsymbol{m}}(f_i) \right\}_n \sim_\lambda \sum_{i=1}^{k} a_i \otimes f_i.$$

## 3 | ISOGEOMETRIC GALERKIN AND COLLOCATION DISCRETIZATIONS

In this section, we outline the isogeometric approach for the Galerkin and collocation discretizations of problem (1). Let

$$\{\hat{\varphi}_1, \dots, \hat{\varphi}_{N+N_b}\} \tag{14}$$

be a set of basis functions defined on the parametric (or reference) domain $[0, 1]^d$, such that $\hat{\varphi}_1, \dots, \hat{\varphi}_N$ vanish on the boundary $\partial([0, 1]^d)$. Suppose that the physical domain $\Omega$ can be described by a global geometry function $\mathbf{G}$, which is defined in terms of the functions $\hat{\varphi}_i$ as follows:

$$\mathbf{G} : [0, 1]^d \to \overline{\Omega}, \quad \mathbf{G}(\hat{\mathbf{x}}) := \sum_{i=1}^{N+N_b} \mathbf{P}_i \hat{\varphi}_i(\hat{\mathbf{x}}), \quad \mathbf{P}_i \in \mathbb{R}^d. \tag{15}$$

We assume that the map $\mathbf{G}$ is invertible and $\mathbf{G}(\partial([0, 1]^d)) = \partial\overline{\Omega}$. In the isogeometric approach, we compute an approximation $u_{\mathcal{W}}$ of $u$ by applying the standard Galerkin or collocation method in the space $\mathcal{W} := \langle \varphi_i : i = 1, \dots, N \rangle$, where

$$\varphi_i(\mathbf{x}) := \hat{\varphi}_i(\mathbf{G}^{-1}(\mathbf{x})) = \hat{\varphi}_i(\hat{\mathbf{x}}), \quad \mathbf{x} = \mathbf{G}(\hat{\mathbf{x}}), \quad i = 1, \dots, N. \tag{16}$$

Since $u_{\mathcal{W}} = \sum_{i=1}^{N} u_i \varphi_i$ for a unique vector $\mathbf{u} := (u_1, \dots, u_N)^T$, the computation of $u_{\mathcal{W}}$ reduces to the computation of the vector $\mathbf{u}$. In the classical formulation of IgA, the basis functions $\hat{\varphi}_i$ are chosen to be B-splines or NURBS.[1-3]

## 3.1 | Isogeometric Galerkin discretization

When considering the Galerkin discretization of (1), we assume that the PDE coefficients $\kappa_{ij}, \alpha_i, \gamma$ belong to $L^\infty(\Omega)$ and $\mathrm{f} \in L^2(\Omega)$. We look for an approximate solution $u_{\mathcal{W}}$ in the finite dimensional subspace $\mathcal{W} \subset H_0^1(\Omega)$ satisfying

$$a(u_{\mathcal{W}}, v) = \mathrm{F}(v), \quad \forall v \in \mathcal{W},$$

where

$$a(u, v) := \int_\Omega ((\nabla u)^T K \nabla v + (\nabla u)^T \boldsymbol{\alpha}\, v + \gamma u v), \quad \mathrm{F}(v) := \int_\Omega \mathrm{f} v.$$

By linearity, the computation of $u_{\mathcal{W}}$ reduces to solving the linear system $A^{\mathcal{G}}\mathbf{u} = \mathbf{f}$, where

$$A^{\mathcal{G}} := [a(\varphi_j, \varphi_i)]_{i,j=1}^N = \left[\int_\Omega ((\nabla \varphi_j)^T K \nabla \varphi_i + (\nabla \varphi_j)^T \boldsymbol{\alpha}\, \varphi_i + \gamma \varphi_j \varphi_i)\right]_{i,j=1}^N,$$

and $\mathbf{f} := [\mathrm{F}(\varphi_i)]_{i=1}^N$. In the isogeometric Galerkin method, the basis functions $\varphi_i$ are defined as in (16). Assuming that $\mathbf{G}$ and $\hat{\varphi}_i$, $i = 1, \dots, N$, are sufficiently regular, we can apply standard differential calculus to express the Galerkin matrix $A^{\mathcal{G}}$ in terms of $\mathbf{G}$ and $\hat{\varphi}_i$, $i = 1, \dots, N$, as follows:

$$A^{\mathcal{G}} = \left[\int_{[0,1]^d} |\det(J_{\mathbf{G}})|\, ((\nabla \hat{\varphi}_j)^T K_{\mathbf{G}} \nabla \hat{\varphi}_i + (\nabla \hat{\varphi}_j)^T \boldsymbol{\alpha}_{\mathbf{G}}\, \hat{\varphi}_i + \gamma_{\mathbf{G}}\, \hat{\varphi}_j \hat{\varphi}_i)\right]_{i,j=1}^N, \tag{17}$$

where

$$K_{\mathbf{G}} := [\kappa_{\mathbf{G},ij}]_{i,j=1}^d := (J_{\mathbf{G}})^{-1} K(\mathbf{G}) (J_{\mathbf{G}})^{-T}, \quad \boldsymbol{\alpha}_{\mathbf{G}} := (\alpha_{\mathbf{G},1}, \dots, \alpha_{\mathbf{G},d})^T := (J_{\mathbf{G}})^{-1} \boldsymbol{\alpha}(\mathbf{G}), \quad \gamma_{\mathbf{G}} := \gamma(\mathbf{G}), \tag{18}$$

and $J_{\mathbf{G}}$ is the Jacobian matrix of $\mathbf{G}$,

$$J_{\mathbf{G}} := \left[\frac{\partial G_i}{\partial \hat{x}_j}\right]_{i,j=1}^d = \left[\frac{\partial x_i}{\partial \hat{x}_j}\right]_{i,j=1}^d.$$

## 3.2 | Isogeometric collocation discretization

When considering the collocation discretization of (1), we assume that the functions $\kappa_{ij}$ belong to $C^1(\Omega) \cap C(\overline{\Omega})$, their partial derivatives are bounded on $\Omega$, and $\alpha_i, \gamma, \mathrm{f} \in C(\overline{\Omega})$. Problem (1) can be reformulated as

$$\begin{cases} -\mathbf{1}(K \circ Hu)\mathbf{1}^T + \boldsymbol{\beta} \cdot \nabla u + \gamma u = \mathrm{f}, & \text{in } \Omega, \\ u = 0, & \text{on } \partial\Omega, \end{cases} \tag{19}$$

where $Hu$ denotes the Hessian of $u$,

$$(Hu)_{ij} := \frac{\partial^2 u}{\partial x_i \partial x_j}, \quad i, j = 1, \dots, d,$$

and $\boldsymbol{\beta}$ collects the coefficients of the first-order derivatives,

$$\beta_j := \alpha_j - \sum_{i=1}^d \frac{\partial \kappa_{ij}}{\partial x_i}, \quad j = 1, \dots, d.$$

Given a finite dimensional approximation space $\mathcal{W}$, consisting of sufficiently smooth functions defined on $\overline{\Omega}$ and vanishing on the boundary $\partial\Omega$, we introduce a set of $N = \dim \mathcal{W}$ collocation points $\{\tau_1, \dots, \tau_N\} \subset \Omega$, and we look for an approximate solution $u_{\mathcal{W}} \in \mathcal{W}$ satisfying

$$-\mathbf{1}(K(\boldsymbol{\tau}_i) \circ H u_{\mathcal{W}}(\boldsymbol{\tau}_i))\mathbf{1}^T + \boldsymbol{\beta}(\boldsymbol{\tau}_i) \cdot \nabla u_{\mathcal{W}}(\boldsymbol{\tau}_i) + \gamma(\boldsymbol{\tau}_i) u_{\mathcal{W}}(\boldsymbol{\tau}_i) = \mathrm{f}(\boldsymbol{\tau}_i), \quad i = 1, \dots, N.$$

By linearity, the computation of $u_{\mathcal{W}}$ reduces to solving the linear system $A^C \mathbf{u} = \mathbf{f}$, where

$$A^C := [-\mathbf{1}(K(\boldsymbol{\tau}_i) \circ H\varphi_j(\boldsymbol{\tau}_i))\mathbf{1}^T + \boldsymbol{\beta}(\boldsymbol{\tau}_i) \cdot \nabla\varphi_j(\boldsymbol{\tau}_i) + \gamma(\boldsymbol{\tau}_i)\varphi_j(\boldsymbol{\tau}_i)]_{i,j=1}^N, \tag{20}$$

and $\mathbf{f} := [\mathrm{f}(\boldsymbol{\tau}_i)]_{i=1}^N$. In the isogeometric collocation method, the functions $\{\varphi_1, \dots, \varphi_N\}$ are defined as in (16) and the collocation points are given by

$$\boldsymbol{\tau}_i := \mathbf{G}(\hat{\boldsymbol{\tau}}_i), \quad i = 1, \dots, N, \tag{21}$$

where $\{\hat{\boldsymbol{\tau}}_1, \dots, \hat{\boldsymbol{\tau}}_N\}$ is a set of $N$ collocation points in the domain $(0, 1)^d$. Assuming that $\mathbf{G}$ and $\hat{\varphi}_i$, $i = 1, \dots, N$, are sufficiently regular, we can apply standard differential calculus to express $A^C$ in terms of $\mathbf{G}$ and $\hat{\varphi}_i$, $\hat{\boldsymbol{\tau}}_i$, $i = 1, \dots, N$. More precisely, for any $u : \overline{\Omega} \to \mathbb{R}$ consider the corresponding function on the parametric domain $[0, 1]^d$,

$$\hat{u} : [0, 1]^d \to \mathbb{R}, \quad \hat{u}(\hat{\mathbf{x}}) := u(\mathbf{x}), \quad \mathbf{x} = \mathbf{G}(\hat{\mathbf{x}}).$$

The function $u$ satisfies (19) if and only if $\hat{u}$ satisfies the transformed problem

$$\begin{cases} -\mathbf{1}(K_{\mathbf{G}} \circ H\hat{u})\mathbf{1}^T + \boldsymbol{\beta}_{\mathbf{G}} \cdot \nabla\hat{u} + \gamma_{\mathbf{G}}\, \hat{u} = \mathrm{f}(\mathbf{G}), & \text{in } (0, 1)^d, \\ \hat{u} = 0, & \text{on } \partial((0, 1)^d), \end{cases} \tag{22}$$

where $H\hat{u}$ is the Hessian of $\hat{u}$,

$$(H\hat{u})_{ij} := \frac{\partial^2 \hat{u}}{\partial \hat{x}_i \partial \hat{x}_j}, \quad i, j = 1, \dots, d,$$

and $K_{\mathbf{G}}$ is the transformed diffusion coefficient matrix in (18), and $\boldsymbol{\beta}_{\mathbf{G}}$ is the transformed advection coefficient vector, whose expression in terms of $K, \boldsymbol{\beta}, \mathbf{G}$ is quite complicated and hence not reported here. For later purposes, we just highlight that the components of $\boldsymbol{\beta}_{\mathbf{G}}$ are bounded on a set $E \subseteq [0, 1]^d$ if $\mathbf{G}$ belongs to $C^1([0, 1]^d)$ with $\det(J_{\mathbf{G}}) \neq 0$ on $[0, 1]^d$ and $\mathbf{G}$ has bounded second-order partial derivatives on $E$. The collocation matrix $A^C$ in (20) can be expressed in terms of $\mathbf{G}$ and $\hat{\varphi}_i$, $\hat{\boldsymbol{\tau}}_i$, $i = 1, \dots, N$, as follows:

$$A^C = [-\mathbf{1}(K_{\mathbf{G}}(\hat{\boldsymbol{\tau}}_i) \circ H\hat{\varphi}_j(\hat{\boldsymbol{\tau}}_i))\mathbf{1}^T + \boldsymbol{\beta}_{\mathbf{G}}(\hat{\boldsymbol{\tau}}_i) \cdot \nabla\hat{\varphi}_j(\hat{\boldsymbol{\tau}}_i) + \gamma_{\mathbf{G}}(\hat{\boldsymbol{\tau}}_i)\hat{\varphi}_j(\hat{\boldsymbol{\tau}}_i)]_{i,j=1}^N. \tag{23}$$

## 4 | B-SPLINES AND NURBS

In the classical formulation of IgA, the basis functions $\hat{\varphi}_i$ in (14) are chosen to be B-splines or NURBS.[1-3] In this article, we focus on B-splines/NURBS defined over uniformly refined knot sequences. Furthermore, the collocation points $\hat{\boldsymbol{\tau}}_i$ in (21) are taken as the Greville abscissae associated with the chosen B-splines/NURBS, a common choice in the literature.[12,25]

### 4.1 | B-splines

For $p, n \geq 1$, consider the uniform knot sequence

$$t_1 = \dots = t_{p+1} = 0 < t_{p+2} < \dots < t_{p+n} < 1 = t_{p+n+1} = \dots = t_{2p+n+1}, \tag{24}$$

where $t_{i+p+1} := i/n$, $i = 0, \dots, n$.

**Definition 4** (Univariate B-splines). The univariate B-splines of degree $p$ on the knot sequence (24) are denoted by

$$N_{i,p,n} : [0,1] \to \mathbb{R}, \quad i = 1, \dots, n+p, \tag{25}$$

and are defined recursively as follows: for $1 \le i \le n+2p$,

$$N_{i,0,n}(x) := \begin{cases} 1, & \text{if } x \in [t_i, t_{i+1}), \\ 0, & \text{elsewhere;} \end{cases}$$

for $1 \le k \le p$ and $1 \le i \le n+2p-k$,

$$N_{i,k,n}(x) := \frac{x - t_i}{t_{i+k} - t_i} N_{i,k-1,n}(x) + \frac{t_{i+k+1} - x}{t_{i+k+1} - t_{i+1}} N_{i+1,k-1,n}(x),$$

where we assume that a fraction with zero denominator is zero.

Let $\mathbb{P}_p$ be the space of polynomials of degree less than or equal to $p$. It is well known[26,27] that $\{N_{1,p,n}, \dots, N_{n+p,p,n}\}$ is a basis for the spline space

$$\mathbb{S}_n^p := \left\{ s \in C^{p-1}([0,1]) : \ s_{\left|\left[\frac{i}{n}, \frac{i+1}{n}\right]\right.} \in \mathbb{P}_p, \ i = 0, \dots, n-1 \right\}.$$

Furthermore, the univariate B-splines have local support given by

$$\operatorname{supp}(N_{i,p,n}) = [t_i, t_{i+p+1}], \quad i = 1, \dots, n+p, \tag{26}$$

and they form a nonnegative partition of unity,

$$\sum_{i=1}^{n+p} N_{i,p,n}(x) = 1, \quad N_{i,p,n}(x) \ge 0, \quad i = 1, \dots, n+p, \quad x \in [0,1]. \tag{27}$$

The absolute values of their derivatives can be bounded as

$$|N'_{i,p,n}| \le 2pn, \quad i = 1, \dots, n+p, \tag{28}$$

$$|N''_{i,p,n}| \le 4p(p-1)n^2, \quad i = 1, \dots, n+p. \tag{29}$$

Except for the boundary functions $N_{1,p,n}$ and $N_{n+p,p,n}$, all the other B-splines vanish on $\partial([0,1])$,

$$N_{i,p,n}(0) = N_{i,p,n}(1) = 0, \quad i = 2, \dots, n+p-1. \tag{30}$$

With each B-spline $N_{i,p,n}$ in (25), one can associate a so-called Greville abscissa, defined by

$$\xi_{i,p,n} := \frac{t_{i+1} + \dots + t_{i+p}}{p}, \quad i = 1, \dots, n+p.$$

From its definition we see that $\xi_{i,p,n}$ lies in the support of $N_{i,p,n}$,

$$\xi_{i,p,n} \in [t_i, t_{i+p+1}] = \operatorname{supp}(N_{i,p,n}), \quad i = 1, \dots, n+p. \tag{31}$$

It can be checked that

$$|\xi_{i,p,n} - \xi_{j,p,n}| \le \frac{|i-j|}{n}, \quad i,j = 1, \dots, n+p, \tag{32}$$

and

$$\left|\xi_{i,p,n} - \frac{i}{n+p}\right| \leq \frac{C_p}{n}, \quad i = 1, \dots, n+p, \tag{33}$$

where $C_p$ depends only on $p$.

Let $\boldsymbol{p} := (p_1, \dots, p_d)$ and $\boldsymbol{n} := (n_1, \dots, n_d)$ be multiindices in $\mathbb{N}^d$. For $j = 1, \dots, d$, we consider the knots $t_{i_j}$, $i_j = 1, \dots, n_j + 2p_j + 1$ given by (24) with $n = n_j$ and $p = p_j$.

**Definition 5** (Multivariate B-splines). The multivariate B-splines

$$N_{\boldsymbol{i},\boldsymbol{p},\boldsymbol{n}} : [0,1]^d \to \mathbb{R}, \quad \boldsymbol{i} = \boldsymbol{1}, \dots, \boldsymbol{n}+\boldsymbol{p}, \tag{34}$$

are defined via tensor products by

$$N_{\boldsymbol{i},\boldsymbol{p},\boldsymbol{n}} := N_{i_1,p_1,n_1} \otimes \dots \otimes N_{i_d,p_d,n_d}. \tag{35}$$

The space spanned by the B-splines in (34) is denoted by $\mathbb{S}_{\boldsymbol{n}}^{\boldsymbol{p}}$. The corresponding Greville abscissae are defined by

$$\boldsymbol{\xi}_{\boldsymbol{i},\boldsymbol{p},\boldsymbol{n}} := (\xi_{i_1,p_1,n_1}, \dots, \xi_{i_d,p_d,n_d}), \quad \boldsymbol{i} = \boldsymbol{1}, \dots, \boldsymbol{n}+\boldsymbol{p}.$$

By (26), we have

$$\operatorname{supp}(N_{\boldsymbol{i},\boldsymbol{p},\boldsymbol{n}}) = [t_{i_1}, t_{i_1+p_1+1}] \times \dots \times [t_{i_d}, t_{i_d+p_d+1}], \quad \boldsymbol{i} = \boldsymbol{1}, \dots, \boldsymbol{n}+\boldsymbol{p}, \tag{36}$$

and from (31) it is clear that

$$\boldsymbol{\xi}_{\boldsymbol{i},\boldsymbol{p},\boldsymbol{n}} \in \operatorname{supp}(N_{\boldsymbol{i},\boldsymbol{p},\boldsymbol{n}}), \quad \boldsymbol{i} = \boldsymbol{1}, \dots, \boldsymbol{n}+\boldsymbol{p}. \tag{37}$$

## 4.2 | NURBS

NURBS are defined in terms of B-splines and weights as follows.

**Definition 6** (NURBS). Given a set of B-splines as in (34) and a vector of positive values $\mathbf{w}_{\boldsymbol{p},\boldsymbol{n}} := (w_{\boldsymbol{1},\boldsymbol{p},\boldsymbol{n}}, \dots, w_{\boldsymbol{n}+\boldsymbol{p},\boldsymbol{p},\boldsymbol{n}})$, called weights, the corresponding NURBS are defined by

$$R_{\boldsymbol{i},\boldsymbol{p},\boldsymbol{n}} : [0,1]^d \to \mathbb{R}, \quad R_{\boldsymbol{i},\boldsymbol{p},\boldsymbol{n}} := \frac{w_{\boldsymbol{i},\boldsymbol{p},\boldsymbol{n}} N_{\boldsymbol{i},\boldsymbol{p},\boldsymbol{n}}}{W_{\boldsymbol{p},\boldsymbol{n}}}, \quad \boldsymbol{i} = \boldsymbol{1}, \dots, \boldsymbol{n}+\boldsymbol{p}, \tag{38}$$

where

$$W_{\boldsymbol{p},\boldsymbol{n}} : [0,1]^d \to \mathbb{R}, \quad W_{\boldsymbol{p},\boldsymbol{n}} := \sum_{\boldsymbol{i}=\boldsymbol{1}}^{\boldsymbol{n}+\boldsymbol{p}} w_{\boldsymbol{i},\boldsymbol{p},\boldsymbol{n}} N_{\boldsymbol{i},\boldsymbol{p},\boldsymbol{n}}. \tag{39}$$

NURBS preserve the main properties of B-splines including local support, nonnegativity, and partition of unity.[28] Moreover, from (27) it is easy to see that they reduce to B-splines whenever all the weights are equal. Due to (30), the functions in (38) vanishing on the boundary $\partial([0,1]^d)$ are

$$R_{\boldsymbol{i},\boldsymbol{p},\boldsymbol{n}}, \quad \boldsymbol{i} = \boldsymbol{2}, \dots, \boldsymbol{n}+\boldsymbol{p}-\boldsymbol{1}. \tag{40}$$

In the NURBS-based IgA framework, the functions $\hat{\varphi}_1, \dots, \hat{\varphi}_{N+N_b}$ in (14) are chosen as the NURBS in (38), the functions $\hat{\varphi}_1, \dots, \hat{\varphi}_N$ are those in (40), and the collocation points $\hat{\boldsymbol{\tau}}_1, \dots, \hat{\boldsymbol{\tau}}_N$ used in (21) are chosen as the Greville abscissae

$$\boldsymbol{\xi}_{\boldsymbol{i},\boldsymbol{p},\boldsymbol{n}}, \quad \boldsymbol{i} = \boldsymbol{2}, \dots, \boldsymbol{n}+\boldsymbol{p}-\boldsymbol{1}. \tag{41}$$

Note that we have $N + N_b = N(\boldsymbol{n} + \boldsymbol{p})$ and $N = N(\boldsymbol{n} + \boldsymbol{p} - \boldsymbol{2})$. IgA based on B-splines is a special instance of this framework obtained by taking all the NURBS weights equal.

*Remark* 2. The use of piecewise rational forms vs piecewise polynomial forms in IgA (that is, NURBS vs B-splines) is motivated by the better capability of representing the physical domain $\Omega$ through a map $\mathbf{G}$. More precisely, contrarily to B-splines, NURBS allow for an exact representation of conic sections and quadric surfaces (see Example 1); these are very common shapes in engineering. For this reason, NURBS in their full generality are the dominant technology in engineering CAD systems, and so in the most common formulation of IgA.

**Example 1.** In this example, we illustrate the NURBS representation of a circular arc. Let $d = 1$ and consider the knot sequence $\{0,0,0,1,1,1\}$, so $n = 1$ and $p = 2$. The circular arc

$$\{(x_1, x_2) : \ x_1^2 + x_2^2 = 1, \ x_1, x_2 \geq 0\}$$

can be described by means of a parametric quadratic NURBS curve defined on the above knot sequence as

$$\mathbf{C}(\hat{x}) = \sum_{i=1}^{3} \mathbf{P}_{i,2,1} R_{i,2,1}(\hat{x}) = \sum_{i=1}^{3} \mathbf{P}_{i,2,1} \frac{w_{i,2,1} N_{i,2,1}(\hat{x})}{W_{2,1}(\hat{x})}, \quad \hat{x} \in [0,1],$$

where

$$\mathbf{P}_{1,2,1} = (1,0)^T, \quad \mathbf{P}_{2,2,1} = (1,1)^T, \quad \mathbf{P}_{3,2,1} = (0,1)^T,$$

and

$$w_{1,2,1} = 1, \quad w_{2,2,1} = \frac{\sqrt{2}}{2}, \quad w_{3,2,1} = 1.$$

When refining the domain in two subintervals ($n = 2$), we obtain the new knot sequence $\{0,0,0,1/2,1,1,1\}$. The same circular arc can be expressed in terms of the new quadratic NURBS as

$$\mathbf{C}(\hat{x}) = \sum_{i=1}^{4} \mathbf{P}_{i,2,2} R_{i,2,2}(\hat{x}) = \sum_{i=1}^{4} \mathbf{P}_{i,2,2} \frac{w_{i,2,2} N_{i,2,2}(\hat{x})}{W_{2,2}(\hat{x})}, \quad \hat{x} \in [0,1],$$

where

$$\mathbf{P}_{1,2,2} = (1,0)^T, \quad \mathbf{P}_{2,2,2} = \left(1, \frac{1}{2}\right)^T, \quad \mathbf{P}_{3,2,2} = \left(\frac{1}{2}, 1\right)^T, \quad \mathbf{P}_{4,2,2} = (0,1)^T,$$

and

$$w_{1,2,2} = 1, \quad w_{2,2,2} = \frac{1}{2} + \frac{\sqrt{2}}{4}, \quad w_{3,2,2} = \frac{1}{2} + \frac{\sqrt{2}}{4}, \quad w_{4,2,2} = 1.$$

Note that $W_{2,1} = W_{2,2}$. The refinement process can be easily iterated. In general, the new weights $w_{i,p,n}$ and control points $\mathbf{P}_{i,p,n}$ of a (refined) NURBS curve can be computed by means of the so-called knot-insertion algorithm.[26-28]

Figure 1 shows the graph of the spline $W_{2,1} = W_{2,2} = W_{2,4}$, together with the three corresponding control polygons, that is, the polygonal line through the set of points $\{(\xi_{i,p,n}, w_{i,p,n}), \ i = 1, \ldots, n + p\}$, for $n = 1,2,4$ and $p = 2$. One can visually verify that the control polygon converges to the graph of the spline for increasing $n$.

## 4.3 | Geometry map in terms of NURBS

In this article, we consider a sequence of spaces obtained by uniform $h$-refinement, that is, by refining the knot sequences uniformly. In particular, from now on, we assume to have a single discretization parameter $n$, which varies in an infinite

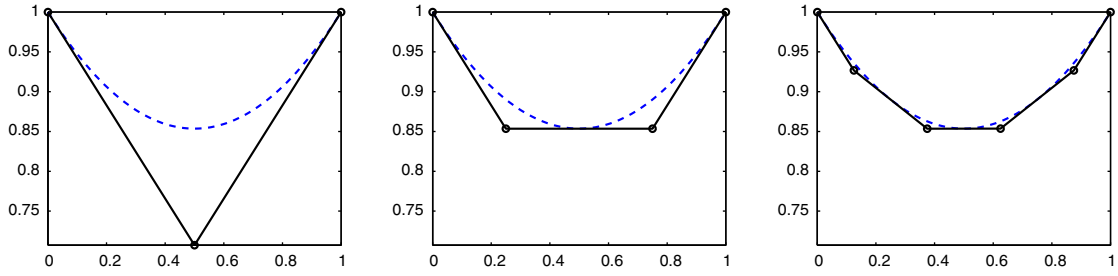

(a) $n = 1$ (b) $n = 2$ (c) $n = 4$

**FIGURE 1** (Example 1). Graph of the functions $W_{2,n}$ (blue dashed line) together with the corresponding control polygons (black full line) for $n = 1,2,4$

set of indices $\mathbb{I} := \{n^{(0)}, n^{(1)}, \dots\} \subseteq \mathbb{N}$ such that

$$\mathbb{S}^{\boldsymbol{p}}_{\boldsymbol{n}^{(0)}} \subseteq \mathbb{S}^{\boldsymbol{p}}_{\boldsymbol{n}^{(i)}}, \quad \forall i \geq 0,$$

where $\boldsymbol{n}^{(i)} := \boldsymbol{\nu} n^{(i)} := (\nu_1 n^{(i)}, \dots, \nu_d n^{(i)}) \in \mathbb{N}^d$, and $\boldsymbol{\nu} := (\nu_1, \dots, \nu_d) \in \mathbb{Q}^d_+ := \{(r_1, \dots, r_d) : r_1, \dots, r_d \in \mathbb{Q}, r_1, \dots, r_d > 0\}$ is an a priori fixed vector. So, when referring to a spline space $\mathbb{S}^{\boldsymbol{p}}_{\boldsymbol{n}}$, the relation $\boldsymbol{n} = \boldsymbol{\nu} n$ for some $n \in \mathbb{I}$ must be kept in mind throughout the remainder of this article.

According to the IgA approach,[1,3] the physical domain $\Omega$ is represented exactly along the entire refinement process by means of the geometry map $\mathbf{G}$ in (15). This map is defined in terms of the NURBS $R_{\boldsymbol{i},\boldsymbol{p},\boldsymbol{n}^{(0)}}$, $\boldsymbol{i} = \mathbf{1}, \dots, \boldsymbol{n}^{(0)} + \boldsymbol{p}$, corresponding to the coarsest discretization $n = n^{(0)}$,

$$\mathbf{G} := \sum_{\boldsymbol{i}=\mathbf{1}}^{\boldsymbol{n}^{(0)}+\boldsymbol{p}} \mathbf{P}_{\boldsymbol{i},\boldsymbol{p},\boldsymbol{n}^{(0)}} \frac{w_{\boldsymbol{i},\boldsymbol{p},\boldsymbol{n}^{(0)}} N_{\boldsymbol{i},\boldsymbol{p},\boldsymbol{n}^{(0)}}}{W_{\boldsymbol{p}}}, \quad W_{\boldsymbol{p}} := \sum_{\boldsymbol{i}=\mathbf{1}}^{\boldsymbol{n}^{(0)}+\boldsymbol{p}} w_{\boldsymbol{i},\boldsymbol{p},\boldsymbol{n}^{(0)}} N_{\boldsymbol{i},\boldsymbol{p},\boldsymbol{n}^{(0)}}, \tag{42}$$

for some given weights $w_{\boldsymbol{i},\boldsymbol{p},\boldsymbol{n}^{(0)}}$ and control points $\mathbf{P}_{\boldsymbol{i},\boldsymbol{p},\boldsymbol{n}^{(0)}} \in \mathbb{R}^d$, $\boldsymbol{i} = \mathbf{1}, \dots, \boldsymbol{n}^{(0)} + \boldsymbol{p}$. Since the coarsest B-splines $N_{\boldsymbol{i},\boldsymbol{p},\boldsymbol{n}^{(0)}}$, $\boldsymbol{i} = \mathbf{1}, \dots, \boldsymbol{n}^{(0)} + \boldsymbol{p}$, belong to each finer space $\mathbb{S}^{\boldsymbol{p}}_{\boldsymbol{n}}$, $n \in \mathbb{I}$, the function $\mathbf{G}$ in (42) can be rewritten in terms of the finer B-splines $N_{\boldsymbol{i},\boldsymbol{p},\boldsymbol{n}}$, $\boldsymbol{i} = \mathbf{1}, \dots, \boldsymbol{n} + \boldsymbol{p}$, by replacing the coarsest B-splines both in numerator and denominator by their representations in terms of the finer B-splines. When doing so, the denominator $W_{\boldsymbol{p}}$ and the map $\mathbf{G}$ do not change. The changing quantities are:

- the coefficients of $W_{\boldsymbol{p}}$ with respect to the new B-spline basis $N_{\boldsymbol{i},\boldsymbol{p},\boldsymbol{n}}$, which are, *by definition*, the weights $w_{\boldsymbol{i},\boldsymbol{p},\boldsymbol{n}}$, $\boldsymbol{i} = \mathbf{1}, \dots, \boldsymbol{n} + \boldsymbol{p}$, see (39);
- the formal expression of $\mathbf{G}$, which is now written in terms of the finer B-splines $N_{\boldsymbol{i},\boldsymbol{p},\boldsymbol{n}}$, and, ultimately, in terms of the finer NURBS $R_{\boldsymbol{i},\boldsymbol{p},\boldsymbol{n}}$, $\boldsymbol{i} = \mathbf{1}, \dots, \boldsymbol{n} + \boldsymbol{p}$.

Since $w_{\boldsymbol{i},\boldsymbol{p},\boldsymbol{n}}$ are the coefficients that represent $W_{\boldsymbol{p}}$ with respect to the basis $N_{\boldsymbol{i},\boldsymbol{p},\boldsymbol{n}}$, $\boldsymbol{i} = \mathbf{1}, \dots, \boldsymbol{n} + \boldsymbol{p}$, and $\boldsymbol{n} = \boldsymbol{\nu} n$, we have[26]

$$\lim_{n \to \infty} \max_{\boldsymbol{i}=\mathbf{1}, \dots, \boldsymbol{n}+\boldsymbol{p}} |W_{\boldsymbol{p}}(\xi_{\boldsymbol{i},\boldsymbol{p},\boldsymbol{n}}) - w_{\boldsymbol{i},\boldsymbol{p},\boldsymbol{n}}| = 0. \tag{43}$$

Thanks to the knot-insertion process,[26,28] the weights $w_{\boldsymbol{i},\boldsymbol{p},\boldsymbol{n}}$, $\boldsymbol{i} = \mathbf{1}, \dots, \boldsymbol{n} + \boldsymbol{p}$, can be computed as successive convex combinations of the weights at the coarsest level $w_{\boldsymbol{i},\boldsymbol{p},\boldsymbol{n}^{(0)}}$, $\boldsymbol{i} = \mathbf{1}, \dots, \boldsymbol{n}^{(0)} + \boldsymbol{p}$ (see Example 1), and so

$$0 < w_{\boldsymbol{p},\min} \leq \min_{\boldsymbol{i}=\mathbf{1}, \dots, \boldsymbol{n}+\boldsymbol{p}} w_{\boldsymbol{i},\boldsymbol{p},\boldsymbol{n}} \leq \max_{\boldsymbol{i}=\mathbf{1}, \dots, \boldsymbol{n}+\boldsymbol{p}} w_{\boldsymbol{i},\boldsymbol{p},\boldsymbol{n}} \leq w_{\boldsymbol{p},\max}, \quad \forall n \in \mathbb{I}, \tag{44}$$

where

$$w_{\boldsymbol{p},\min} := \min_{\boldsymbol{i}=\mathbf{1}, \dots, \boldsymbol{n}^{(0)}+\boldsymbol{p}} w_{\boldsymbol{i},\boldsymbol{p},\boldsymbol{n}^{(0)}}, \quad w_{\boldsymbol{p},\max} := \max_{\boldsymbol{i}=\mathbf{1}, \dots, \boldsymbol{n}^{(0)}+\boldsymbol{p}} w_{\boldsymbol{i},\boldsymbol{p},\boldsymbol{n}^{(0)}}.$$

Finally, since the B-splines form a nonnegative partition of unity, we also have

$$0 < w_{\boldsymbol{p},\min} \le W_{\boldsymbol{p}}(\hat{\mathbf{x}}) \le w_{\boldsymbol{p},\max}, \quad \hat{\mathbf{x}} \in [0,1]^d. \tag{45}$$

*Remark* 3. Both the numerator and denominator of the geometry map $\mathbf{G}$ given in (42) are piecewise polynomial functions of class $C^{\min(\boldsymbol{p})-1}([0,1]^d)$. In particular, they reduce to a $\boldsymbol{p}$-degree tensor-product polynomial on each of the hyperrectangles

$$\mathfrak{R}_{\boldsymbol{i}} := [t_{i_1}, t_{i_1+1}] \times \ldots \times [t_{i_d}, t_{i_d+1}], \quad \boldsymbol{i} = \boldsymbol{p}+\mathbf{1}, \ldots, \boldsymbol{n}^{(0)}+\boldsymbol{p},$$

which form a partition of $[0,1]^d$ in view of (24). Moreover, from (45) we see that the denominator $W_{\boldsymbol{p}}$ is positive on $[0,1]^d$. As a consequence, all the partial derivatives of $\mathbf{G}$ are bounded on the interior of each $\mathfrak{R}_{\boldsymbol{i}}$, and so on

$$\mathfrak{Q} := \bigcup_{\boldsymbol{i}=\boldsymbol{p}+\mathbf{1}}^{\boldsymbol{n}^{(0)}+\boldsymbol{p}} {}^{o}\mathfrak{R}_{\boldsymbol{i}}. \tag{46}$$

For $\boldsymbol{p}=\mathbf{2}$ the collocation points in (41) all belong to $\mathfrak{Q}$ for every $\boldsymbol{n}$. Therefore, for any $\boldsymbol{p}\ge\mathbf{2}$ the map $\mathbf{G}$ belongs to $C^1([0,1]^d)$ and its second-order partial derivatives are bounded on the set

$$\bigcup_{\boldsymbol{n}} \{\boldsymbol{\xi}_{\boldsymbol{i}+\mathbf{1},\boldsymbol{p},\boldsymbol{n}},\ \boldsymbol{i}=\mathbf{2}, \ldots, \boldsymbol{n}+\boldsymbol{p}-\mathbf{1}\}. \tag{47}$$

## 5 | SPECTRAL DISTRIBUTION OF NURBS-BASED ISOGEOMETRIC MATRICES

This section contains our main results: the computation of the spectral distribution of the NURBS-based isogeometric Galerkin and collocation matrices by the identification of the corresponding symbols. To this end, we first describe in more detail the matrices we are interested in.

### 5.1 | Univariate building-block matrices

We start by defining some matrices that will form the univariate building blocks of our spectral analysis: for $p \ge 1$,

$$K_n^{\mathcal{G},p} := \frac{1}{n}\left[\int_{[0,1]} N'_{j+1,p,n} N'_{i+1,p,n}\right]_{i,j=1}^{n+p-2}, \quad H_n^{\mathcal{G},p} := \left[\int_{[0,1]} N'_{j+1,p,n} N_{i+1,p,n}\right]_{i,j=1}^{n+p-2}, \quad M_n^{\mathcal{G},p} := n\left[\int_{[0,1]} N_{j+1,p,n} N_{i+1,p,n}\right]_{i,j=1}^{n+p-2}, \tag{48}$$

and for $p \ge 2$,

$$K_n^{\mathcal{C},p} := \frac{1}{n^2}[-N''_{j+1,p,n}(\xi_{i+1,p,n})]_{i,j=1}^{n+p-2}, \quad H_n^{\mathcal{C},p} := \frac{1}{n}[N'_{j+1,p,n}(\xi_{i+1,p,n})]_{i,j=1}^{n+p-2}, \quad M_n^{\mathcal{C},p} := [N_{j+1,p,n}(\xi_{i+1,p,n})]_{i,j=1}^{n+p-2}. \tag{49}$$

By (31) and using the fact that $[t_i, t_{i+p+1}] \cap (t_j, t_{j+p+1})$ is empty if $|i-j| > p$, we have

$$\begin{aligned} &(K_n^{\mathcal{G},p})_{ij} = (H_n^{\mathcal{G},p})_{ij} = (M_n^{\mathcal{G},p})_{ij} = 0, \\ &(K_n^{\mathcal{C},p})_{ij} = (H_n^{\mathcal{C},p})_{ij} = (M_n^{\mathcal{C},p})_{ij} = 0, \end{aligned} \quad \text{if} \quad |i-j| > p. \tag{50}$$

Therefore, all these matrices are banded, with a bandwidth independent of $n$. Moreover, by Lemma 8 of Reference 13 and Lemma 4.1 of Reference 12 their spectral norms are uniformly bounded with respect to $n$,

$$\begin{aligned} &\|K_n^{\mathcal{G},p}\| \le 4p, \quad \|H_n^{\mathcal{G},p}\| \le 2, \quad \|M_n^{\mathcal{G},p}\| \le 1, \\ &\|K_n^{\mathcal{C},p}\| \le 2p(p-1)\sqrt{3p}, \quad \|H_n^{\mathcal{C},p}\| \le p\sqrt{3p}, \quad \|M_n^{\mathcal{C},p}\| \le \sqrt{3p/2}. \end{aligned} \tag{51}$$

Since we are using the knot sequence (24), almost all the B-splines in (25) are a translated and scaled version of the same function. The cardinal B-spline of degree $p$ is denoted by $\phi_p$ and is defined recursively by

$$\phi_0(t) := \begin{cases} 1, & \text{if } t \in [0,1), \\ 0, & \text{elsewhere,} \end{cases}$$

and

$$\phi_p(t) := \frac{t}{p}\phi_{p-1}(t) + \frac{p+1-t}{p}\phi_{p-1}(t-1), \quad p \geq 1.$$

This is a nonnegative piecewise polynomial of degree $p$ in $C^{p-1}(\mathbb{R})$. It is symmetric with respect to $(p+1)/2$, which is the midpoint of its support $[0, p+1]$. From Lemma 4 of Reference 13 (see also Reference 27) we know that the inner products of the derivatives of cardinal B-splines can be expressed as

$$\int_{\mathbb{R}} \phi_p^{(r)}(t)\phi_p^{(s)}(t+k)\mathrm{d}t = (-1)^r \phi_{2p+1}^{(r+s)}(p+1+k) = (-1)^s \phi_{2p+1}^{(r+s)}(p+1-k).$$

It can be easily checked that, for $x \in [0,1]$ and $n \geq p+1$,

$$N_{i,p,n}(x) = \phi_p(nx - i + p + 1), \quad i = p+1, \ldots, n.$$

The above equalities imply that for $i,j = 2p, \ldots, n-p-1$,

$$n\int_{[0,1]} N_{i+1,p,n}(x)N_{j+1,p,n}(x)\mathrm{d}x = \phi_{2p+1}(p+1+i-j), \tag{52}$$

$$\int_{[0,1]} N_{i+1,p,n}(x)N'_{j+1,p,n}(x)\mathrm{d}x = \dot{\phi}_{2p+1}(p+1+i-j), \tag{53}$$

$$\frac{1}{n}\int_{[0,1]} N'_{i+1,p,n}(x)N'_{j+1,p,n}(x)\mathrm{d}x = -\ddot{\phi}_{2p+1}(p+1+i-j), \tag{54}$$

where $\dot{\phi}_p$ and $\ddot{\phi}_p$ denote the first- and second-order derivatives of $\phi_p$, respectively. Furthermore, from (24) we deduce that

$$\xi_{i,p,n} = \frac{i}{n} - \frac{p+1}{2n}, \quad i = p+1, \ldots, n,$$

and we obtain for $i,j = p, \ldots, n-1$,

$$N_{j+1,p,n}(\xi_{i+1,p,n}) = \phi_p\left(\frac{p+1}{2} + i - j\right), \tag{55}$$

$$\frac{1}{n}N'_{j+1,p,n}(\xi_{i+1,p,n}) = \dot{\phi}_p\left(\frac{p+1}{2} + i - j\right), \tag{56}$$

$$\frac{1}{n^2}N''_{j+1,p,n}(\xi_{i+1,p,n}) = \ddot{\phi}_p\left(\frac{p+1}{2} + i - j\right). \tag{57}$$

It follows that the central rows identified by the indices $i = 3p+1, \ldots, n-2p-2$ of the pairs of matrices

$$K_n^{\mathcal{G},p} \text{ and } K_{n-p-1}^{\mathcal{C},2p+1}, \quad H_n^{\mathcal{G},p} \text{ and } H_{n-p-1}^{\mathcal{C},2p+1}, \quad M_n^{\mathcal{G},p} \text{ and } M_{n-p-1}^{\mathcal{C},2p+1}$$

are identical (see Section 4.1 of Reference 12).

The Toeplitz matrices $T_{n+p-2}(f_p)$, $T_{n+p-2}(g_p)$, $T_{n+p-2}(h_p)$ and their generating functions,

$$f_p(\theta) := -\ddot{\phi}_p\left(\frac{p+1}{2}\right) - 2\sum_{k=1}^{\lfloor p/2 \rfloor} \ddot{\phi}_p\left(\frac{p+1}{2} - k\right)\cos(k\theta), \tag{58}$$

$$g_p(\theta) := -2\sum_{k=1}^{\lfloor p/2\rfloor} \dot{\phi}_p\left(\frac{p+1}{2}-k\right)\sin(k\theta), \tag{59}$$

$$h_p(\theta) := \phi_p\left(\frac{p+1}{2}\right) + 2\sum_{k=1}^{\lfloor p/2\rfloor} \phi_p\left(\frac{p+1}{2}-k\right)\cos(k\theta), \tag{60}$$

will play a fundamental role later on. Since $f_p$, $g_p$, $h_p$ are trigonometric polynomials of degree $\lfloor p/2\rfloor$, the matrices $T_{n+p-2}(f_p)$, $T_{n+p-2}(g_p)$, $T_{n+p-2}(h_p)$ are banded, with a bandwidth independent of $n$.

Finally, when comparing (58), (59), (60) with (57), (56), (55), respectively, we observe that the matrices $K_n^{\mathcal{C},p}, H_n^{\mathcal{C},p}, M_n^{\mathcal{C},p}$ defined in (49) are small-rank perturbations of the Toeplitz matrices $T_{n+p-2}(f_p)$, $\mathrm{i}\,T_{n+p-2}(g_p)$, $T_{n+p-2}(h_p)$, respectively. In view of (52) to (54), there is a similar relation between the matrices $K_n^{\mathcal{G},p}$, $H_n^{\mathcal{G},p}$, $M_n^{\mathcal{G},p}$ defined in (48) and the Toeplitz matrices $T_{n+p-2}(f_{2p+1})$, $\mathrm{i}\,T_{n+p-2}(g_{2p+1})$, $T_{n+p-2}(h_{2p+1})$, respectively. More precisely, it can be checked[12,13] that

$$\mathrm{rank}(K_n^{\mathcal{G},p} - T_{n+p-2}(f_{2p+1})) \le 4p, \quad \mathrm{rank}(K_n^{\mathcal{C},p} - T_{n+p-2}(f_p)) \le 3p, \tag{61}$$

$$\mathrm{rank}(H_n^{\mathcal{G},p} - \mathrm{i}\,T_{n+p-2}(g_{2p+1})) \le 4p, \quad \mathrm{rank}(H_n^{\mathcal{C},p} - \mathrm{i}\,T_{n+p-2}(g_p)) \le 3p, \tag{62}$$

$$\mathrm{rank}(M_n^{\mathcal{G},p} - T_{n+p-2}(h_{2p+1})) \le 4p, \quad \mathrm{rank}(M_n^{\mathcal{C},p} - T_{n+p-2}(h_p)) \le 3p. \tag{63}$$

*Remark* 4. Up to some scaling factors, the matrices defined in (48) and (49) are matrices appearing in isogeometric Galerkin and collocation discretizations based on B-splines applied in the simplest scenario: the univariate problem (1) with constant coefficients and no geometry map, see (17) and (23). The above discussion shows that such matrices are small-rank perturbations of Toeplitz matrices generated by the functions in (58) to (60), which are also the corresponding spectral symbols. Hence, from the spectral point of view, the only difference between the isogeometric Galerkin and collocation methods based on B-splines of degree $p$ is the degree parameter in the generating functions (58) to (60), namely, $2p+1$ and $p$ in the Galerkin and collocation case, respectively.

## 5.2 | NURBS-based isogeometric matrices

With the choices of $\hat{\varphi}_i$ and $\hat{\boldsymbol{\tau}}_i$ as in (40) and (41), we obtain from (17) and (23) two matrices, which from now on will be denoted by $A_{\mathbf{G},\boldsymbol{n}}^{\mathcal{G},\boldsymbol{p}}$ and $A_{\mathbf{G},\boldsymbol{n}}^{\mathcal{C},\boldsymbol{p}}$, in order to emphasize their dependence on $\mathbf{G}$, $\boldsymbol{p}$, $\boldsymbol{n}$. We adopt for the NURBS in (40), as well as for the associated Greville abscissae in (41), the lexicographic ordering (6). This ordering is followed when assembling the matrices $A_{\mathbf{G},\boldsymbol{n}}^{\mathcal{G},\boldsymbol{p}}$ and $A_{\mathbf{G},\boldsymbol{n}}^{\mathcal{C},\boldsymbol{p}}$, which can then be expressed in multiindex notation as follows:

$$A_{\mathbf{G},\boldsymbol{n}}^{\mathcal{G},\boldsymbol{p}} = \left[\int_{[0,1]^d} |\det(J_{\mathbf{G}})|\,((\nabla R_{\boldsymbol{j}+\mathbf{1},\boldsymbol{p},\boldsymbol{n}})^T K_{\mathbf{G}} \nabla R_{\boldsymbol{i}+\mathbf{1},\boldsymbol{p},\boldsymbol{n}} + (\nabla R_{\boldsymbol{j}+\mathbf{1},\boldsymbol{p},\boldsymbol{n}})^T \boldsymbol{\alpha}_{\mathbf{G}}\, R_{\boldsymbol{i}+\mathbf{1},\boldsymbol{p},\boldsymbol{n}} + \gamma_{\mathbf{G}}\, R_{\boldsymbol{j}+\mathbf{1},\boldsymbol{p},\boldsymbol{n}} R_{\boldsymbol{i}+\mathbf{1},\boldsymbol{p},\boldsymbol{n}})\right]_{\boldsymbol{i},\boldsymbol{j}=\mathbf{1}}^{\boldsymbol{n}+\boldsymbol{p}-\mathbf{2}}, \tag{64}$$

and

$$A_{\mathbf{G},\boldsymbol{n}}^{\mathcal{C},\boldsymbol{p}} = [-\mathbf{1}(K_{\mathbf{G}}(\boldsymbol{\xi}_{\boldsymbol{i}+\mathbf{1},\boldsymbol{p},\boldsymbol{n}}) \circ H R_{\boldsymbol{j}+\mathbf{1},\boldsymbol{p},\boldsymbol{n}}(\boldsymbol{\xi}_{\boldsymbol{i}+\mathbf{1},\boldsymbol{p},\boldsymbol{n}}))\mathbf{1}^T + \boldsymbol{\beta}_{\mathbf{G}}(\boldsymbol{\xi}_{\boldsymbol{i}+\mathbf{1},\boldsymbol{p},\boldsymbol{n}}) \cdot \nabla R_{\boldsymbol{j}+\mathbf{1},\boldsymbol{p},\boldsymbol{n}}(\boldsymbol{\xi}_{\boldsymbol{i}+\mathbf{1},\boldsymbol{p},\boldsymbol{n}}) + \gamma_{\mathbf{G}}(\boldsymbol{\xi}_{\boldsymbol{i}+\mathbf{1},\boldsymbol{p},\boldsymbol{n}}) R_{\boldsymbol{j}+\mathbf{1},\boldsymbol{p},\boldsymbol{n}}(\boldsymbol{\xi}_{\boldsymbol{i}+\mathbf{1},\boldsymbol{p},\boldsymbol{n}})]_{\boldsymbol{i},\boldsymbol{j}=\mathbf{1}}^{\boldsymbol{n}+\boldsymbol{p}-\mathbf{2}}. \tag{65}$$

The Galerkin matrix $A_{\mathbf{G},\boldsymbol{n}}^{\mathcal{G},\boldsymbol{p}}$ is defined for all $\boldsymbol{p} \ge \mathbf{1}$, whereas the collocation matrix $A_{\mathbf{G},\boldsymbol{n}}^{\mathcal{C},\boldsymbol{p}}$ is defined for all $\boldsymbol{p} \ge \mathbf{2}$. By Remark 3 the condition $\boldsymbol{p} \ge \mathbf{2}$ ensures that the expressions $HR_{\boldsymbol{j}+\mathbf{1},\boldsymbol{p},\boldsymbol{n}}(\boldsymbol{\xi}_{\boldsymbol{i}+\mathbf{1},\boldsymbol{p},\boldsymbol{n}})$ are well defined.

For $s, t = 1, \dots, d$ and $\boldsymbol{i} = \mathbf{1}, \dots, \boldsymbol{n}+\boldsymbol{p}$, from (38) we derive

$$\frac{\partial R_{\boldsymbol{i},\boldsymbol{p},\boldsymbol{n}}}{\partial \hat{x}_s} = \frac{w_{\boldsymbol{i},\boldsymbol{p},\boldsymbol{n}}}{W_{\boldsymbol{p}}} \frac{\partial N_{\boldsymbol{i},\boldsymbol{p},\boldsymbol{n}}}{\partial \hat{x}_s} - \frac{w_{\boldsymbol{i},\boldsymbol{p},\boldsymbol{n}}}{W_{\boldsymbol{p}}^2} \frac{\partial W_{\boldsymbol{p}}}{\partial \hat{x}_s} N_{\boldsymbol{i},\boldsymbol{p},\boldsymbol{n}}, \tag{66}$$

$$\frac{\partial^2 R_{\boldsymbol{i},\boldsymbol{p},\boldsymbol{n}}}{\partial \hat{x}_s \partial \hat{x}_t} = \frac{w_{\boldsymbol{i},\boldsymbol{p},\boldsymbol{n}}}{W_{\boldsymbol{p}}} \frac{\partial^2 N_{\boldsymbol{i},\boldsymbol{p},\boldsymbol{n}}}{\partial \hat{x}_s \partial \hat{x}_t} - \frac{w_{\boldsymbol{i},\boldsymbol{p},\boldsymbol{n}}}{W_{\boldsymbol{p}}^2} \frac{\partial W_{\boldsymbol{p}}}{\partial \hat{x}_t} \frac{\partial N_{\boldsymbol{i},\boldsymbol{p},\boldsymbol{n}}}{\partial \hat{x}_s} - \frac{w_{\boldsymbol{i},\boldsymbol{p},\boldsymbol{n}}}{W_{\boldsymbol{p}}^2} \frac{\partial W_{\boldsymbol{p}}}{\partial \hat{x}_s} \frac{\partial N_{\boldsymbol{i},\boldsymbol{p},\boldsymbol{n}}}{\partial \hat{x}_t} - \frac{w_{\boldsymbol{i},\boldsymbol{p},\boldsymbol{n}}}{W_{\boldsymbol{p}}^3} \left(W_{\boldsymbol{p}} \frac{\partial^2 W_{\boldsymbol{p}}}{\partial \hat{x}_s \partial \hat{x}_t} - 2 \frac{\partial W_{\boldsymbol{p}}}{\partial \hat{x}_s} \frac{\partial W_{\boldsymbol{p}}}{\partial \hat{x}_t}\right) N_{\boldsymbol{i},\boldsymbol{p},\boldsymbol{n}}. \tag{67}$$

Using some elementary calculations, from (38) and (66) we see that the Galerkin matrix (64) can be decomposed as

$$A_{\mathbf{G},\boldsymbol{n}}^{\mathcal{G},\boldsymbol{p}} = K_{\mathbf{G},\boldsymbol{n}}^{\mathcal{G},\boldsymbol{p}} + R_{\mathbf{G},\boldsymbol{n}}^{\mathcal{G},\boldsymbol{p}}, \tag{68}$$

where

$$K_{\mathbf{G},\boldsymbol{n}}^{\mathcal{G},\boldsymbol{p}} := \left[\sum_{s,t=1}^{d}\int_{[0,1]^d} |\det(J_{\mathbf{G}})|\ \kappa_{\mathbf{G},st}\ \frac{w_{\boldsymbol{j+1},\boldsymbol{p},\boldsymbol{n}}}{W_{\boldsymbol{p}}}\ \frac{w_{\boldsymbol{i+1},\boldsymbol{p},\boldsymbol{n}}}{W_{\boldsymbol{p}}}\ \frac{\partial N_{\boldsymbol{j+1},\boldsymbol{p},\boldsymbol{n}}}{\partial \hat{x}_s}\ \frac{\partial N_{\boldsymbol{i+1},\boldsymbol{p},\boldsymbol{n}}}{\partial \hat{x}_t}\right]_{\boldsymbol{i},\boldsymbol{j}=\boldsymbol{1}}^{\boldsymbol{n+p-2}}, \tag{69}$$

and $R_{\mathbf{G},\boldsymbol{n}}^{\mathcal{G},\boldsymbol{p}}$ is a matrix whose entries contain only products involving lower order derivatives of B-splines, see (A1). Moreover, it is useful to consider the further decomposition

$$K_{\mathbf{G},\boldsymbol{n}}^{\mathcal{G},\boldsymbol{p}} = \hat{K}_{\mathbf{G},\boldsymbol{n}}^{\mathcal{G},\boldsymbol{p}} + (K_{\mathbf{G},\boldsymbol{n}}^{\mathcal{G},\boldsymbol{p}} - \hat{K}_{\mathbf{G},\boldsymbol{n}}^{\mathcal{G},\boldsymbol{p}}),$$

where

$$\hat{K}_{\mathbf{G},\boldsymbol{n}}^{\mathcal{G},\boldsymbol{p}} := \left[\int_{[0,1]^d} |\det(J_{\mathbf{G}})|\ (\nabla N_{\boldsymbol{j+1},\boldsymbol{p},\boldsymbol{n}})^T K_{\mathbf{G}}\ \nabla N_{\boldsymbol{i+1},\boldsymbol{p},\boldsymbol{n}}\right]_{\boldsymbol{i},\boldsymbol{j}=\boldsymbol{1}}^{\boldsymbol{n+p-2}} \tag{70}$$

is the Galerkin diffusion matrix based on B-splines.

Similarly, the collocation matrix $A_{\mathbf{G},\boldsymbol{n}}^{\mathcal{C},\boldsymbol{p}}$ in (65) can be decomposed as

$$A_{\mathbf{G},\boldsymbol{n}}^{\mathcal{C},\boldsymbol{p}} = K_{\mathbf{G},\boldsymbol{n}}^{\mathcal{C},\boldsymbol{p}} + R_{\mathbf{G},\boldsymbol{n}}^{\mathcal{C},\boldsymbol{p}}, \tag{71}$$

where

$$K_{\mathbf{G},\boldsymbol{n}}^{\mathcal{C},\boldsymbol{p}} := \left[-\sum_{s,t=1}^{d}\kappa_{\mathbf{G},st}(\boldsymbol{\xi}_{\boldsymbol{i+1},\boldsymbol{p},\boldsymbol{n}})\ \frac{w_{\boldsymbol{j+1},\boldsymbol{p},\boldsymbol{n}}}{W_{\boldsymbol{p}}(\boldsymbol{\xi}_{\boldsymbol{i+1},\boldsymbol{p},\boldsymbol{n}})}\ \frac{\partial^2 N_{\boldsymbol{j+1},\boldsymbol{p},\boldsymbol{n}}}{\partial \hat{x}_s \partial \hat{x}_t}(\boldsymbol{\xi}_{\boldsymbol{i+1},\boldsymbol{p},\boldsymbol{n}})\right]_{\boldsymbol{i},\boldsymbol{j}=\boldsymbol{1}}^{\boldsymbol{n+p-2}}, \tag{72}$$

and $R_{\mathbf{G},\boldsymbol{n}}^{\mathcal{C},\boldsymbol{p}}$ is a matrix whose entries contain only products involving lower order derivatives of B-splines, see (B1). Again, it is useful to consider the further decomposition

$$K_{\mathbf{G},\boldsymbol{n}}^{\mathcal{C},\boldsymbol{p}} = \hat{K}_{\mathbf{G},\boldsymbol{n}}^{\mathcal{C},\boldsymbol{p}} + (K_{\mathbf{G},\boldsymbol{n}}^{\mathcal{C},\boldsymbol{p}} - \hat{K}_{\mathbf{G},\boldsymbol{n}}^{\mathcal{C},\boldsymbol{p}}),$$

where

$$\hat{K}_{\mathbf{G},\boldsymbol{n}}^{\mathcal{C},\boldsymbol{p}} := [-\mathbf{1}(K_{\mathbf{G}}(\boldsymbol{\xi}_{\boldsymbol{i+1},\boldsymbol{p},\boldsymbol{n}})\circ HN_{\boldsymbol{j+1},\boldsymbol{p},\boldsymbol{n}}(\boldsymbol{\xi}_{\boldsymbol{i+1},\boldsymbol{p},\boldsymbol{n}}))\mathbf{1}^T]_{\boldsymbol{i},\boldsymbol{j}=\boldsymbol{1}}^{\boldsymbol{n+p-2}} \tag{73}$$

is the collocation diffusion matrix based on B-splines. Note that such a matrix can be expressed as (see Lemma 3)

$$\hat{K}_{\mathbf{G},\boldsymbol{n}}^{\mathcal{C},\boldsymbol{p}} = \sum_{s,t=1}^{d} n_s n_t D_{\boldsymbol{n}}^{\boldsymbol{p}}(\kappa_{\mathbf{G},st})\hat{K}_{\boldsymbol{n},st}^{\mathcal{C},\boldsymbol{p}}, \tag{74}$$

where $D_{\boldsymbol{n}}^{\boldsymbol{p}}(a)$ denotes the $d$-level diagonal matrix of size $N(\boldsymbol{n}+\boldsymbol{p}-\boldsymbol{2})$ containing samples of the function $a : [0,1]^d \to \mathbb{R}$ at the Greville abscissae (41),

$$D_{\boldsymbol{n}}^{\boldsymbol{p}}(a) := \mathrm{diag}_{\boldsymbol{i}=\boldsymbol{1},\ldots,\boldsymbol{n+p-2}}\, a(\boldsymbol{\xi}_{\boldsymbol{i+1},\boldsymbol{p},\boldsymbol{n}}), \tag{75}$$

and

$$\hat{K}_{\boldsymbol{n},st}^{\mathcal{C},\boldsymbol{p}} := \begin{cases} (\otimes_{r=1}^{s-1} M_{n_r}^{\mathcal{C},p_r}) \otimes K_{n_s}^{\mathcal{C},p_s} \otimes (\otimes_{r=s+1}^{d} M_{n_r}^{\mathcal{C},p_r}), & s = t, \\ -(\otimes_{r=1}^{s-1} M_{n_r}^{\mathcal{C},p_r}) \otimes H_{n_s}^{\mathcal{C},p_s} \otimes (\otimes_{r=s+1}^{t-1} M_{n_r}^{\mathcal{C},p_r}) \otimes H_{n_t}^{\mathcal{C},p_t} \otimes (\otimes_{r=t+1}^{d} M_{n_r}^{\mathcal{C},p_r}), & s < t, \\ -(\otimes_{r=1}^{t-1} M_{n_r}^{\mathcal{C},p_r}) \otimes H_{n_t}^{\mathcal{C},p_t} \otimes (\otimes_{r=t+1}^{s-1} M_{n_r}^{\mathcal{C},p_r}) \otimes H_{n_s}^{\mathcal{C},p_s} \otimes (\otimes_{r=s+1}^{d} M_{n_r}^{\mathcal{C},p_r}), & s > t, \end{cases} \tag{76}$$

with the matrices $K_n^{\mathcal{C},p}, H_n^{\mathcal{C},p}, M_n^{\mathcal{C},p}$ defined in (49). The matrix in (76) is nothing else than the matrix obtained after the discretization of the second-order derivative $-\frac{\partial^2}{\partial x_s \partial x_t}$ using B-splines and no geometry map. A similar structure can be derived for the B-spline Galerkin diffusion matrix (in the case of constant coefficients); we refer the reader to the literature[14] for more details.

*Remark* 5. In view of Theorem 1, the matrices $R_{\mathbf{G},\boldsymbol{n}}^{\mathcal{G},\boldsymbol{p}}$ and $R_{\mathbf{G},\boldsymbol{n}}^{\mathcal{C},\boldsymbol{p}}$ can be regarded as "residual terms." Indeed, we shall see later that their spectral norms are negligible with respect to the norms of $K_{\mathbf{G},\boldsymbol{n}}^{\mathcal{G},\boldsymbol{p}}$ and $K_{\mathbf{G},\boldsymbol{n}}^{\mathcal{C},\boldsymbol{p}}$, respectively, when the discretization parameters $\boldsymbol{n}$ are large. Furthermore, since the weights $w_{\boldsymbol{j},\boldsymbol{p},\boldsymbol{n}}$ approach the values $W_{\boldsymbol{p}}(\boldsymbol{\xi}_{\boldsymbol{i},\boldsymbol{p},\boldsymbol{n}})$ for large $\boldsymbol{n}$ if $\boldsymbol{i}$ and $\boldsymbol{j}$ are close enough, see (43), it turns out that $K_{\mathbf{G},\boldsymbol{n}}^{\mathcal{G},\boldsymbol{p}}$ and $K_{\mathbf{G},\boldsymbol{n}}^{\mathcal{C},\boldsymbol{p}}$ are small perturbations in spectral norm of $\hat{K}_{\mathbf{G},\boldsymbol{n}}^{\mathcal{G},\boldsymbol{p}}$ and $\hat{K}_{\mathbf{G},\boldsymbol{n}}^{\mathcal{C},\boldsymbol{p}}$, respectively. These are the main ingredients used in the following section to derive the symbol of the matrices (64) and (65).

## 5.3 | The symbol of NURBS-based isogeometric matrices

We are now ready to provide the symbol of the matrices arising from NURBS-based isogeometric Galerkin and collocation discretizations. To improve the readability of the section, several technical results are deferred to Appendix A (Galerkin case) and Appendix B (collocation case).

Let $H_{\boldsymbol{p}}$ be the $d \times d$ symmetric matrix of continuous functions defined by

$$(H_{\boldsymbol{p}})_{st} := \begin{cases} (\otimes_{r=1}^{s-1} h_{p_r}) \otimes f_{p_s} \otimes (\otimes_{r=s+1}^{d} h_{p_r}), & s = t, \\ (\otimes_{r=1}^{s-1} h_{p_r}) \otimes g_{p_s} \otimes (\otimes_{r=s+1}^{t-1} h_{p_r}) \otimes g_{p_t} \otimes (\otimes_{r=t+1}^{d} h_{p_r}), & s < t, \\ (\otimes_{r=1}^{t-1} h_{p_r}) \otimes g_{p_t} \otimes (\otimes_{r=t+1}^{s-1} h_{p_r}) \otimes g_{p_s} \otimes (\otimes_{r=s+1}^{d} h_{p_r}), & s > t, \end{cases} \tag{77}$$

where $f_p, g_p, h_p$ are given in (58) to (60). Since $g_{p_s} \otimes g_{p_t} = -(\mathrm{i}g_{p_s} \otimes \mathrm{i}g_{p_t})$, we clearly observe a similarity between the matrix in (76) and the Toeplitz matrix $T_{\boldsymbol{n}+\boldsymbol{p}-\boldsymbol{2}}((H_{\boldsymbol{p}})_{st})$ associated with the function in (77); see also (11) and (61) to (63).

The next theorem describes the symbol of a sequence of NURBS-based isogeometric Galerkin matrices.

**Theorem 3.** *Let $\boldsymbol{\nu} \in \mathbb{Q}_+^d$ and $\boldsymbol{p} \geq \mathbf{1}$. Assume that the PDE coefficients $\kappa_{ij}, \alpha_i, \gamma$ belong to $L^\infty(\Omega)$ and let $\mathbf{G}$ be given by (42) with $\det(J_{\mathbf{G}}) \neq 0$ on $[0,1]^d$. Then, the sequence of matrices $\{n^{d-2} A_{\mathbf{G},\boldsymbol{n}}^{\mathcal{G},\boldsymbol{p}}\}_n$, with $\boldsymbol{n} := \boldsymbol{\nu} n$, has an asymptotic spectral distribution described by the symbol $f_{\mathbf{G},\boldsymbol{p}}^{\mathcal{G},\boldsymbol{\nu}} : [0,1]^d \times [-\pi,\pi]^d \to \mathbb{R}$,*

$$f_{\mathbf{G},\boldsymbol{p}}^{\mathcal{G},\boldsymbol{\nu}}(\hat{\mathbf{x}}, \boldsymbol{\theta}) := \frac{|\det(J_{\mathbf{G}}(\hat{\mathbf{x}}))|}{N(\boldsymbol{\nu})} \, \boldsymbol{\nu}(K_{\mathbf{G}}(\hat{\mathbf{x}}) \circ H_{2\boldsymbol{p}+\mathbf{1}}(\boldsymbol{\theta}))\boldsymbol{\nu}^T. \tag{78}$$

*In formulas, $\{n^{d-2} A_{\mathbf{G},\boldsymbol{n}}^{\mathcal{G},\boldsymbol{p}}\}_n \sim_\lambda f_{\mathbf{G},\boldsymbol{p}}^{\mathcal{G},\boldsymbol{\nu}}$.*

*Proof.* The proof is an application of Theorem 1. We consider the following decomposition of $n^{d-2} A_{\mathbf{G},\boldsymbol{n}}^{\mathcal{G},\boldsymbol{p}}$:

$$n^{d-2} A_{\mathbf{G},\boldsymbol{n}}^{\mathcal{G},\boldsymbol{p}} = n^{d-2} \hat{K}_{\mathbf{G},\boldsymbol{n}}^{\mathcal{G},\boldsymbol{p}} + (n^{d-2} K_{\mathbf{G},\boldsymbol{n}}^{\mathcal{G},\boldsymbol{p}} - n^{d-2} \hat{K}_{\mathbf{G},\boldsymbol{n}}^{\mathcal{G},\boldsymbol{p}}) + n^{d-2} R_{\mathbf{G},\boldsymbol{n}}^{\mathcal{G},\boldsymbol{p}},$$

and we prove that all the hypotheses of Theorem 1 are satisfied with

$$X_{\boldsymbol{m}} := n^{d-2} \hat{K}_{\mathbf{G},\boldsymbol{n}}^{\mathcal{G},\boldsymbol{p}}, \quad Y_{\boldsymbol{m}} := (n^{d-2} K_{\mathbf{G},\boldsymbol{n}}^{\mathcal{G},\boldsymbol{p}} - n^{d-2} \hat{K}_{\mathbf{G},\boldsymbol{n}}^{\mathcal{G},\boldsymbol{p}}) + n^{d-2} R_{\mathbf{G},\boldsymbol{n}}^{\mathcal{G},\boldsymbol{p}}, \quad Z_{\boldsymbol{m}} := n^{d-2} A_{\mathbf{G},\boldsymbol{n}}^{\mathcal{G},\boldsymbol{p}}.$$

More precisely,

- $\hat{K}_{\mathbf{G},\boldsymbol{n}}^{\mathcal{G},\boldsymbol{p}}$ is Hermitian, see (70), and from Theorem 2.1 of Reference 15 (note that the map $\mathbf{G}$ belongs to $C^1([0,1]^d)$ for $\boldsymbol{p} \geq \mathbf{2}$ but by Remark 3 one can check that the theorem holds for any $\boldsymbol{p} \geq \mathbf{1}$) we deduce $\{n^{d-2} \hat{K}_{\mathbf{G},\boldsymbol{n}}^{\mathcal{G},\boldsymbol{p}}\}_n \sim_\lambda f_{\mathbf{G},\boldsymbol{p}}^{\mathcal{G},\boldsymbol{\nu}}$;
- Lemma 1 says that $\|n^{d-2} \hat{K}_{\mathbf{G},\boldsymbol{n}}^{\mathcal{G},\boldsymbol{p}}\|$, $\|n^{d-2} K_{\mathbf{G},\boldsymbol{n}}^{\mathcal{G},\boldsymbol{p}}\|$ are uniformly bounded with respect to $n$ and $\|n^{d-2} R_{\mathbf{G},\boldsymbol{n}}^{\mathcal{G},\boldsymbol{p}}\| \leq C/n$, where $C$ is a constant independent of $n$;

- Lemma 2 says that $\|n^{d-2}K_{\mathbf{G},\boldsymbol{n}}^{\mathcal{G},\boldsymbol{p}} - n^{d-2}\hat{K}_{\mathbf{G},\boldsymbol{n}}^{\mathcal{G},\boldsymbol{p}}\| \to 0$ as $n \to \infty$. By the inequality in (3), the above bounds imply

$$\|n^{d-2}K_{\mathbf{G},\boldsymbol{n}}^{\mathcal{G},\boldsymbol{p}} - n^{d-2}\hat{K}_{\mathbf{G},\boldsymbol{n}}^{\mathcal{G},\boldsymbol{p}} + n^{d-2}R_{\mathbf{G},\boldsymbol{n}}^{\mathcal{G},\boldsymbol{p}}\|_1 = o(N(\boldsymbol{n}+\boldsymbol{p}-\boldsymbol{2})).$$

This concludes the proof. ∎

The next theorem describes the symbol of a sequence of NURBS-based isogeometric collocation matrices.

**Theorem 4.** *Let $\boldsymbol{\nu} \in \mathbb{Q}_+^d$ and $\boldsymbol{p} \geq \boldsymbol{2}$. Assume that the PDE coefficients $\kappa_{ij}, \alpha_i, \gamma$ belong to $C(\overline{\Omega})$, and that each $\kappa_{ij}$ has continuous and bounded partial derivatives on $\Omega$. Let $\mathbf{G}$ be given by (42) with $\det(J_{\mathbf{G}}) \neq 0$ on $[0,1]^d$. Then, the sequence of matrices $\{n^{-2}A_{\mathbf{G},\boldsymbol{n}}^{\mathcal{C},\boldsymbol{p}}\}_n$, with $\boldsymbol{n} := \boldsymbol{\nu}n$, has an asymptotic spectral distribution described by the symbol $f_{\mathbf{G},\boldsymbol{p}}^{\mathcal{C},\boldsymbol{\nu}} : [0,1]^d \times [-\pi,\pi]^d \to \mathbb{R}$,*

$$f_{\mathbf{G},\boldsymbol{p}}^{\mathcal{C},\boldsymbol{\nu}}(\hat{\mathbf{x}},\boldsymbol{\theta}) := \boldsymbol{\nu}(K_{\mathbf{G}}(\hat{\mathbf{x}}) \circ H_{\boldsymbol{p}}(\boldsymbol{\theta}))\boldsymbol{\nu}^T. \tag{79}$$

*In formulas, $\{n^{-2}A_{\mathbf{G},\boldsymbol{n}}^{\mathcal{C},\boldsymbol{p}}\}_n \sim_\lambda f_{\mathbf{G},\boldsymbol{p}}^{\mathcal{C},\boldsymbol{\nu}}$.*

*Proof.* The proof is again an application of Theorem 1. We consider the following decomposition of $n^{-2}A_{\mathbf{G},\boldsymbol{n}}^{\mathcal{C},\boldsymbol{p}}$:

$$n^{-2}A_{\mathbf{G},\boldsymbol{n}}^{\mathcal{C},\boldsymbol{p}} = n^{-2}\tilde{K}_{\mathbf{G},\boldsymbol{n}}^{\mathcal{C},\boldsymbol{p}} + (n^{-2}K_{\mathbf{G},\boldsymbol{n}}^{\mathcal{C},\boldsymbol{p}} - n^{-2}\tilde{K}_{\mathbf{G},\boldsymbol{n}}^{\mathcal{C},\boldsymbol{p}}) + n^{-2}R_{\mathbf{G},\boldsymbol{n}}^{\mathcal{C},\boldsymbol{p}},$$

where

$$\tilde{K}_{\mathbf{G},\boldsymbol{n}}^{\mathcal{C},\boldsymbol{p}} := \sum_{s,t=1}^{d} n_s n_t \tilde{D}_{\boldsymbol{n}+\boldsymbol{p}-\boldsymbol{2}}(\kappa_{\mathbf{G},st}) \circ T_{\boldsymbol{n}+\boldsymbol{p}-\boldsymbol{2}}((H_{\boldsymbol{p}})_{st}), \tag{80}$$

and we prove that all the hypotheses of Theorem 1 are satisfied with

$$X_{\boldsymbol{m}} := n^{-2}\tilde{K}_{\mathbf{G},\boldsymbol{n}}^{\mathcal{C},\boldsymbol{p}}, \quad Y_{\boldsymbol{m}} := (n^{-2}K_{\mathbf{G},\boldsymbol{n}}^{\mathcal{C},\boldsymbol{p}} - n^{-2}\tilde{K}_{\mathbf{G},\boldsymbol{n}}^{\mathcal{C},\boldsymbol{p}}) + n^{-2}R_{\mathbf{G},\boldsymbol{n}}^{\mathcal{C},\boldsymbol{p}}, \quad Z_{\boldsymbol{m}} := n^{-2}A_{\mathbf{G},\boldsymbol{n}}^{\mathcal{C},\boldsymbol{p}}.$$

More precisely,

- $\tilde{K}_{\mathbf{G},\boldsymbol{n}}^{\mathcal{C},\boldsymbol{p}}$ is Hermitian, because the Hadamard product of Hermitian matrices is Hermitian, the matrix $\tilde{D}_{\boldsymbol{n}+\boldsymbol{p}-\boldsymbol{2}}(a)$ is Hermitian (actually, real and symmetric) for all real-valued functions $a : [0,1]^d \to \mathbb{R}$, see (12), and the matrix $T_{\boldsymbol{n}+\boldsymbol{p}-\boldsymbol{2}}(f)$ is Hermitian for all real-valued functions $f \in L^1([-\pi,\pi]^d)$, see (9). Moreover, since $\boldsymbol{n} = \boldsymbol{\nu}n$, we can write

$$n^{-2}\tilde{K}_{\mathbf{G},\boldsymbol{n}}^{\mathcal{C},\boldsymbol{p}} = \sum_{s,t=1}^{d} \nu_s \nu_t \tilde{D}_{\boldsymbol{n}+\boldsymbol{p}-\boldsymbol{2}}(\kappa_{\mathbf{G},st}) \circ T_{\boldsymbol{n}+\boldsymbol{p}-\boldsymbol{2}}((H_{\boldsymbol{p}})_{st}). \tag{81}$$

  By comparing (81) with (79), we deduce that $\{n^{-2}\tilde{K}_{\mathbf{G},\boldsymbol{n}}^{\mathcal{C},\boldsymbol{p}}\}_n \sim_\lambda f_{\mathbf{G},\boldsymbol{p}}^{\mathcal{C},\boldsymbol{\nu}}$ as a consequence of Theorem 2;
- Lemma 4 says that $\|n^{-2}\tilde{K}_{\mathbf{G},\boldsymbol{n}}^{\mathcal{C},\boldsymbol{p}}\|$, $\|n^{-2}K_{\mathbf{G},\boldsymbol{n}}^{\mathcal{C},\boldsymbol{p}}\|$ are uniformly bounded with respect to $n$ and $\|n^{-2}R_{\mathbf{G},\boldsymbol{n}}^{\mathcal{C},\boldsymbol{p}}\| \leq C/n$, where $C$ is a constant independent of $n$;
- Lemma 5 says that $\|n^{-2}K_{\mathbf{G},\boldsymbol{n}}^{\mathcal{C},\boldsymbol{p}} - n^{-2}\tilde{K}_{\mathbf{G},\boldsymbol{n}}^{\mathcal{C},\boldsymbol{p}}\|_1 = o(N(\boldsymbol{n}+\boldsymbol{p}-\boldsymbol{2}))$. By the inequality (3), the above bounds imply

$$\|n^{-2}K_{\mathbf{G},\boldsymbol{n}}^{\mathcal{C},\boldsymbol{p}} - n^{-2}\tilde{K}_{\mathbf{G},\boldsymbol{n}}^{\mathcal{C},\boldsymbol{p}} + n^{-2}R_{\mathbf{G},\boldsymbol{n}}^{\mathcal{C},\boldsymbol{p}}\|_1 = o(N(\boldsymbol{n}+\boldsymbol{p}-\boldsymbol{2})).$$

This concludes the proof. ∎

We end this section with some important remarks.

*Remark* 6. Theorems 3 and 4 are formulated in the isoparametric spirit of IgA by assuming that the geometry map $\mathbf{G}$ is expressed in terms of the same NURBS as used for the discretization. However, as can be seen from the proofs of Lemmas 1 and 4, the above theorems still hold for any geometry map $\mathbf{G}$ that is $C^1([0,1]^d)$ in the Galerkin case and $C^2([0,1]^d)$ in

the collocation case. The only requirement is that the function $W_{\boldsymbol{p}}$ defining the considered sequence of NURBS remains unchanged along the entire refinement process.

*Remark* 7. The symbol of the Galerkin matrices based on NURBS is the same as the symbol of the Galerkin matrices based on B-splines for problem (1); compare Theorem 3 with Theorem 4.1 of Reference 14 and Theorem 2.1 of Reference 15. Similarly, the symbol of the collocation matrices based on NURBS is the same as the symbol of the collocation matrices based on B-splines for problem (1); compare Theorem 4 with Equation (5.16) of Reference 12. Hence, isogeometric B-spline and NURBS discretizations are completely equivalent from the asymptotic spectral point of view. We refer the reader to Section 3 of Reference 12 and Section 5 of Reference 14 and Section 3 of Reference 15 for a study of the properties of the matrix $H_{\boldsymbol{p}}$ and the symbols (78), (79).

*Remark* 8. The structure of the symbol obtained in Theorems 3 and 4 is intrinsic to the discretization of PDEs by any local method; see Sections 1 and 4.6 of Reference 14 for further details. More precisely, the symbol incorporates

- the discretization technique, identified by a set of trigonometric polynomials in the Fourier variables $\boldsymbol{\theta} := (\theta_1, \dots, \theta_d) \in [-\pi, \pi]^d$;
- the geometry of the physical domain $\Omega$, identified by the map $\mathbf{G}$ in the parametric variables $\hat{\mathbf{x}} := (\hat{x}_1, \dots, \hat{x}_d) \in [0, 1]^d$;
- the diffusion coefficients of the PDE, identified by the matrix $K$ in the physical variables $\mathbf{x} := (x_1, \dots, x_d) \in \Omega$.

*Remark* 9. Thanks to the tensor-product structure of the discretization spaces, the symbol in the multivariate setting is obtained by a "natural tensor-product assembling" of the symbols of the univariate building-block matrices in (48) and (49). This can be seen by comparing the matrix $H_{\boldsymbol{p}}$ in (77) with the tensor-product construction of the diffusion matrix in (76) and by taking into account the results of Section 5.1. As a consequence, a deep knowledge of the properties of the univariate functions $f_p$, $g_p$, $h_p$ given in (58) to (60) is basically sufficient to understand the behavior of $f^{\mathcal{G},\boldsymbol{\nu}}_{\mathbf{G},\boldsymbol{p}}$ and $f^{\mathcal{C},\boldsymbol{\nu}}_{\mathbf{G},\boldsymbol{p}}$; we refer the reader to the related literature.[12-15,18]

*Remark* 10. The formal structure of $f^{\mathcal{C},\boldsymbol{\nu}}_{\mathbf{G},\boldsymbol{p}}$ is completely analogous to the structure of the diffusion term $-\mathbf{1}(K_{\mathbf{G}} \circ H\hat{u})\mathbf{1}^T$ associated with problem (22). The similarity is particularly clear if we equally discretize every direction, that is, if we choose $\boldsymbol{\nu} = \mathbf{1}$. In view of this similarity, the matrix $H_{\boldsymbol{p}}$ is sometimes referred to as the symbol of the negative Hessian operator, although this terminology is not rigorous from the mathematical point of view.

*Remark* 11. NURBS-based isogeometric Galerkin and collocation discretizations are equivalent from the spectral point of view. Indeed, up to a scaling depending on the Jacobian of the geometry map, the symbol $f^{\mathcal{G},\boldsymbol{\nu}}_{\mathbf{G},\boldsymbol{p}}$ of the Galerkin matrices based on $\boldsymbol{p}$-degree NURBS agrees with the symbol $f^{\mathcal{C},\boldsymbol{\nu}}_{\mathbf{G},2\boldsymbol{p}+\mathbf{1}}$ of the collocation matrices based on $(2\boldsymbol{p}+\mathbf{1})$-degree NURBS. This result is not surprising taking into account the equivalence of the corresponding univariate building-block matrices, see Remark 4.

## 6 | NUMERICAL EXAMPLES

In this section, we present a selection of one-dimensional (1D) and two-dimensional (2D) numerical examples to illustrate the effectiveness of the symbols (78) and (79) in describing the spectra of the NURBS-based Galerkin and collocation matrices. The numerical results show that there is a very good match between the eigenvalues of the normalized discretization matrices and uniformly sampled values of the symbol, also when the NURBS weights are highly nonuniform. This indicates that the symbol provides a reliable and accurate spectral description for general NURBS-based discretizations.

### 6.1 | 1D examples

Here, we focus on our model problem (1) with $d = 1$, $\alpha = \gamma = 0$, and $\Omega = (0, 1)$. The diffusion coefficient $\kappa$ and the geometry map $G$ are specified in each example. We consider univariate NURBS basis functions of the form (38) with different $p$ and $n$. According to Section 4.3, first we specify an initial weight vector $\mathbf{w}_{p,n^{(0)}}$, and then the weight vector $\mathbf{w}_{p,n}$ is constructed from $\mathbf{w}_{p,n^{(0)}}$ so that it represents the function $W_p$ in (42) in the form (39) for each $n$. In all the 1D examples we set $n^{(0)} = 1$. Therefore, the considered initial weight vectors $\mathbf{w}_{p,n^{(0)}}$ consist of $p + 1$ components; their values are specified in each example.

Since $d=1$, according to Theorem 3, the symbol of the corresponding NURBS-based Galerkin matrices has the form

$$f_{G,p}^{\mathcal{G},1}(\hat{x},\theta)=\frac{\kappa(G(\hat{x}))}{|G'(\hat{x})|}f_{2p+1}(\theta),\quad \hat{x}\in[0,1],\quad \theta\in[-\pi,\pi], \tag{82}$$

where $f_p$ is defined in (60). Similarly, Theorem 4 says that the symbol of the corresponding NURBS-based collocation matrices is given by

$$f_{G,p}^{\mathcal{C},1}(\hat{x},\theta)=\frac{\kappa(G(\hat{x}))}{(G'(\hat{x}))^2}f_p(\theta),\quad \hat{x}\in[0,1],\quad \theta\in[-\pi,\pi]. \tag{83}$$

As explained in Remark 1, the spectrum of a normalized Galerkin matrix $\frac{1}{n}A_{G,n}^{\mathcal{G},p}$ or a normalized collocation matrix $\frac{1}{n^2}A_{G,n}^{\mathcal{C},p}$ behaves approximately like a uniform sampling of these symbols. To obtain such a sampling, we select a set consisting of $m\times m$ uniformly distributed points, namely,

$$\left\{\frac{i}{m},\ i=1,\ \dots,m\right\}\times\left\{\frac{i\pi}{m},\ i=1,\ \dots,m\right\}, \tag{84}$$

where we assume for the sake of simplicity that the considered matrices are of size $m^2$. Note that it suffices to consider the interval $[0,\pi]$ for the Fourier variable $\theta$ due to the symmetry of the function $f_p$.

If $\kappa=1$ and $G(\hat{x})=\hat{x}$, then the expressions in (82) and (83) reduce to

$$f_{G,p}^{\mathcal{G},1}(\theta)=f_{2p+1}(\theta),\quad f_{G,p}^{\mathcal{C},1}(\theta)=f_p(\theta),\quad \theta\in[-\pi,\pi], \tag{85}$$

respectively. In other words, in this case, we may ignore the parametric variable $\hat{x}$, and we simply sample the symbol in a set consisting of $m$ uniformly distributed points in the Fourier variable $\theta$,

$$\left\{\frac{i\pi}{m},\ i=1,\ \dots,m\right\}, \tag{86}$$

where $m$ is the size of the considered matrices.

**Example 2** (Constant diffusion coefficient and identity geometry map). We consider $\kappa=1$ and $G(\hat{x})=\hat{x}$; this means that the symbols are given by (85). In this example, we aim to show the (minimal) effect of the weights on the eigenvalues of the NURBS-based Galerkin and collocation matrices. Taking into account Remark 6, we apply Theorems 3 and 4 in their full generality, so that the geometry map is not required to be in the NURBS span as in (42). This gives us more flexibility in playing with the choices of the weights. We compare the eigenvalues of a normalized Galerkin matrix $\frac{1}{n}A_{G,n}^{\mathcal{G},p}$ and a normalized collocation matrix $\frac{1}{n^2}A_{G,n}^{\mathcal{C},p}$ with the samples of $f_{2p+1}$ and $f_p$, respectively, over the uniform grid (86) with $m=n+p-2$. To make a fair comparison, both the eigenvalues and the symbol values are sorted.

We first consider the NURBS-based Galerkin discretization. The eigenvalues of $\frac{1}{n}A_{G,n}^{\mathcal{G},p}$ and the samples of $f_{2p+1}$ are depicted in Figure 2 for the values $p=2,3$ and $m=25,75$ ($n=m-p+2$), and the initial weight vectors

$$\mathbf{w}_{2,1}=\left(1,\frac{\sqrt{2}}{2},1\right),\quad \mathbf{w}_{3,1}=\left(1,\frac{\sqrt{2}}{2},\frac{\sqrt{2}}{2},1\right),$$

and

$$\mathbf{w}_{2,1}=\left(1,20,\frac{1}{20}\right),\quad \mathbf{w}_{3,1}=\left(1,20,\frac{1}{20},1\right).$$

For the sake of comparison, we also depict each time the (sorted) eigenvalues obtained with a standard B-spline discretization of the same degree, which is a special NURBS case using the weights $\mathbf{w}_{p,1}=(1,1,\dots,1)$. Although we are presenting an asymptotic theory, the matching between the symbol samples and the computed eigenvalues is almost perfect (up to few outliers) even for very low dimension ($m=25$).

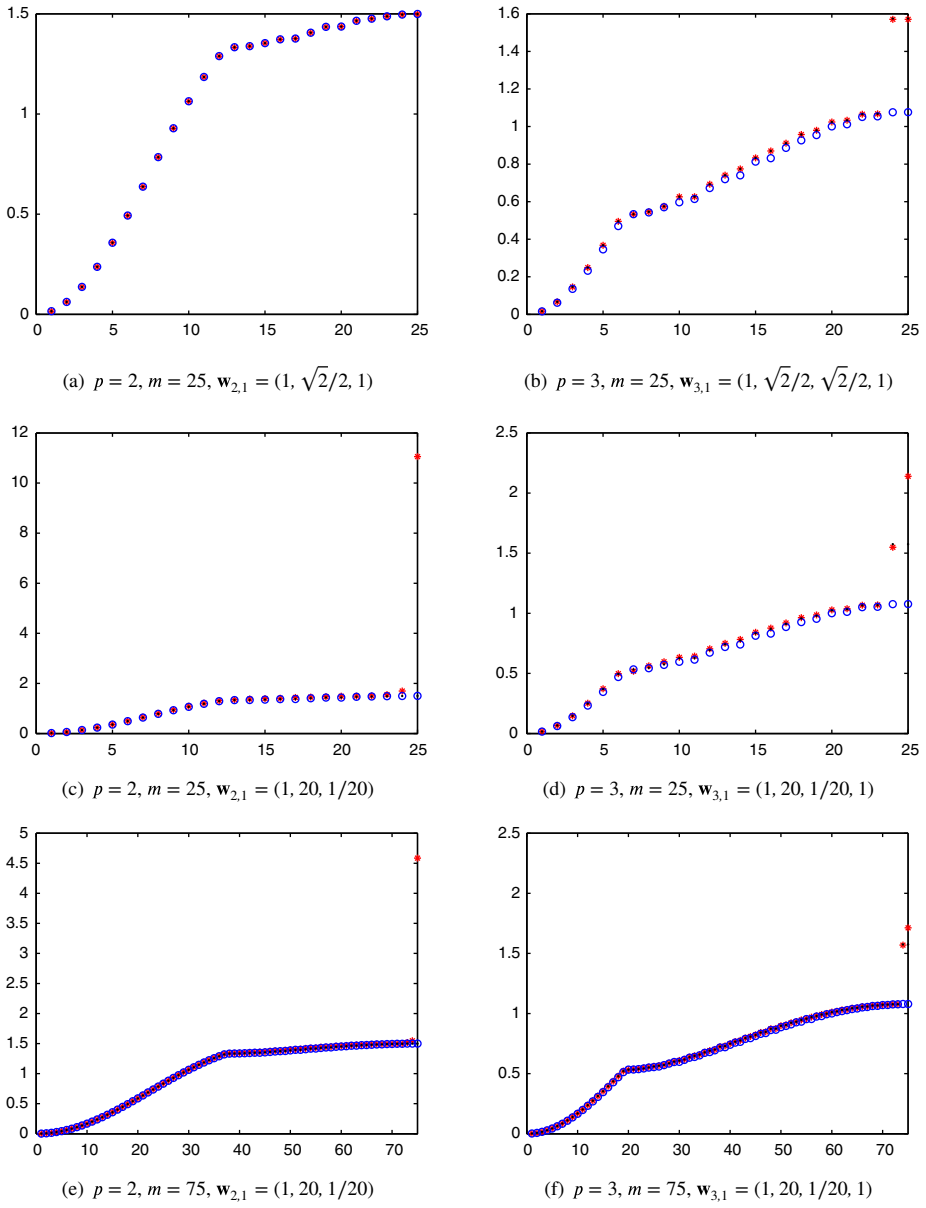

(a) $p = 2$, $m = 25$, $\mathbf{w}_{2,1} = (1, \sqrt{2}/2, 1)$

(b) $p = 3$, $m = 25$, $\mathbf{w}_{3,1} = (1, \sqrt{2}/2, \sqrt{2}/2, 1)$

(c) $p = 2$, $m = 25$, $\mathbf{w}_{2,1} = (1, 20, 1/20)$

(d) $p = 3$, $m = 25$, $\mathbf{w}_{3,1} = (1, 20, 1/20, 1)$

(e) $p = 2$, $m = 75$, $\mathbf{w}_{2,1} = (1, 20, 1/20)$

(f) $p = 3$, $m = 75$, $\mathbf{w}_{3,1} = (1, 20, 1/20, 1)$

**FIGURE 2** (Example 2: Constant diffusion coefficient, identity geometry map, and Galerkin discretization). Samples of the symbol $f_{2p+1}$ over the uniform grid (86) (blue circles) are compared with the eigenvalues of $\frac{1}{n}A_{G,n}^{\mathcal{G},p}$ in the NURBS case (red stars) and in the B-spline case (black dots) with $n = m - p + 2$

The results in case of NURBS-based collocation are similar. Figure 3 shows the samples of $f_p$ and the eigenvalues of the normalized collocation matrices $\frac{1}{n^2}A_{G,n}^{C,p}$, for the same values of $p$, $m$, and $\mathbf{w}_{p,1}$ as above. The (sorted) eigenvalues in the B-spline case are also shown. Even though the collocation matrices are not symmetric, the eigenvalues are all real in this example. In general, however, this is not always the case, but from the theory we may expect that the imaginary part of the eigenvalues is not relevant for large enough $n$ since the symbol is real.

*Remark* 12. From the previous example, we observe that the number of outliers is basically the same for general NURBS as for B-splines. We refer the reader to the related B-spline literature[11,12,14] for other examples and comments about their dependence on the salient parameters of the discretization.

**Example 3** (Variable diffusion coefficient and NURBS geometry map). We now consider $\kappa(x) = e^{x-1}$ and the geometry map

$$G(\hat{x}) = \frac{10\hat{x}(1-\hat{x}) + 100\hat{x}^2}{(1-\hat{x})^2 + 20\hat{x}(1-\hat{x}) + 100\hat{x}^2}, \quad \hat{x} \in [0,1], \tag{87}$$

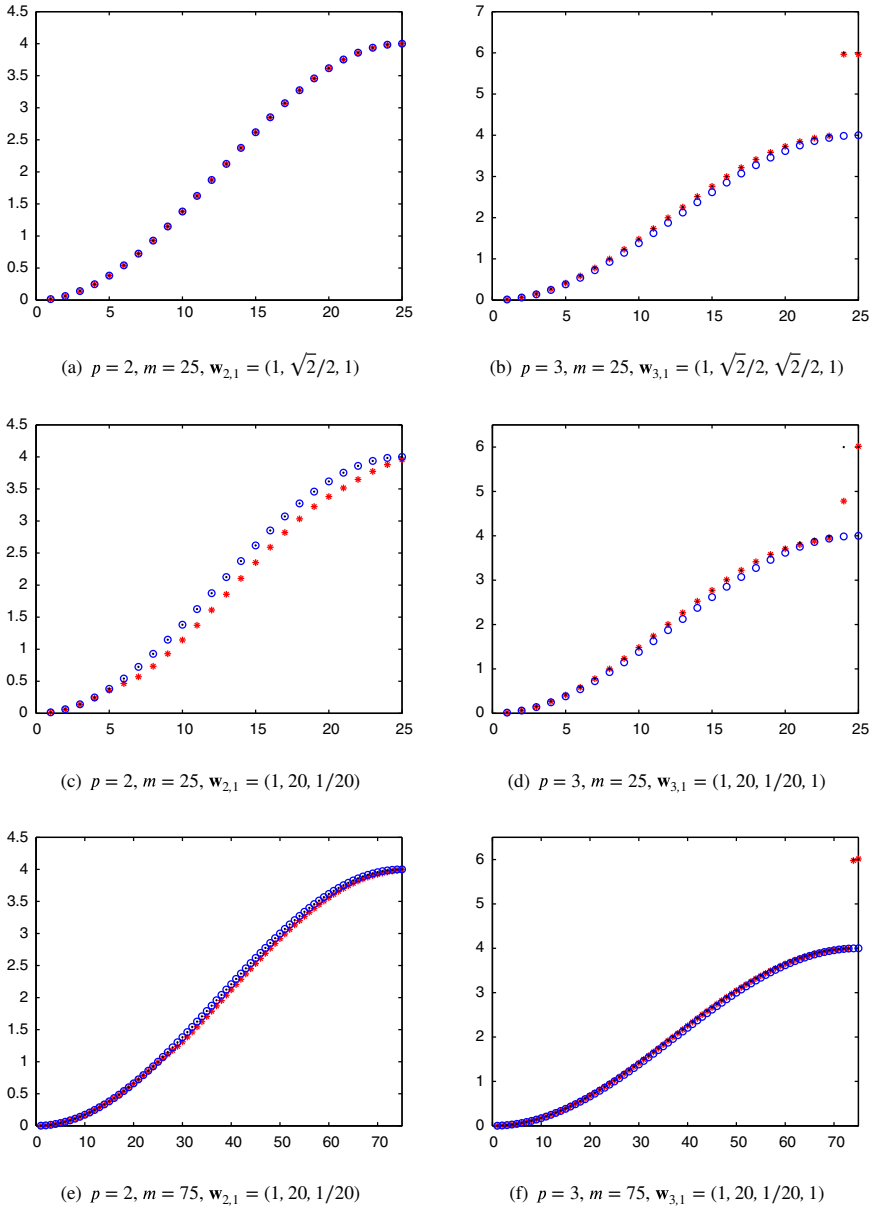

(a) $p = 2$, $m = 25$, $\mathbf{w}_{2,1} = (1, \sqrt{2}/2, 1)$

(b) $p = 3$, $m = 25$, $\mathbf{w}_{3,1} = (1, \sqrt{2}/2, \sqrt{2}/2, 1)$

(c) $p = 2$, $m = 25$, $\mathbf{w}_{2,1} = (1, 20, 1/20)$

(d) $p = 3$, $m = 25$, $\mathbf{w}_{3,1} = (1, 20, 1/20, 1)$

(e) $p = 2$, $m = 75$, $\mathbf{w}_{2,1} = (1, 20, 1/20)$

(f) $p = 3$, $m = 75$, $\mathbf{w}_{3,1} = (1, 20, 1/20, 1)$

**FIGURE 3** (Example 2: Constant diffusion coefficient, identity geometry map, and collocation discretization). Samples of the symbol $f_p$ over the uniform grid (86) (blue circles) are compared with the eigenvalues of $\frac{1}{n^2}A^{C,p}_{G,n}$ in the NURBS case (red stars) and in the B-spline case (black dots) with $n = m - p + 2$

whose graph is depicted in Figure 4. This map can be written in NURBS form (42), with the weights and control points given in Table 1 for $p = 2,3$ and $n^{(0)} = 1$. We compare the eigenvalues of a normalized Galerkin matrix $\frac{1}{n}A^{G,p}_{G,n}$ and a normalized collocation matrix $\frac{1}{n^2}A^{C,p}_{G,n}$ with the samples of the symbols $f^{G,1}_{G,p}$ and $f^{C,1}_{G,p}$ in (82) and (83), respectively, over the uniform tensor-product grid (84) with $m^2 = n + p - 2$. To make a fair comparison, both the eigenvalues and the symbol values are sorted. In addition to a plot of both sets of sorted values, we also show a bivariate plot taking into account the positional information of the symbol samples.

We first consider the NURBS-based Galerkin discretization. The eigenvalues of $\frac{1}{n}A^{G,p}_{G,n}$ and the sampled values of $f^{G,1}_{G,p}$ are depicted in Figure 5 for the values $p = 2,3$ and $m = 15$ ($n = 227 - p$). As explained before, the initial weight vector $\mathbf{w}_{p,1}$ used to build the NURBS basis functions in (38) is specified by the geometry map (see Table 1), so

$$\mathbf{w}_{2,1} = \left(\frac{1}{10}, 1, 10\right), \quad \mathbf{w}_{3,1} = \left(\frac{1}{10}, \frac{7}{10}, 4, 10\right).$$

The results in case of NURBS-based collocation are similar. Figure 6 shows the sampled values of $f^{C,1}_{G,p}$ and the eigenvalues of the corresponding normalized collocation matrices $\frac{1}{n^2}A^{C,p}_{G,n}$ for the same values of $p$, $m$, and $\mathbf{w}_{p,1}$. Just like in the previous example, the eigenvalues are all real.

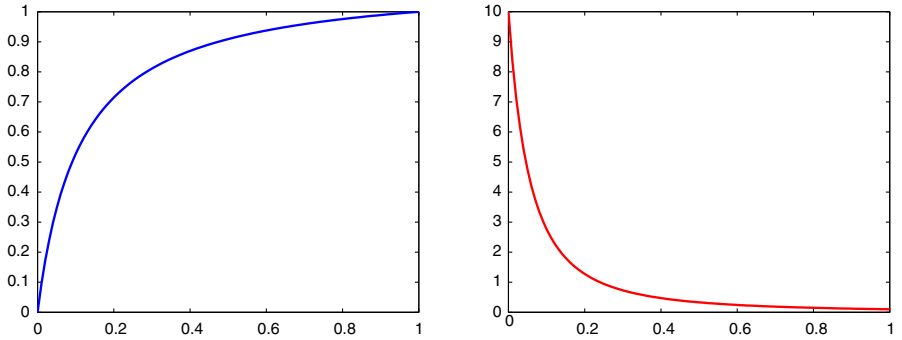


(a) geometry map (b) first derivative

**FIGURE 4** (Example 3). Graph of the geometry map in (87) and its first derivative

**TABLE 1** (Example 3). Weights and control points of the geometry function in (87), expressed in the form (42) with $p=2,3$ and $n^{(0)}=1$

| | $p=2$ | | $p=3$ | |
|---|---|---|---|---|
| $i$ | $w_{i,2,1}$ | $P_{i,2,1}$ | $w_{i,3,1}$ | $P_{i,3,1}$ |
| 1 | 1/10 | 0 | 1/10 | 0 |
| 2 | 1 | 1/2 | 7/10 | 10/21 |
| 3 | 10 | 1 | 4 | 11/12 |
| 4 | – | – | 10 | 1 |

## 6.2 | 2D examples

We now focus on our model problem (1) with $d=2$, $\boldsymbol{\alpha}=\mathbf{0}$, $\gamma=0$, and $K=I$. For a given geometry map $\mathbf{G}$, the symbols of the normalized NURBS-based Galerkin and collocation matrices are specified in (78) and (79), respectively. According to (18), in this case we have

$$K_{\mathbf{G}} = (J_{\mathbf{G}})^{-1}(J_{\mathbf{G}})^{-T}, \tag{88}$$

and according to (77),

$$H_{\boldsymbol{p}}(\theta_1,\theta_2) = \begin{bmatrix} f_{p_1}(\theta_1)h_{p_2}(\theta_2) & g_{p_1}(\theta_1)g_{p_2}(\theta_2) \\ g_{p_1}(\theta_1)g_{p_2}(\theta_2) & h_{p_1}(\theta_1)f_{p_2}(\theta_2) \end{bmatrix}. \tag{89}$$

Whenever the geometry map is conformal (that is, it preserves the angles), the matrix (88) is diagonal and then the symbols (78) and (79) only depend on the diagonal entries of the matrix (89).

From Remark 1, we know that the spectrum of a normalized Galerkin matrix $A^{\mathcal{G},\boldsymbol{p}}_{\mathbf{G},\boldsymbol{n}}$ or a normalized collocation matrix $\frac{1}{n^2}A^{\mathcal{C},\boldsymbol{p}}_{\mathbf{G},\boldsymbol{n}}$ behaves approximately like a uniform sampling of these symbols. To obtain such a sampling, we select a set consisting of $m^4$ uniformly distributed points, namely,

$$\left\{\left(\frac{i}{m},\frac{j}{m}\right),\ i,j=1,\ \dots\ ,m\right\}\times\left\{\left(\frac{i\pi}{m},\frac{j\pi}{m}\right),\ i,j=1,\ \dots\ ,m\right\}, \tag{90}$$

where we assume for the sake of simplicity that the considered matrices are of size $m^4$. Note that, under the condition that the matrix (88) is diagonal, it suffices to consider the interval $[0,\pi]$ for the Fourier variables $\theta_1,\theta_2$ due to the symmetry of the diagonal entries of the matrix (89).

**Example 4** (Poisson problem on a quarter of annulus). We consider the 2D Poisson problem, with homogeneous Dirichlet boundary conditions, on the quarter of annulus depicted in Figure 7. This domain can be exactly described by a geometry map $\mathbf{G}$ represented in terms of NURBS of at least bidegree $\boldsymbol{p}^{(0)}=(1,2)$ and $\boldsymbol{n}^{(0)}=(1,1)$. In this case, the

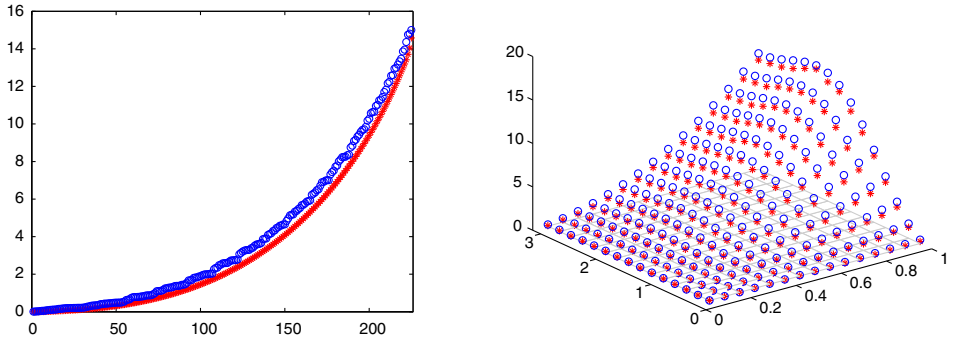

(a) $p = 2$, $m = 15$, $\mathbf{w}_{2,1} = (1/10, 1, 10)$

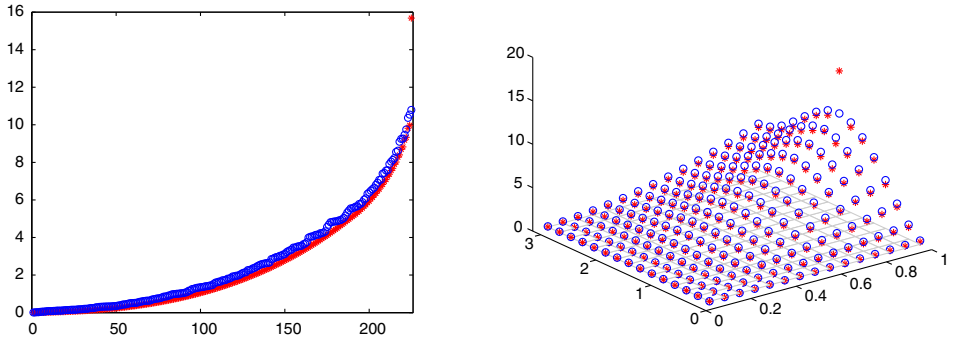

(b) $p = 3$, $m = 15$, $\mathbf{w}_{3,1} = (1/10, 7/10, 4, 10)$

**FIGURE 5** (Example 3: Variable diffusion coefficient, NURBS geometry map, and Galerkin discretization). Samples of the symbol $f^{\mathcal{G},1}_{G,p}$ over the uniform tensor-product grid in (84) (blue circles) are compared with the eigenvalues of $\frac{1}{n}A^{\mathcal{G},p}_{G,n}$ (red stars) with $n = m^2 - p + 2$. Left: sorted values of the eigenvalues and symbol samples. Right: bivariate plot on the grid (84)

tensor-product knot sequence is $\{0,0,1,1\} \times \{0,0,0,1,1,1\}$ and

$$\mathbf{G}(\hat{x}_1, \hat{x}_2) = \sum_{\boldsymbol{i}=(1,1)}^{(2,3)} \mathbf{P}_{\boldsymbol{i},\boldsymbol{p}^{(0)},\boldsymbol{n}^{(0)}} \frac{w_{\boldsymbol{i},\boldsymbol{p}^{(0)},\boldsymbol{n}^{(0)}} N_{\boldsymbol{i},\boldsymbol{p}^{(0)},\boldsymbol{n}^{(0)}}(\hat{x}_1, \hat{x}_2)}{W_{\boldsymbol{p}^{(0)},\boldsymbol{n}^{(0)}}(\hat{x}_1, \hat{x}_2)}, \tag{91}$$

where

$$\begin{aligned} &\mathbf{P}_{(1,1),\boldsymbol{p}^{(0)},\boldsymbol{n}^{(0)}} = (1,0)^T, \quad \mathbf{P}_{(1,2),\boldsymbol{p}^{(0)},\boldsymbol{n}^{(0)}} = (1,1)^T, \quad \mathbf{P}_{(1,3),\boldsymbol{p}^{(0)},\boldsymbol{n}^{(0)}} = (0,1)^T, \\ &\mathbf{P}_{(2,1),\boldsymbol{p}^{(0)},\boldsymbol{n}^{(0)}} = (4,0)^T, \quad \mathbf{P}_{(2,2),\boldsymbol{p}^{(0)},\boldsymbol{n}^{(0)}} = (4,4)^T, \quad \mathbf{P}_{(2,3),\boldsymbol{p}^{(0)},\boldsymbol{n}^{(0)}} = (0,4)^T, \end{aligned}$$

and

$$w_{(i,1),\boldsymbol{p}^{(0)},\boldsymbol{n}^{(0)}} = 1, \quad w_{(i,2),\boldsymbol{p}^{(0)},\boldsymbol{n}^{(0)}} = \frac{\sqrt{2}}{2}, \quad w_{(i,3),\boldsymbol{p}^{(0)},\boldsymbol{n}^{(0)}} = 1, \quad i = 1,2, \tag{92}$$

see also Example 1. Note that the above geometry map is conformal (see Figure 7), so that the matrix (88) is diagonal.

We investigate the symbols of NURBS discretizations with $\boldsymbol{\nu} = (1,1)$ and $\boldsymbol{p} = (p,p)$ for $p \geq 2$, as per Section 4.3. In particular, we compare (the modulus of) the eigenvalues of a normalized Galerkin matrix $A^{\mathcal{G},\boldsymbol{p}}_{\mathbf{G},\boldsymbol{n}}$ and a normalized collocation matrix $\frac{1}{n^2}A^{C,\boldsymbol{p}}_{\mathbf{G},\boldsymbol{n}}$ with the samples of the functions in (78) and (79), respectively, over the uniform tensor-product grid (90) with $m^2 = n + p - 2$. To make a fair comparison, both the eigenvalues and the symbol values are sorted. The weights in (38) are obtained from the expressions in (92) by using degree elevation and knot insertion, in order to maintain the exact representation of the considered geometry map.

We first consider the NURBS-based Galerkin discretization. The eigenvalues of $A^{\mathcal{G},\boldsymbol{p}}_{\mathbf{G},\boldsymbol{n}}$ and the sampled values of $f^{\mathcal{G},(1,1)}_{\mathbf{G},\boldsymbol{p}}$ are depicted in Figure 8 (top) for the values $p = 2,3$ and $m = 10$ ($n = 102 - p$). The results in case of NURBS-based collocation are similar. Figure 8 (bottom) shows the sampled values of $f^{C,(1,1)}_{\mathbf{G},\boldsymbol{p}}$ and the modulus of the eigenvalues of the corresponding normalized collocation matrices $\frac{1}{n^2}A^{C,\boldsymbol{p}}_{\mathbf{G},\boldsymbol{n}}$ for the same values of $p$ and $m$. The nonreal eigenvalues can be

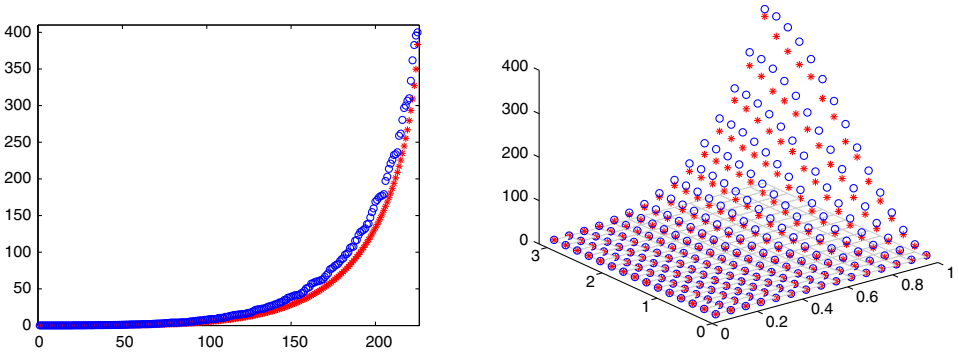

(a) $p = 2$, $m = 15$, $\mathbf{w}_{2,1} = (1/10, 1, 10)$

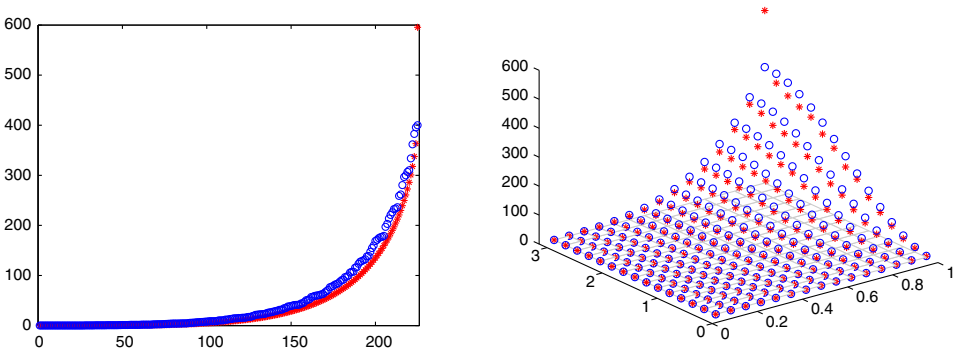

(b) $p = 3$, $m = 15$, $\mathbf{w}_{3,1} = (1/10, 7/10, 4, 10)$

**FIGURE 6** (Example 3: Variable diffusion coefficient, NURBS geometry map, and collocation discretization). Samples of the symbol $f_{G,p}^{C,1}$ over the uniform tensor-product grid in (84) (blue circles) are compared with the eigenvalues of $\frac{1}{n^2}A_{G,n}^{C,p}$ (red stars) with $n = m^2 - p + 2$. Left: sorted values of the eigenvalues and symbol samples. Right: bivariate plot on the grid (84)

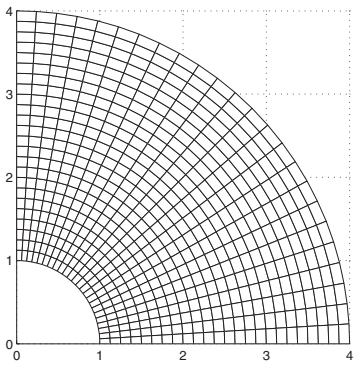

**FIGURE 7** (Example 4). Physical domain with coordinate lines obtained by the geometry map (91)

classified as outliers: their number is 52 and 62 for $p = 2,3$, respectively, so very small compared with the total dimension ($10^4$) of the corresponding NURBS matrices.

## 7 | CONCLUSION

In this article, we have analyzed the spectral properties of (sequences of) matrices arising from NURBS-based isogeometric Galerkin and collocation methods for second-order elliptic PDEs in their full generality: multivariate setting, variable coefficients, and nontrivial geometry map. The spectral analysis completes the already known analysis for isogeometric Galerkin and collocation methods based on B-splines. More precisely, we have shown that an asymptotic spectral distribution exists in both the Galerkin and collocation NURBS case, and it is compactly described by a spectral symbol whose main properties can be summarized as follows:

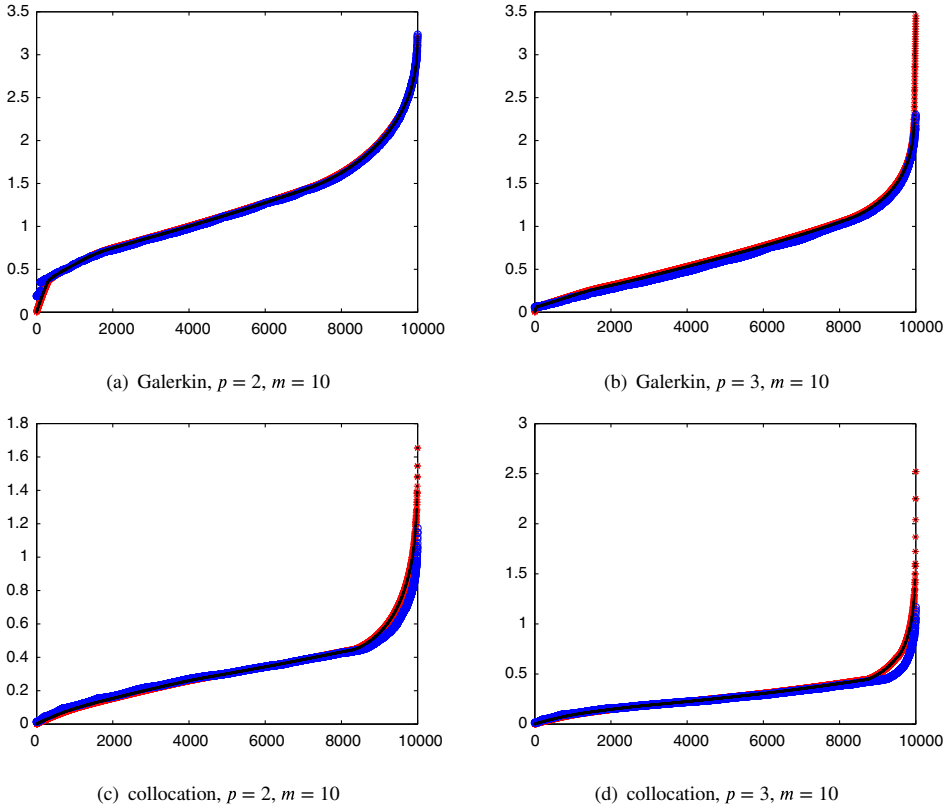

(a) Galerkin, $p = 2$, $m = 10$

(b) Galerkin, $p = 3$, $m = 10$

(c) collocation, $p = 2$, $m = 10$

(d) collocation, $p = 3$, $m = 10$

**FIGURE 8** (Example 4: Poisson problem on a quarter of annulus). Top: samples of the Galerkin symbol $f_{\mathbf{G},\boldsymbol{p}}^{\mathcal{G},(1,1)}$ over the uniform grid (90) (blue circles) are compared with the eigenvalues of $A_{\mathbf{G},\boldsymbol{n}}^{\mathcal{G},\boldsymbol{p}}$ in the NURBS case (red stars) and in the B-spline case (black dots). Bottom: samples of the collocation symbol $f_{\mathbf{G},\boldsymbol{p}}^{C,(1,1)}$ over the uniform grid (90) (blue circles) are compared with the modulus of the eigenvalues of $\frac{1}{n^2}A_{\mathbf{G},\boldsymbol{n}}^{C,\boldsymbol{p}}$ in the NURBS case (red stars) and in the B-spline case (black dots). In all cases, $m = 10$ and $n = m^2 - p + 2$

- the symbol depends on the discretization technique, on the geometry of the physical domain, and on the diffusion coefficients of the PDE;
- the formal structure of the symbol is completely analogous to the structure of the diffusion term of the PDE;
- the symbol in the multivariate setting is obtained by means of a "natural tensor-product assembling" of the symbols of certain univariate building-block matrices;
- up to a scaling depending on the Jacobian of the geometry map, the symbol of the Galerkin matrices based on $\boldsymbol{p}$-degree NURBS is equivalent to the symbol of the collocation matrices based on $(2\boldsymbol{p}+\mathbf{1})$-degree NURBS;
- the NURBS symbol is the same as the symbol derived for B-spline discretizations of the same problem, both in the Galerkin and collocation case.

The knowledge of the NURBS symbol and its properties suggests several interesting consequences:

- the same symbol-based fast solvers developed for B-spline discretizations[5,17,18] may be also successfully applied in the context of NURBS discretizations;
- it may further help to understand and explain the numerically observed excellent behavior of isogeometric methods to approximate the spectrum of the underlying continuous differential operators.[4,11]

## ACKNOWLEDGEMENTS

C.G., C.M., and H.S. are partially supported by the Beyond Borders Program of the University of Rome Tor Vergata through the project ASTRID (CUP E84I19002250005) and by the MIUR Excellence Department Project awarded to the Department of Mathematics, University of Rome Tor Vergata (CUP E83C18000100006). S.S.-C. is partially supported by Donation KAW 2013.0341 from the Knut & Alice Wallenberg Foundation in collaboration with the Royal Swedish Academy of Sciences. All the authors are members of the INdAM Research group GNCS (Istituto Nazionale di Alta Matematica—Gruppo Nazionale per il Calcolo Scientifico).

## CONFLICT OF INTEREST

This work does not have any conflicts of interest.

## ORCID

*Carlo Garoni* http://orcid.org/0000-0001-9720-092X
*Carla Manni* https://orcid.org/0000-0002-1519-4106
*Stefano Serra-Capizzano* http://orcid.org/0000-0001-9477-109X
*Hendrik Speleers* https://orcid.org/0000-0003-4110-3308

## REFERENCES

1. Cottrell JA, Hughes TJR, Bazilevs Y. Isogeometric analysis: Toward integration of CAD and FEA. Chichester, England: John Wiley & Sons, 2009.
2. Hughes TJR, Cottrell JA, Bazilevs Y. Isogeometric analysis: CAD, finite elements, NURBS, exact geometry and mesh refinement. Comput Methods Appl Mech Eng. 2005;194:4135–4195.
3. Beirão da Veiga L, Buffa A, Sangalli G, Vázquez R. Mathematical analysis of variational isogeometric methods. Acta Numer. 2014;23:157–287.
4. Hughes TJR, Evans JA, Reali A. Finite element and NURBS approximations of eigenvalue, boundary-value, and initial-value problems. Comput Methods Appl Mech Eng. 2014;272:290–320.
5. Donatelli M, Garoni C, Manni C, Serra-Capizzano S, Speleers H. Robust and optimal multi-iterative techniques for IgA Galerkin linear systems. Comput Methods Appl Mech Eng. 2015;284:230–264.
6. Hofreither C, Takacs S. Robust multigrid for isogeometric analysis based on stable splittings of spline spaces. SIAM J Numer Anal. 2017;55:2004–2024.
7. Beckermann B, Kuijlaars ABJ. Superlinear convergence of conjugate gradients. SIAM J Numer Anal. 2001;39:300–329.
8. Kuijlaars ABJ. Convergence analysis of Krylov subspace iterations with methods from potential theory. SIAM Rev. 2006;48:3–40.
9. Aricó A, Donatelli M, Serra-Capizzano S. V-cycle optimal convergence for certain (multilevel) structured linear systems. SIAM J Matrix Anal Appl. 2004;26:186–214.
10. Serra-Capizzano S. The rate of convergence of Toeplitz based PCG methods for second order nonlinear boundary value problems. Numer Math. 1999;81:461–495.
11. Garoni C, Speleers H, Ekström S-E, Reali A, Serra-Capizano S, Hughes TJR. Symbol-based analysis of finite element and isogeometric B-spline discretizations of eigenvalue problems: Exposition and review, Arch Comput Methods Eng. 2019;26:1639–1690.
12. Donatelli M, Garoni C, Manni C, Serra-Capizzano S, Speleers H. Spectral analysis and spectral symbol of matrices in isogeometric collocation methods. Math Comp. 2016;85:1639–1680.
13. Garoni C, Manni C, Pelosi F, Serra-Capizzano S, Speleers H. On the spectrum of stiffness matrices arising from isogeometric analysis. Numer Math. 2014;127:751–799.
14. Garoni C, Manni C, Serra-Capizzano S, Sesana D, Speleers H. Spectral analysis and spectral symbol of matrices in isogeometric Galerkin methods. Math Comp. 2017;86:1343–1373.
15. Garoni C, Manni C, Serra-Capizzano S, Sesana D, Speleers H. Lusin theorem, GLT sequences and matrix computations: An application to the spectral analysis of PDE discretization matrices. J Math Anal Appl. 2017;446:365–382.
16. Garoni C, Serra-Capizzano S. Generalized locally Toeplitz sequences: Theory and applications. Vol II. Cham: Springer International Publishing, 2018.
17. Donatelli M, Garoni C, Manni C, Serra-Capizzano S, Speleers H. Robust and optimal multi-iterative techniques for IgA collocation linear systems. Comput Methods Appl Mech Eng. 2015;284:1120–1146.
18. Donatelli M, Garoni C, Manni C, Serra-Capizzano S, Speleers H. Symbol-based multigrid methods for Galerkin B-spline isogeometric analysis. SIAM J Numer Anal. 2017;55:31–62.
19. Beirão da Veiga L, Cho D, Pavarino L, Scacchi S. Overlapping Schwarz methods for isogeometric analysis. SIAM J Numer Anal. 2012;50:1394–1416.
20. Buffa A, Harbrecht H, Kunoth A, Sangalli G. BPX-preconditioning for isogeometric analysis. Comput Methods Appl Mech Eng. 2013;265:63–70.
21. Sangalli G, Tani M. Isogeometric preconditioners based on fast solvers for the Sylvester equation. SIAM J Sci Comput. 2016;38:A3644–A3671.
22. Hofreither C, Takacs S, Zulehner W. A robust multigrid method for isogeometric analysis in two dimensions using boundary correction. Comput Methods Appl Mech Eng. 2017;316:22–42.
23. Serra-Capizzano S, Tilli P. On unitarily invariant norms of matrix-valued linear positive operators. J Inequal Appl. 2002;7:309–330.

24. Golinskii L, Serra-Capizzano S. The asymptotic properties of the spectrum of nonsymmetrically perturbed Jacobi matrix sequences. J Approx Theory. 2007;144:84–102.
25. Auricchio F, Beirão da Veiga L, Hughes TJR, Reali A, Sangalli G. Isogeometric collocation methods. Math Models Methods Appl Sci. 2010;20:2075–2107.
26. de Boor C. A practical guide to splines. Revised ed. New York, NY: Springer-Verlag, 2001.
27. Lyche T, Manni C, Speleers H. Foundations of spline theory: B-splines, spline approximation, and hierarchical refinement. In: Lyche T, Manni C & Speleers H (eds), Splines and PDEs: From approximation theory to numerical linear algebra. Lecture Notes in Mathematics, 2219, pp. 1–76, New York, NY: Springer International Publishing, 2018.
28. Piegl L, Tiller W. The NURBS book. 2nd ed. Berlin, Germany: Springer-Verlag, 1997.

**How to cite this article:** Garoni C, Manni C, Serra-Capizzano S, Speleers H. NURBS in isogeometric discretization methods: A spectral analysis. *Numer Linear Algebra Appl*. 2020;e2318.
https://doi.org/10.1002/nla.2318

## APPENDIX A. LEMMAS FOR THE PROOF OF THEOREM 3

This appendix collects the technical results used in the proof of Theorem 3. Throughout the appendix, the symbol $C$ stands for a generic constant independent of $n$. We start by noting that the matrix $R_{\mathbf{G},\boldsymbol{n}}^{\mathcal{G},\boldsymbol{p}}$ in (68) has the following expression:

$$\begin{aligned}
R_{\mathbf{G},\boldsymbol{n}}^{\mathcal{G},\boldsymbol{p}} = \Bigg[ & -\sum_{s,t=1}^{d} \int_{[0,1]^d} |\det(J_{\mathbf{G}})|\, \kappa_{\mathbf{G},st}\, \frac{w_{\boldsymbol{j}+\mathbf{1},\boldsymbol{p},\boldsymbol{n}}}{W_{\boldsymbol{p}}}\, \frac{w_{\boldsymbol{i}+\mathbf{1},\boldsymbol{p},\boldsymbol{n}}}{W_{\boldsymbol{p}}^2}\, \frac{\partial W_{\boldsymbol{p}}}{\partial \hat{x}_t}\, \frac{\partial N_{\boldsymbol{j}+\mathbf{1},\boldsymbol{p},\boldsymbol{n}}}{\partial \hat{x}_s}\, N_{\boldsymbol{i}+\mathbf{1},\boldsymbol{p},\boldsymbol{n}} \\
& - \sum_{s,t=1}^{d} \int_{[0,1]^d} |\det(J_{\mathbf{G}})|\, \kappa_{\mathbf{G},st}\, \frac{w_{\boldsymbol{j}+\mathbf{1},\boldsymbol{p},\boldsymbol{n}}}{W_{\boldsymbol{p}}^2}\, \frac{w_{\boldsymbol{i}+\mathbf{1},\boldsymbol{p},\boldsymbol{n}}}{W_{\boldsymbol{p}}}\, \frac{\partial W_{\boldsymbol{p}}}{\partial \hat{x}_s}\, N_{\boldsymbol{j}+\mathbf{1},\boldsymbol{p},\boldsymbol{n}}\, \frac{\partial N_{\boldsymbol{i}+\mathbf{1},\boldsymbol{p},\boldsymbol{n}}}{\partial \hat{x}_t} \\
& + \sum_{s,t=1}^{d} \int_{[0,1]^d} |\det(J_{\mathbf{G}})|\, \kappa_{\mathbf{G},st}\, \frac{w_{\boldsymbol{j}+\mathbf{1},\boldsymbol{p},\boldsymbol{n}}}{W_{\boldsymbol{p}}^2}\, \frac{w_{\boldsymbol{i}+\mathbf{1},\boldsymbol{p},\boldsymbol{n}}}{W_{\boldsymbol{p}}^2}\, \frac{\partial W_{\boldsymbol{p}}}{\partial \hat{x}_s}\, \frac{\partial W_{\boldsymbol{p}}}{\partial \hat{x}_t}\, N_{\boldsymbol{j}+\mathbf{1},\boldsymbol{p},\boldsymbol{n}}\, N_{\boldsymbol{i}+\mathbf{1},\boldsymbol{p},\boldsymbol{n}} \\
& + \sum_{s=1}^{d} \int_{[0,1]^d} |\det(J_{\mathbf{G}})|\, \alpha_{\mathbf{G},s}\, \frac{w_{\boldsymbol{j}+\mathbf{1},\boldsymbol{p},\boldsymbol{n}}}{W_{\boldsymbol{p}}}\, \frac{w_{\boldsymbol{i}+\mathbf{1},\boldsymbol{p},\boldsymbol{n}}}{W_{\boldsymbol{p}}}\, \frac{\partial N_{\boldsymbol{j}+\mathbf{1},\boldsymbol{p},\boldsymbol{n}}}{\partial \hat{x}_s}\, N_{\boldsymbol{i}+\mathbf{1},\boldsymbol{p},\boldsymbol{n}} \\
& - \sum_{s=1}^{d} \int_{[0,1]^d} |\det(J_{\mathbf{G}})|\, \alpha_{\mathbf{G},s}\, \frac{w_{\boldsymbol{j}+\mathbf{1},\boldsymbol{p},\boldsymbol{n}}}{W_{\boldsymbol{p}}^2}\, \frac{w_{\boldsymbol{i}+\mathbf{1},\boldsymbol{p},\boldsymbol{n}}}{W_{\boldsymbol{p}}}\, \frac{\partial W_{\boldsymbol{p}}}{\partial \hat{x}_s}\, N_{\boldsymbol{j}+\mathbf{1},\boldsymbol{p},\boldsymbol{n}}\, N_{\boldsymbol{i}+\mathbf{1},\boldsymbol{p},\boldsymbol{n}} \\
& + \int_{[0,1]^d} |\det(J_{\mathbf{G}})|\, \gamma_{\mathbf{G}}\, \frac{w_{\boldsymbol{j}+\mathbf{1},\boldsymbol{p},\boldsymbol{n}}}{W_{\boldsymbol{p}}}\, \frac{w_{\boldsymbol{i}+\mathbf{1},\boldsymbol{p},\boldsymbol{n}}}{W_{\boldsymbol{p}}}\, N_{\boldsymbol{j}+\mathbf{1},\boldsymbol{p},\boldsymbol{n}}\, N_{\boldsymbol{i}+\mathbf{1},\boldsymbol{p},\boldsymbol{n}} \Bigg]_{\boldsymbol{i},\boldsymbol{j}=\mathbf{1}}^{\boldsymbol{n}+\boldsymbol{p}-\mathbf{2}}.
\end{aligned} \tag{A1}$$

**Lemma 1.** *Let $\hat{K}_{\mathbf{G},\boldsymbol{n}}^{\mathcal{G},\boldsymbol{p}}$, $K_{\mathbf{G},\boldsymbol{n}}^{\mathcal{G},\boldsymbol{p}}$, and $R_{\mathbf{G},\boldsymbol{n}}^{\mathcal{G},\boldsymbol{p}}$ be given as in (70), (69), and (A1), respectively. Under the assumptions of Theorem 3,*

- *$\|n^{d-2}\hat{K}_{\mathbf{G},\boldsymbol{n}}^{\mathcal{G},\boldsymbol{p}}\|$, $\|n^{d-2}K_{\mathbf{G},\boldsymbol{n}}^{\mathcal{G},\boldsymbol{p}}\|$ are uniformly bounded with respect to $n$;*
- *$\|n^{d-2}R_{\mathbf{G},\boldsymbol{n}}^{\mathcal{G},\boldsymbol{p}}\| \le C/n$.*

*Proof.* It suffices to prove that:

(a) the number of nonzero entries in each row and column of $\hat{K}_{\mathbf{G},\boldsymbol{n}}^{\mathcal{G},\boldsymbol{p}}$, $K_{\mathbf{G},\boldsymbol{n}}^{\mathcal{G},\boldsymbol{p}}$, $R_{\mathbf{G},\boldsymbol{n}}^{\mathcal{G},\boldsymbol{p}}$ is bounded by $C$;
(b) the modulus of each entry of $\hat{K}_{\mathbf{G},\boldsymbol{n}}^{\mathcal{G},\boldsymbol{p}}$, $K_{\mathbf{G},\boldsymbol{n}}^{\mathcal{G},\boldsymbol{p}}$ is bounded by $Cn^{2-d}$, and the modulus of each entry of $R_{\mathbf{G},\boldsymbol{n}}^{\mathcal{G},\boldsymbol{p}}$ is bounded by $Cn^{1-d}$.

The items (a) and (b) imply that

$$\|n^{d-2}\hat{K}_{\mathbf{G},\boldsymbol{n}}^{\mathcal{G},\boldsymbol{p}}\|_\infty,\ \|(n^{d-2}\hat{K}_{\mathbf{G},\boldsymbol{n}}^{\mathcal{G},\boldsymbol{p}})^T\|_\infty,\ \|n^{d-2}K_{\mathbf{G},\boldsymbol{n}}^{\mathcal{G},\boldsymbol{p}}\|_\infty,\ \|(n^{d-2}K_{\mathbf{G},\boldsymbol{n}}^{\mathcal{G},\boldsymbol{p}})^T\|_\infty \le C,$$

and

$$\|n^{d-2}R^{\mathcal{G},\boldsymbol{p}}_{\mathbf{G},\boldsymbol{n}}\|_\infty,\ \|(n^{d-2}R^{\mathcal{G},\boldsymbol{p}}_{\mathbf{G},\boldsymbol{n}})^T\|_\infty \le \frac{C}{n}.$$

Then, the stated bounds follow from (2).

To prove (a), we note that $\mathrm{supp}(N_{\boldsymbol{i}+\mathbf{1},\boldsymbol{p},\boldsymbol{n}}) \cap \mathrm{supp}(N_{\boldsymbol{j}+\mathbf{1},\boldsymbol{p},\boldsymbol{n}})$ has zero measure if $\|\boldsymbol{i}-\boldsymbol{j}\|_\infty > \|\boldsymbol{p}\|_\infty$, see (36). Hence, looking at the definitions of $\hat{K}^{\mathcal{G},\boldsymbol{p}}_{\mathbf{G},\boldsymbol{n}}$, $K^{\mathcal{G},\boldsymbol{p}}_{\mathbf{G},\boldsymbol{n}}$, $R^{\mathcal{G},\boldsymbol{p}}_{\mathbf{G},\boldsymbol{n}}$ in (70), (69), (A1), we observe that

$$(\hat{K}^{\mathcal{G},\boldsymbol{p}}_{\mathbf{G},\boldsymbol{n}})_{\boldsymbol{ij}} = (K^{\mathcal{G},\boldsymbol{p}}_{\mathbf{G},\boldsymbol{n}})_{\boldsymbol{ij}} = (R^{\mathcal{G},\boldsymbol{p}}_{\mathbf{G},\boldsymbol{n}})_{\boldsymbol{ij}} = 0, \quad \text{if} \quad \|\boldsymbol{i}-\boldsymbol{j}\|_\infty > \|\boldsymbol{p}\|_\infty, \tag{A2}$$

and so each row and column of $\hat{K}^{\mathcal{G},\boldsymbol{p}}_{\mathbf{G},\boldsymbol{n}}$, $K^{\mathcal{G},\boldsymbol{p}}_{\mathbf{G},\boldsymbol{n}}$, $R^{\mathcal{G},\boldsymbol{p}}_{\mathbf{G},\boldsymbol{n}}$ contains at most $N(2\boldsymbol{p}+\mathbf{1})$ nonzero entries.

To prove (b), we highlight the following properties:

- for all $s,t = 1,\dots,d$, the functions $\kappa_{\mathbf{G},st}$, $\alpha_{\mathbf{G},s}$, $\gamma_{\mathbf{G}}$, $|\det(J_{\mathbf{G}})|$ are in $L^\infty(\mathfrak{Q})$, because the functions $\kappa_{st}$, $\alpha_s$, $\gamma$ are in $L^\infty(\Omega)$, the determinant $\det(J_{\mathbf{G}})$ does not vanish on $[0,1]^d$, and the partial derivatives of $\mathbf{G}$ are bounded on the set $\mathfrak{Q}$ defined in (46);
- the partial derivatives of $W_{\boldsymbol{p}}$ are bounded on $\mathfrak{Q}$;
- $w_{\boldsymbol{i},\boldsymbol{p},\boldsymbol{n}} \le w_{\boldsymbol{p},\max}$ for all $\boldsymbol{i} = \mathbf{1},\dots,\boldsymbol{n}+\boldsymbol{p}$ and $W_{\boldsymbol{p}} \ge w_{\boldsymbol{p},\min}$ on $[0,1]^d$, see (44) and (45);
- by (27), (28), and (35), for $\boldsymbol{i} = \mathbf{1},\dots,\boldsymbol{n}+\boldsymbol{p}$ and $s = 1,\dots,d$ we have

$$0 \le N_{\boldsymbol{i},\boldsymbol{p},\boldsymbol{n}} \le 1, \quad \left|\frac{\partial N_{\boldsymbol{i},\boldsymbol{p},\boldsymbol{n}}}{\partial \hat{x}_s}\right| \le Cn;$$

- $\mu_d(\mathrm{supp}(N_{\boldsymbol{i}+\mathbf{1},\boldsymbol{p},\boldsymbol{n}})) \le Cn^{-d}$ and each integral appearing in (69), (70), (A1) reduces to an integral over $\mathrm{supp}(N_{\boldsymbol{i}+\mathbf{1},\boldsymbol{p},\boldsymbol{n}}) \cap \mathfrak{Q}$.

Thanks to the above properties, we can easily deduce that the modulus of the $(\boldsymbol{i},\boldsymbol{j})$th entry of $\hat{K}^{\mathcal{G},\boldsymbol{p}}_{\mathbf{G},\boldsymbol{n}}$, $K^{\mathcal{G},\boldsymbol{p}}_{\mathbf{G},\boldsymbol{n}}$ is bounded by $Cn^{2-d}$ and the modulus of the $(\boldsymbol{i},\boldsymbol{j})$th entry of $R^{\mathcal{G},\boldsymbol{p}}_{\mathbf{G},\boldsymbol{n}}$ is bounded by $Cn^{1-d}$. For example, for the matrix $\hat{K}^{\mathcal{G},\boldsymbol{p}}_{\mathbf{G},\boldsymbol{n}}$ in (70) we have

$$|(\hat{K}^{\mathcal{G},\boldsymbol{p}}_{\mathbf{G},\boldsymbol{n}})_{\boldsymbol{ij}}| = \left|\sum_{s,t=1}^{d}\int_{[0,1]^d} |\det(J_{\mathbf{G}})|\ \kappa_{\mathbf{G},st}\ \frac{\partial N_{\boldsymbol{j}+\mathbf{1},\boldsymbol{p},\boldsymbol{n}}}{\partial \hat{x}_s}\ \frac{\partial N_{\boldsymbol{i}+\mathbf{1},\boldsymbol{p},\boldsymbol{n}}}{\partial \hat{x}_t}\right| \le Cn^2 \sum_{s,t=1}^{d}\int_{\mathrm{supp}(N_{\boldsymbol{i}+\mathbf{1},\boldsymbol{p},\boldsymbol{n}})\cap\mathfrak{Q}} 1 \le Cn^{2-d}.$$

■

**Lemma 2.** *Let $K^{\mathcal{G},\boldsymbol{p}}_{\mathbf{G},\boldsymbol{n}}$ and $\hat{K}^{\mathcal{G},\boldsymbol{p}}_{\mathbf{G},\boldsymbol{n}}$ be given as in (69) and (70), respectively. Under the assumptions of Theorem 3, we have that $\|n^{d-2}K^{\mathcal{G},\boldsymbol{p}}_{\mathbf{G},\boldsymbol{n}} - n^{d-2}\hat{K}^{\mathcal{G},\boldsymbol{p}}_{\mathbf{G},\boldsymbol{n}}\| \to 0$ as $n \to \infty$.*

*Proof.* We start by showing that the modulus of each entry of $K^{\mathcal{G},\boldsymbol{p}}_{\mathbf{G},\boldsymbol{n}} - \hat{K}^{\mathcal{G},\boldsymbol{p}}_{\mathbf{G},\boldsymbol{n}}$ is bounded by $C\varepsilon_n n^{-d+2}$, where $\varepsilon_n \to 0$ as $n \to \infty$. From (A2) it follows that $(K^{\mathcal{G},\boldsymbol{p}}_{\mathbf{G},\boldsymbol{n}} - \hat{K}^{\mathcal{G},\boldsymbol{p}}_{\mathbf{G},\boldsymbol{n}})_{\boldsymbol{ij}} = 0$ if $\|\boldsymbol{i}-\boldsymbol{j}\|_\infty > \|\boldsymbol{p}\|_\infty$. On the other hand, for $\boldsymbol{i},\boldsymbol{j}$ such that $\|\boldsymbol{i}-\boldsymbol{j}\|_\infty \le \|\boldsymbol{p}\|_\infty$, we have

$$\begin{aligned}|(K^{\mathcal{G},\boldsymbol{p}}_{\mathbf{G},\boldsymbol{n}} - \hat{K}^{\mathcal{G},\boldsymbol{p}}_{\mathbf{G},\boldsymbol{n}})_{\boldsymbol{ij}}| &\le \sum_{s,t=1}^{d}\int_{[0,1]^d} |\det(J_{\mathbf{G}})|\ |\kappa_{\mathbf{G},st}| \left|\frac{w_{\boldsymbol{j}+\mathbf{1},\boldsymbol{p},\boldsymbol{n}}}{W_{\boldsymbol{p}}}\ \frac{w_{\boldsymbol{i}+\mathbf{1},\boldsymbol{p},\boldsymbol{n}}}{W_{\boldsymbol{p}}} - 1\right| \left|\frac{\partial N_{\boldsymbol{j}+\mathbf{1},\boldsymbol{p},\boldsymbol{n}}}{\partial \hat{x}_s}\right| \left|\frac{\partial N_{\boldsymbol{i}+\mathbf{1},\boldsymbol{p},\boldsymbol{n}}}{\partial \hat{x}_t}\right| \\ &\le Cn^2 \sum_{s,t=1}^{d}\int_{\mathrm{supp}(N_{\boldsymbol{i}+\mathbf{1},\boldsymbol{p},\boldsymbol{n}})} \left|\frac{w_{\boldsymbol{j}+\mathbf{1},\boldsymbol{p},\boldsymbol{n}}}{W_{\boldsymbol{p}}}\ \frac{w_{\boldsymbol{i}+\mathbf{1},\boldsymbol{p},\boldsymbol{n}}}{W_{\boldsymbol{p}}} - 1\right| \le Cn^2 \int_{\mathrm{supp}(N_{\boldsymbol{i}+\mathbf{1},\boldsymbol{p},\boldsymbol{n}})} |w_{\boldsymbol{j}+\mathbf{1},\boldsymbol{p},\boldsymbol{n}} w_{\boldsymbol{i}+\mathbf{1},\boldsymbol{p},\boldsymbol{n}} - W^2_{\boldsymbol{p}}|,\end{aligned} \tag{A3}$$

using (69), (70), and the highlighted properties in the proof of Lemma 1. From (36) we know that $\|\hat{\mathbf{x}}-\hat{\mathbf{y}}\|_\infty \le C/n$ for any $\hat{\mathbf{x}},\hat{\mathbf{y}} \in \mathrm{supp}(N_{\boldsymbol{i}+\mathbf{1},\boldsymbol{p},\boldsymbol{n}})$. In combination with (37), we deduce that $\|\boldsymbol{\xi}_{\boldsymbol{i}+\mathbf{1},\boldsymbol{p},\boldsymbol{n}} - \hat{\mathbf{x}}\|_\infty \le C/n$ for every $\hat{\mathbf{x}} \in \mathrm{supp}(N_{\boldsymbol{i}+\mathbf{1},\boldsymbol{p},\boldsymbol{n}})$,

and so

$$|W_{\boldsymbol{p}}(\boldsymbol{\xi}_{\boldsymbol{i}+\mathbf{1},\boldsymbol{p},\boldsymbol{n}})^2 - W_{\boldsymbol{p}}(\hat{\mathbf{x}})^2| \leq \omega_{W_{\boldsymbol{p}}^2}\left(\frac{C}{n}\right),$$

where $\omega_\psi(\cdot)$ is the modulus of continuity of $\psi : [0,1]^d \to \mathbb{R}$,

$$\omega_\psi(\delta) := \sup_{\hat{\mathbf{x}},\hat{\mathbf{y}}\in[0,1]^d,\ \|\hat{\mathbf{x}}-\hat{\mathbf{y}}\|_\infty \leq \delta} |\psi(\hat{\mathbf{x}}) - \psi(\hat{\mathbf{y}})|.$$

In addition, since we are dealing with the case $\|\boldsymbol{i}-\boldsymbol{j}\|_\infty \leq \|\boldsymbol{p}\|_\infty$, by (32) we have

$$\|\boldsymbol{\xi}_{\boldsymbol{i}+\mathbf{1},\boldsymbol{p},\boldsymbol{n}} - \boldsymbol{\xi}_{\boldsymbol{j}+\mathbf{1},\boldsymbol{p},\boldsymbol{n}}\|_\infty \leq \frac{\|\boldsymbol{i}-\boldsymbol{j}\|_\infty}{\min(\boldsymbol{n})} \leq \frac{\|\boldsymbol{p}\|_\infty}{\min(\boldsymbol{n})} \leq \frac{C}{n}. \tag{A4}$$

Therefore, given any $\hat{\mathbf{x}} \in \mathrm{supp}(N_{\boldsymbol{i}+\mathbf{1},\boldsymbol{p},\boldsymbol{n}})$ and $\|\boldsymbol{i}-\boldsymbol{j}\|_\infty \leq \|\boldsymbol{p}\|_\infty$, the integrand of the last integral in (A3) can be bounded using (44) and (45) as follows:

$$\begin{aligned}
|w_{\boldsymbol{j}+\mathbf{1},\boldsymbol{p},\boldsymbol{n}} w_{\boldsymbol{i}+\mathbf{1},\boldsymbol{p},\boldsymbol{n}} - W_{\boldsymbol{p}}(\hat{\mathbf{x}})^2| &\leq |(w_{\boldsymbol{j}+\mathbf{1},\boldsymbol{p},\boldsymbol{n}} - W_{\boldsymbol{p}}(\boldsymbol{\xi}_{\boldsymbol{j}+\mathbf{1},\boldsymbol{p},\boldsymbol{n}}))w_{\boldsymbol{i}+\mathbf{1},\boldsymbol{p},\boldsymbol{n}}| + |W_{\boldsymbol{p}}(\boldsymbol{\xi}_{\boldsymbol{j}+\mathbf{1},\boldsymbol{p},\boldsymbol{n}})(w_{\boldsymbol{i}+\mathbf{1},\boldsymbol{p},\boldsymbol{n}} - W_{\boldsymbol{p}}(\boldsymbol{\xi}_{\boldsymbol{i}+\mathbf{1},\boldsymbol{p},\boldsymbol{n}}))| \\
&\quad + |W_{\boldsymbol{p}}(\boldsymbol{\xi}_{\boldsymbol{i}+\mathbf{1},\boldsymbol{p},\boldsymbol{n}})(W_{\boldsymbol{p}}(\boldsymbol{\xi}_{\boldsymbol{j}+\mathbf{1},\boldsymbol{p},\boldsymbol{n}}) - W_{\boldsymbol{p}}(\boldsymbol{\xi}_{\boldsymbol{i}+\mathbf{1},\boldsymbol{p},\boldsymbol{n}}))| + |W_{\boldsymbol{p}}(\boldsymbol{\xi}_{\boldsymbol{i}+\mathbf{1},\boldsymbol{p},\boldsymbol{n}})^2 - W_{\boldsymbol{p}}(\hat{\mathbf{x}})^2| \\
&\leq 2w_{\boldsymbol{p},\max} \max_{\boldsymbol{\ell}=\mathbf{1},\dots,\boldsymbol{n}+\boldsymbol{p}} |w_{\boldsymbol{\ell},\boldsymbol{p},\boldsymbol{n}} - W_{\boldsymbol{p}}(\boldsymbol{\xi}_{\boldsymbol{\ell},\boldsymbol{p},\boldsymbol{n}})| + w_{\boldsymbol{p},\max}\ \omega_{W_{\boldsymbol{p}}}\left(\frac{C}{n}\right) + \omega_{W_{\boldsymbol{p}}^2}\left(\frac{C}{n}\right) =: \varepsilon_n,
\end{aligned} \tag{A5}$$

where $\varepsilon_n \to 0$ by (43) and the continuity of $W_{\boldsymbol{p}}$. When combining (A3), (A5), and the last highlighted property in the proof of Lemma 1, we get

$$|(K_{\mathbf{G},\boldsymbol{n}}^{\mathcal{G},\boldsymbol{p}} - \hat{K}_{\mathbf{G},\boldsymbol{n}}^{\mathcal{G},\boldsymbol{p}})_{\boldsymbol{ij}}| \leq C\varepsilon_n n^{2-d}.$$

Furthermore, by (A2), it is clear that the number of nonzero entries in each row and column of $K_{\mathbf{G},\boldsymbol{n}}^{\mathcal{G},\boldsymbol{p}} - \hat{K}_{\mathbf{G},\boldsymbol{n}}^{\mathcal{G},\boldsymbol{p}}$ is bounded by a constant independent of $n$. Hence,

$$\|n^{d-2}K_{\mathbf{G},\boldsymbol{n}}^{\mathcal{G},\boldsymbol{p}} - n^{d-2}\hat{K}_{\mathbf{G},\boldsymbol{n}}^{\mathcal{G},\boldsymbol{p}}\|_\infty,\ \|(n^{d-2}K_{\mathbf{G},\boldsymbol{n}}^{\mathcal{G},\boldsymbol{p}} - n^{d-2}\hat{K}_{\mathbf{G},\boldsymbol{n}}^{\mathcal{G},\boldsymbol{p}})^T\|_\infty \leq C\varepsilon_n,$$

and the application of (2) completes the proof. ∎

## APPENDIX B. LEMMAS FOR THE PROOF OF THEOREM 4

This appendix collects the technical results used in the proof of Theorem 4. Again, the symbol $C$ stands for a generic constant independent of $n$. We start by noting that the matrix $R_{\mathbf{G},\boldsymbol{n}}^{C,\boldsymbol{p}}$ in (71) has the following expression:

$$\begin{aligned}
R_{\mathbf{G},\boldsymbol{n}}^{C,\boldsymbol{p}} = \Bigg[ &\sum_{s,t=1}^{d} \kappa_{\mathbf{G},st}(\boldsymbol{\xi}_{\boldsymbol{i}+\mathbf{1},\boldsymbol{p},\boldsymbol{n}})\ \frac{w_{\boldsymbol{j}+\mathbf{1},\boldsymbol{p},\boldsymbol{n}}}{W_{\boldsymbol{p}}(\boldsymbol{\xi}_{\boldsymbol{i}+\mathbf{1},\boldsymbol{p},\boldsymbol{n}})^2}\ \frac{\partial W_{\boldsymbol{p}}}{\partial \hat{x}_t}(\boldsymbol{\xi}_{\boldsymbol{i}+\mathbf{1},\boldsymbol{p},\boldsymbol{n}})\ \frac{\partial N_{\boldsymbol{j}+\mathbf{1},\boldsymbol{p},\boldsymbol{n}}}{\partial \hat{x}_s}(\boldsymbol{\xi}_{\boldsymbol{i}+\mathbf{1},\boldsymbol{p},\boldsymbol{n}}) \\
&+ \sum_{s,t=1}^{d} \kappa_{\mathbf{G},st}(\boldsymbol{\xi}_{\boldsymbol{i}+\mathbf{1},\boldsymbol{p},\boldsymbol{n}})\ \frac{w_{\boldsymbol{j}+\mathbf{1},\boldsymbol{p},\boldsymbol{n}}}{W_{\boldsymbol{p}}(\boldsymbol{\xi}_{\boldsymbol{i}+\mathbf{1},\boldsymbol{p},\boldsymbol{n}})^2}\ \frac{\partial W_{\boldsymbol{p}}}{\partial \hat{x}_s}(\boldsymbol{\xi}_{\boldsymbol{i}+\mathbf{1},\boldsymbol{p},\boldsymbol{n}})\ \frac{\partial N_{\boldsymbol{j}+\mathbf{1},\boldsymbol{p},\boldsymbol{n}}}{\partial \hat{x}_t}(\boldsymbol{\xi}_{\boldsymbol{i}+\mathbf{1},\boldsymbol{p},\boldsymbol{n}}) \\
&+ \sum_{s,t=1}^{d} \kappa_{\mathbf{G},st}(\boldsymbol{\xi}_{\boldsymbol{i}+\mathbf{1},\boldsymbol{p},\boldsymbol{n}})\ \frac{w_{\boldsymbol{j}+\mathbf{1},\boldsymbol{p},\boldsymbol{n}}}{W_{\boldsymbol{p}}(\boldsymbol{\xi}_{\boldsymbol{i}+\mathbf{1},\boldsymbol{p},\boldsymbol{n}})^2}\ \frac{\partial^2 W_{\boldsymbol{p}}}{\partial \hat{x}_s \partial \hat{x}_t}(\boldsymbol{\xi}_{\boldsymbol{i}+\mathbf{1},\boldsymbol{p},\boldsymbol{n}}) N_{\boldsymbol{j}+\mathbf{1},\boldsymbol{p},\boldsymbol{n}}(\boldsymbol{\xi}_{\boldsymbol{i}+\mathbf{1},\boldsymbol{p},\boldsymbol{n}}) \\
&- 2\sum_{s,t=1}^{d} \kappa_{\mathbf{G},st}(\boldsymbol{\xi}_{\boldsymbol{i}+\mathbf{1},\boldsymbol{p},\boldsymbol{n}})\ \frac{w_{\boldsymbol{j}+\mathbf{1},\boldsymbol{p},\boldsymbol{n}}}{W_{\boldsymbol{p}}(\boldsymbol{\xi}_{\boldsymbol{i}+\mathbf{1},\boldsymbol{p},\boldsymbol{n}})^3}\ \frac{\partial W_{\boldsymbol{p}}}{\partial \hat{x}_s}(\boldsymbol{\xi}_{\boldsymbol{i}+\mathbf{1},\boldsymbol{p},\boldsymbol{n}}) \frac{\partial W_{\boldsymbol{p}}}{\partial \hat{x}_t}(\boldsymbol{\xi}_{\boldsymbol{i}+\mathbf{1},\boldsymbol{p},\boldsymbol{n}}) N_{\boldsymbol{j}+\mathbf{1},\boldsymbol{p},\boldsymbol{n}}(\boldsymbol{\xi}_{\boldsymbol{i}+\mathbf{1},\boldsymbol{p},\boldsymbol{n}})
\end{aligned}$$

$$+\sum_{s=1}^{d}\beta_{\mathbf{G},s}(\xi_{\boldsymbol{i+1},\boldsymbol{p},\boldsymbol{n}})\ \frac{w_{\boldsymbol{j+1},\boldsymbol{p},\boldsymbol{n}}}{W_{\boldsymbol{p}}(\xi_{\boldsymbol{i+1},\boldsymbol{p},\boldsymbol{n}})}\ \frac{\partial N_{\boldsymbol{j+1},\boldsymbol{p},\boldsymbol{n}}}{\partial\hat{x}_s}(\xi_{\boldsymbol{i+1},\boldsymbol{p},\boldsymbol{n}})$$
$$-\sum_{s=1}^{d}\beta_{\mathbf{G},s}(\xi_{\boldsymbol{i+1},\boldsymbol{p},\boldsymbol{n}})\ \frac{w_{\boldsymbol{j+1},\boldsymbol{p},\boldsymbol{n}}}{W_{\boldsymbol{p}}(\xi_{\boldsymbol{i+1},\boldsymbol{p},\boldsymbol{n}})^2}\ \frac{\partial W_{\boldsymbol{p}}}{\partial\hat{x}_s}(\xi_{\boldsymbol{i+1},\boldsymbol{p},\boldsymbol{n}})\ N_{\boldsymbol{j+1},\boldsymbol{p},\boldsymbol{n}}(\xi_{\boldsymbol{i+1},\boldsymbol{p},\boldsymbol{n}})$$
$$+\gamma_{\mathbf{G}}(\xi_{\boldsymbol{i+1},\boldsymbol{p},\boldsymbol{n}})\ \frac{w_{\boldsymbol{j+1},\boldsymbol{p},\boldsymbol{n}}}{W_{\boldsymbol{p}}(\xi_{\boldsymbol{i+1},\boldsymbol{p},\boldsymbol{n}})}\ N_{\boldsymbol{j+1},\boldsymbol{p},\boldsymbol{n}}(\xi_{\boldsymbol{i+1},\boldsymbol{p},\boldsymbol{n}})\Bigg]_{\boldsymbol{i,j=1}}^{\boldsymbol{n+p-2}}. \tag{B1}$$

**Lemma 3.** *The matrix $\hat{K}_{\mathbf{G},\boldsymbol{n}}^{\mathcal{C},\boldsymbol{p}}$ defined in (73) can be expressed in the form (74).*

*Proof.* Looking at (73), we see that $\hat{K}_{\mathbf{G},\boldsymbol{n}}^{\mathcal{C},\boldsymbol{p}}$ can be decomposed as

$$\hat{K}_{\mathbf{G},\boldsymbol{n}}^{\mathcal{C},\boldsymbol{p}}=\sum_{s,t=1}^{d}D_{\boldsymbol{n}}^{\boldsymbol{p}}(\kappa_{\mathbf{G},st})\left[-\frac{\partial^2 N_{\boldsymbol{j+1},\boldsymbol{p},\boldsymbol{n}}}{\partial\hat{x}_s\partial\hat{x}_t}(\xi_{\boldsymbol{i+1},\boldsymbol{p},\boldsymbol{n}})\right]_{\boldsymbol{i,j=1}}^{\boldsymbol{n+p-2}}.$$

Thus, to prove (74), it suffices to show that

$$n_s n_t\hat{K}_{\boldsymbol{n},st}^{\mathcal{C},\boldsymbol{p}}=\left[-\frac{\partial^2 N_{\boldsymbol{j+1},\boldsymbol{p},\boldsymbol{n}}}{\partial\hat{x}_s\partial\hat{x}_t}(\xi_{\boldsymbol{i+1},\boldsymbol{p},\boldsymbol{n}})\right]_{\boldsymbol{i,j=1}}^{\boldsymbol{n+p-2}},\quad s,t=1,\ \dots\ ,d. \tag{B2}$$

By property (8), for every $s=1,\dots,d$ and every $\boldsymbol{i},\boldsymbol{j}=\boldsymbol{1},\dots,\boldsymbol{n}+\boldsymbol{p}-\boldsymbol{2}$ we have

$$(n_s^2\hat{K}_{\boldsymbol{n},ss}^{\mathcal{C},\boldsymbol{p}})_{\boldsymbol{ij}}=(n_s^2K_{n_s}^{\mathcal{C},p_s})_{i_sj_s}\prod_{\substack{r=1\\r\neq s}}^{d}(M_{n_r}^{\mathcal{C},p_r})_{i_rj_r}=-\frac{\partial^2 N_{\boldsymbol{j+1},\boldsymbol{p},\boldsymbol{n}}}{\partial\hat{x}_s^2}(\xi_{\boldsymbol{i+1},\boldsymbol{p},\boldsymbol{n}}).$$

This proves (B2) for $s=t$. For the case $s\neq t$, the proof is analogous. ∎

**Lemma 4.** *Let $\tilde{K}_{\mathbf{G},\boldsymbol{n}}^{\mathcal{C},\boldsymbol{p}}$, $K_{\mathbf{G},\boldsymbol{n}}^{\mathcal{C},\boldsymbol{p}}$, and $R_{\mathbf{G},\boldsymbol{n}}^{\mathcal{C},\boldsymbol{p}}$ be given as in (80), (72), and (B1), respectively. Under the assumptions of Theorem 4,*

- *$\|n^{-2}\tilde{K}_{\mathbf{G},\boldsymbol{n}}^{\mathcal{C},\boldsymbol{p}}\|$, $\|n^{-2}K_{\mathbf{G},\boldsymbol{n}}^{\mathcal{C},\boldsymbol{p}}\|$ are uniformly bounded with respect to n;*
- *$\|n^{-2}R_{\mathbf{G},\boldsymbol{n}}^{\mathcal{C},\boldsymbol{p}}\|\leq C/n$.*

*Proof.* It suffices to prove that:

(a) the number of nonzero entries in each row and column of $\tilde{K}_{\mathbf{G},\boldsymbol{n}}^{\mathcal{C},\boldsymbol{p}}$, $K_{\mathbf{G},\boldsymbol{n}}^{\mathcal{C},\boldsymbol{p}}$, $R_{\mathbf{G},\boldsymbol{n}}^{\mathcal{C},\boldsymbol{p}}$ is bounded by $C$;
(b) the modulus of each entry of $\tilde{K}_{\mathbf{G},\boldsymbol{n}}^{\mathcal{C},\boldsymbol{p}}$, $K_{\mathbf{G},\boldsymbol{n}}^{\mathcal{C},\boldsymbol{p}}$ is bounded by $Cn^2$, and the modulus of each entry of $R_{\mathbf{G},\boldsymbol{n}}^{\mathcal{C},\boldsymbol{p}}$ is bounded by $Cn$.

The items (a) and (b) imply that

$$\|n^{-2}\tilde{K}_{\mathbf{G},\boldsymbol{n}}^{\mathcal{C},\boldsymbol{p}}\|_\infty,\ \|(n^{-2}\tilde{K}_{\mathbf{G},\boldsymbol{n}}^{\mathcal{C},\boldsymbol{p}})^T\|_\infty,\ \|n^{-2}K_{\mathbf{G},\boldsymbol{n}}^{\mathcal{C},\boldsymbol{p}}\|_\infty,\ \|(n^{-2}K_{\mathbf{G},\boldsymbol{n}}^{\mathcal{C},\boldsymbol{p}})^T\|_\infty\leq C,$$

and

$$\|n^{-2}R_{\mathbf{G},\boldsymbol{n}}^{\mathcal{C},\boldsymbol{p}}\|_\infty,\ \|(n^{-2}R_{\mathbf{G},\boldsymbol{n}}^{\mathcal{C},\boldsymbol{p}})^T\|_\infty\leq\frac{C}{n}.$$

Then, the stated bounds follow from (2).

To prove (a) for $\tilde{K}_{\mathbf{G},\boldsymbol{n}}^{\mathcal{C},\boldsymbol{p}}$, we observe that, for all $s,t=1,\dots,d$,

$$(\tilde{D}_{\boldsymbol{n+p-2}}(\kappa_{\mathbf{G},st})\circ T_{\boldsymbol{n+p-2}}((H_{\boldsymbol{p}})_{st}))_{\boldsymbol{ij}}=(\tilde{D}_{\boldsymbol{n+p-2}}(\kappa_{\mathbf{G},st}))_{\boldsymbol{ij}}(T_{\boldsymbol{n+p-2}}((H_{\boldsymbol{p}})_{st}))_{\boldsymbol{ij}}=\kappa_{\mathbf{G},st}\left(\frac{\boldsymbol{i}\wedge\boldsymbol{j}}{\boldsymbol{n+p-2}}\right)(T_{\boldsymbol{n+p-2}}((H_{\boldsymbol{p}})_{st}))_{\boldsymbol{ij}}. \tag{B3}$$

Using the relation (11), we have

$$T_{\boldsymbol{n}+\boldsymbol{p}-\boldsymbol{2}}((H_{\boldsymbol{p}})_{st}) = \begin{cases} (\bigotimes_{r=1}^{s-1} T_{n_r+p_r-2}(h_{p_r})) \otimes T_{n_s+p_s-2}(f_{p_s}) \otimes (\bigotimes_{r=s+1}^{d} T_{n_r+p_r-2}(h_{p_r})), & s=t, \\ (\bigotimes_{r=1}^{s-1} T_{n_r+p_r-2}(h_{p_r})) \otimes T_{n_s+p_s-2}(g_{p_s}) \otimes (\bigotimes_{r=s+1}^{t-1} T_{n_r+p_r-2}(h_{p_r})) & \\ \qquad \otimes T_{n_t+p_t-2}(g_{p_t}) \otimes (\bigotimes_{r=t+1}^{d} T_{n_r+p_r-2}(h_{p_r})), & s<t, \\ (\bigotimes_{r=1}^{t-1} T_{n_r+p_r-2}(h_{p_r})) \otimes T_{n_t+p_t-2}(g_{p_t}) \otimes (\bigotimes_{r=t+1}^{s-1} T_{n_r+p_r-2}(h_{p_r})) & \\ \qquad \otimes T_{n_s+p_s-2}(g_{p_s}) \otimes (\bigotimes_{r=s+1}^{d} T_{n_r+p_r-2}(h_{p_r})), & s>t. \end{cases} \tag{B4}$$

Since the Toeplitz matrices associated with $f_p$, $g_p$, $h_p$ are banded with bandwidth $2\lfloor p/2 \rfloor + 1$, the property (8) implies

$$(T_{\boldsymbol{n}+\boldsymbol{p}-\boldsymbol{2}}((H_{\boldsymbol{p}})_{st}))_{\boldsymbol{ij}} = 0, \quad \text{if} \quad \|\boldsymbol{i}-\boldsymbol{j}\|_\infty > \|\boldsymbol{p}/2\|_\infty. \tag{B5}$$

Hence, the entry (B3) is zero if $\|\boldsymbol{i}-\boldsymbol{j}\|_\infty > \|\boldsymbol{p}/2\|_\infty$, and the number of nonzero entries in each row and column of $\tilde{K}_{\mathbf{G},\boldsymbol{n}}^{C,\boldsymbol{p}}$ is at most $N(\boldsymbol{p}+\boldsymbol{1})$.

To prove (a) for $K_{\mathbf{G},\boldsymbol{n}}^{C,\boldsymbol{p}}$ and $R_{\mathbf{G},\boldsymbol{n}}^{C,\boldsymbol{p}}$, we note that $\operatorname{supp}(N_{\boldsymbol{i}+\boldsymbol{1},\boldsymbol{p},\boldsymbol{n}}) \cap \operatorname{supp}(N_{\boldsymbol{j}+\boldsymbol{1},\boldsymbol{p},\boldsymbol{n}}) = \emptyset$ if $\|\boldsymbol{i}-\boldsymbol{j}\|_\infty > \|\boldsymbol{p}+\boldsymbol{1}\|_\infty$, see (36), and we recall that $\boldsymbol{\xi}_{\boldsymbol{i}+\boldsymbol{1},\boldsymbol{p},\boldsymbol{n}} \in \operatorname{supp}(N_{\boldsymbol{i}+\boldsymbol{1},\boldsymbol{p},\boldsymbol{n}})$, see (37). Hence, by (72) and (B1),

$$(K_{\mathbf{G},\boldsymbol{n}}^{C,\boldsymbol{p}})_{\boldsymbol{ij}} = (R_{\mathbf{G},\boldsymbol{n}}^{C,\boldsymbol{p}})_{\boldsymbol{ij}} = 0, \quad \text{if} \quad \|\boldsymbol{i}-\boldsymbol{j}\|_\infty > \|\boldsymbol{p}+\boldsymbol{1}\|_\infty,$$

and so each row and column of $K_{\mathbf{G},\boldsymbol{n}}^{C,\boldsymbol{p}}$ and $R_{\mathbf{G},\boldsymbol{n}}^{C,\boldsymbol{p}}$ contains at most $N(2\boldsymbol{p}+\boldsymbol{3})$ nonzero entries.

To prove (b) for $\tilde{K}_{\mathbf{G},\boldsymbol{n}}^{C,\boldsymbol{p}}$, we note that the modulus of (B3) is bounded by

$$\|\kappa_{\mathbf{G},st}\|_\infty \|T_{\boldsymbol{n}+\boldsymbol{p}-\boldsymbol{2}}((H_{\boldsymbol{p}})_{st})\|,$$

which in turn is bounded by a constant independent of $n$, thanks to (10). Hence, the modulus of the $(\boldsymbol{i},\boldsymbol{j})$th entry of the matrix $\tilde{K}_{\mathbf{G},\boldsymbol{n}}^{C,\boldsymbol{p}}$ in (80) is bounded by $Cn^2$.

To prove (b) for $K_{\mathbf{G},\boldsymbol{n}}^{C,\boldsymbol{p}}$ and $R_{\mathbf{G},\boldsymbol{n}}^{C,\boldsymbol{p}}$, it suffices to take into account the following properties:

- for all $s,t = 1,\dots,d$, the functions $\kappa_{\mathbf{G},st}$, $\beta_{\mathbf{G},s}$, $\gamma_{\mathbf{G}}$ are bounded on the set (47), because the functions $\kappa_{st}$, $\alpha_s$, $\gamma$ are in $C(\overline{\Omega})$, the partial derivatives of $\kappa_{st}$ are bounded on $\Omega$, the determinant $\det(J_{\mathbf{G}})$ does not vanish on $[0,1]^d$, and $\mathbf{G}$ plus its first- and second-order partial derivatives are bounded on the set (47), see Remark 3;
- $W_{\boldsymbol{p}}$ plus its first- and second-order partial derivatives are bounded on the set (47), see Remark 3;
- $w_{\boldsymbol{j},\boldsymbol{p},\boldsymbol{n}} \le w_{\boldsymbol{p},\max}$ and $W_{\boldsymbol{p}} \ge w_{\boldsymbol{p},\min}$ on $[0,1]^d$, see (44) and (45);
- by (27) to (29) and (35), for $\boldsymbol{j} = \boldsymbol{1},\dots,\boldsymbol{n}+\boldsymbol{p}$ and $s,t = 1,\dots,d$ we have

$$0 \le N_{\boldsymbol{j},\boldsymbol{p},\boldsymbol{n}} \le 1, \quad \left|\frac{\partial N_{\boldsymbol{j},\boldsymbol{p},\boldsymbol{n}}}{\partial \hat{x}_s}\right| \le Cn, \quad \left|\frac{\partial^2 N_{\boldsymbol{j},\boldsymbol{p},\boldsymbol{n}}}{\partial \hat{x}_s \partial \hat{x}_t}\right| \le Cn^2.$$

The above properties immediately imply that the modulus of the $(\boldsymbol{i},\boldsymbol{j})$th entry of $K_{\mathbf{G},\boldsymbol{n}}^{C,\boldsymbol{p}}$ in (72) is bounded by $Cn^2$ and the modulus of the $(\boldsymbol{i},\boldsymbol{j})$th entry of $R_{\mathbf{G},\boldsymbol{n}}^{C,\boldsymbol{p}}$ in (B1) is bounded by $Cn$. ∎

**Lemma 5.** *Let $K_{\mathbf{G},\boldsymbol{n}}^{C,\boldsymbol{p}}$ and $\tilde{K}_{\mathbf{G},\boldsymbol{n}}^{C,\boldsymbol{p}}$ be given as in (72) and (80), respectively. Under the assumptions of Theorem 4, we have that $\|n^{-2}K_{\mathbf{G},\boldsymbol{n}}^{C,\boldsymbol{p}} - n^{-2}\tilde{K}_{\mathbf{G},\boldsymbol{n}}^{C,\boldsymbol{p}}\|_1 = o(N(\boldsymbol{n}+\boldsymbol{p}-\boldsymbol{2}))$.*

*Proof.* Let $w_{\boldsymbol{p},\boldsymbol{n}} : [0,1]^d \to \mathbb{R}$ be any function such that $w_{\boldsymbol{p},\boldsymbol{n}}(\boldsymbol{\xi}_{\boldsymbol{i},\boldsymbol{p},\boldsymbol{n}}) = w_{\boldsymbol{i},\boldsymbol{p},\boldsymbol{n}}$ for all $\boldsymbol{i} = \boldsymbol{1},\dots,\boldsymbol{n}+\boldsymbol{p}$. Using this function, the diagonal matrix in (75) has the form

$$D_{\boldsymbol{n}}^{\boldsymbol{p}}(w_{\boldsymbol{p},\boldsymbol{n}}) = \operatorname{diag}_{\boldsymbol{i}=\boldsymbol{1},\dots,\boldsymbol{n}+\boldsymbol{p}-\boldsymbol{2}} w_{\boldsymbol{i}+\boldsymbol{1},\boldsymbol{p},\boldsymbol{n}},$$

and we have

$$K_{\mathbf{G},\boldsymbol{n}}^{C,\boldsymbol{p}} = D_{\boldsymbol{n}}^{\boldsymbol{p}}\left(\frac{1}{W_{\boldsymbol{p}}}\right)\hat{K}_{\mathbf{G},\boldsymbol{n}}^{C,\boldsymbol{p}} D_{\boldsymbol{n}}^{\boldsymbol{p}}(w_{\boldsymbol{p},\boldsymbol{n}}). \tag{B6}$$

We decompose the matrix $n^{-2}K_{\mathbf{G},\boldsymbol{n}}^{C,\boldsymbol{p}} - n^{-2}\tilde{K}_{\mathbf{G},\boldsymbol{n}}^{C,\boldsymbol{p}}$ by using (72), (74), (80), and (B6) as follows:

$$n^{-2}K_{\mathbf{G},\boldsymbol{n}}^{C,\boldsymbol{p}} - n^{-2}\tilde{K}_{\mathbf{G},\boldsymbol{n}}^{C,\boldsymbol{p}} = D_{\boldsymbol{n}}^{\boldsymbol{p}}\left(\frac{1}{W_{\boldsymbol{p}}}\right) n^{-2}\hat{K}_{\mathbf{G},\boldsymbol{n}}^{C,\boldsymbol{p}} D_{\boldsymbol{n}}^{\boldsymbol{p}}(w_{\boldsymbol{p},\boldsymbol{n}}) - n^{-2}\hat{K}_{\mathbf{G},\boldsymbol{n}}^{C,\boldsymbol{p}} + n^{-2}\hat{K}_{\mathbf{G},\boldsymbol{n}}^{C,\boldsymbol{p}} - n^{-2}\tilde{K}_{\mathbf{G},\boldsymbol{n}}^{C,\boldsymbol{p}} = S_1 + S_2 + S_3,$$

where

$$S_1 := D_{\boldsymbol{n}}^{\boldsymbol{p}}\left(\frac{1}{W_{\boldsymbol{p}}}\right) n^{-2}\hat{K}_{\mathbf{G},\boldsymbol{n}}^{C,\boldsymbol{p}} D_{\boldsymbol{n}}^{\boldsymbol{p}}(w_{\boldsymbol{p},\boldsymbol{n}}) - n^{-2}\hat{K}_{\mathbf{G},\boldsymbol{n}}^{C,\boldsymbol{p}}, \tag{B7}$$

$$S_2 := \sum_{s,t=1}^{d} \nu_s\nu_t D_{\boldsymbol{n}}^{\boldsymbol{p}}(\kappa_{\mathbf{G},st})(\hat{K}_{\boldsymbol{n},st}^{C,\boldsymbol{p}} - T_{\boldsymbol{n}+\boldsymbol{p}-\mathbf{2}}((H_{\boldsymbol{p}})_{st})), \tag{B8}$$

$$S_3 := \sum_{s,t=1}^{d} \nu_s\nu_t (D_{\boldsymbol{n}}^{\boldsymbol{p}}(\kappa_{\mathbf{G},st}) T_{\boldsymbol{n}+\boldsymbol{p}-\mathbf{2}}((H_{\boldsymbol{p}})_{st}) - \tilde{D}_{\boldsymbol{n}+\boldsymbol{p}-\mathbf{2}}(\kappa_{\mathbf{G},st}) \circ T_{\boldsymbol{n}+\boldsymbol{p}-\mathbf{2}}((H_{\boldsymbol{p}})_{st})). \tag{B9}$$

We prove that the trace-norms of the terms (B7), (B8), (B9) are $o(N(\boldsymbol{n}+\boldsymbol{p}-\mathbf{2}))$.

We start with (B8). In view of (76) and (B4), from (5) and (61) to (63) we obtain that

$$\operatorname{rank}(\hat{K}_{\boldsymbol{n},st}^{C,\boldsymbol{p}} - T_{\boldsymbol{n}+\boldsymbol{p}-\mathbf{2}}((H_{\boldsymbol{p}})_{st})) \le N(\boldsymbol{n}+\boldsymbol{p}-\mathbf{2}) \sum_{k=1}^{d} \frac{3p_k}{n_k+p_k-2}, \quad s,t = 1, \dots, d.$$

Hence, the trace-norm of the $(s,t)$th term in the summation (B8) can be bounded using (3) as

$$\|\nu_s\nu_t D_{\boldsymbol{n}}^{\boldsymbol{p}}(\kappa_{\mathbf{G},st})(\hat{K}_{\mathbf{G},st}^{C,\boldsymbol{p}} - T_{\boldsymbol{n}+\boldsymbol{p}-\mathbf{2}}((H_{\boldsymbol{p}})_{st}))\|_1 \le C\, N(\boldsymbol{n}+\boldsymbol{p}-\mathbf{2}) \sum_{k=1}^{d} \frac{3p_k}{n_k+p_k-2}, \tag{B10}$$

where $C$ is a constant independent of $n$ that provides an upper bound for the spectral norm of the matrix in the left-hand side of (B10). Note that such a constant exists because of (76), (51), (4), (10), and the fact that $\kappa_{\mathbf{G},st}$ is bounded. It follows that the trace-norm in (B10) is $o(N(\boldsymbol{n}+\boldsymbol{p}-\mathbf{2}))$, and so the trace-norm of the summation (B10) is $o(N(\boldsymbol{n}+\boldsymbol{p}-\mathbf{2}))$ as well.

Regarding the summation in (B9), we show that its spectral norm tends to 0 when $n \to \infty$. This result, together with (3), ensures that the trace-norm of (B9) is $o(N(\boldsymbol{n}+\boldsymbol{p}-\mathbf{2}))$. To this end, we show that:

(a1) the number of nonzero entries in each row and column of the $(s,t)$th term in (B9) is bounded by $C$;
(b1) the modulus of each entry of the $(s,t)$th term in (B9) is bounded by a quantity which tends to 0 as $n \to \infty$.

For $\boldsymbol{i},\boldsymbol{j} = \mathbf{1}, \dots, \boldsymbol{n}+\boldsymbol{p}-\mathbf{2}$, the $(\boldsymbol{i},\boldsymbol{j})$th entry of the $(s,t)$th term in (B9) is given by

$$\nu_s\nu_t \left(\kappa_{\mathbf{G},st}(\boldsymbol{\xi}_{\boldsymbol{i}+\mathbf{1},\boldsymbol{p},\boldsymbol{n}}) - \kappa_{\mathbf{G},st}\left(\frac{\boldsymbol{i}\wedge\boldsymbol{j}}{\boldsymbol{n}+\boldsymbol{p}-\mathbf{2}}\right)\right)(T_{\boldsymbol{n}+\boldsymbol{p}-\mathbf{2}}((H_{\boldsymbol{p}})_{st}))_{\boldsymbol{ij}}. \tag{B11}$$

Due to (B5), the entry (B11) is zero if $\|\boldsymbol{i}-\boldsymbol{j}\|_\infty > \|\boldsymbol{p}/2\|_\infty$, which proves the statement (a1). Furthermore, $\|\boldsymbol{i}-\boldsymbol{j}\|_\infty \le \|\boldsymbol{p}/2\|_\infty$ implies $|i_k - j_k| \le \|\boldsymbol{p}/2\|_\infty$ for all $k = 1, \dots, d$. Hence, by (33),

$$\left|\xi_{i_k+1,p_k,n_k} - \frac{(\boldsymbol{i}\wedge\boldsymbol{j})_k}{n_k+p_k-2}\right| \le \frac{C}{n_k}, \quad k = 1, \dots, d,$$

and so

$$\left\|\boldsymbol{\xi}_{\boldsymbol{i}+\mathbf{1},\boldsymbol{p},\boldsymbol{n}} - \frac{\boldsymbol{i}\wedge\boldsymbol{j}}{\boldsymbol{n}+\boldsymbol{p}-\mathbf{2}}\right\|_\infty \le \frac{C}{n}.$$

Thus,

$$\left|\kappa_{\mathbf{G},st}(\boldsymbol{\xi}_{\boldsymbol{i}+\mathbf{1},\boldsymbol{p},\boldsymbol{n}}) - \kappa_{\mathbf{G},st}\left(\frac{\boldsymbol{i}\wedge\boldsymbol{j}}{\boldsymbol{n}+\boldsymbol{p}-\mathbf{2}}\right)\right| \leq C\ \omega_{\kappa_{\mathbf{G},st}}\left(\frac{1}{n}\right). \tag{B12}$$

The inequalities (B12) and (10) lead to

$$\left|\nu_s\nu_t\left(\kappa_{\mathbf{G},st}(\boldsymbol{\xi}_{\boldsymbol{i}+\mathbf{1},\boldsymbol{p},\boldsymbol{n}}) - \kappa_{\mathbf{G},st}\left(\frac{\boldsymbol{i}\wedge\boldsymbol{j}}{\boldsymbol{n}+\boldsymbol{p}-\mathbf{2}}\right)\right)(T_{\boldsymbol{n}+\boldsymbol{p}-\mathbf{2}}((H_{\boldsymbol{p}})_{st}))_{\boldsymbol{ij}}\right| \leq C\ \omega_{\kappa_{\mathbf{G},st}}\left(\frac{1}{n}\right),$$

which proves the statement (b1).

Finally, we show that also the trace-norm of (B7) is $o(N(\boldsymbol{n}+\boldsymbol{p}-\mathbf{2}))$. As before, it suffices to prove that the spectral norm of (B7) tends to 0 as $n\to\infty$. Following the same line of arguments, we then show that:

(a2) the number of nonzero entries in each row and column of (B7) is bounded by $C$;
(b2) the modulus of each entry of (B7) is bounded by a quantity that tends to 0 as $n\to\infty$.

For $\boldsymbol{i},\boldsymbol{j}=\mathbf{1},\dots,\boldsymbol{n}+\boldsymbol{p}-\mathbf{2}$, the $(\boldsymbol{i},\boldsymbol{j})$th entry of (B7) is

$$\left(D_{\boldsymbol{n}}^{\boldsymbol{p}}\left(\frac{1}{W_{\boldsymbol{p}}}\right)n^{-2}\hat{K}_{\mathbf{G},\boldsymbol{n}}^{C,\boldsymbol{p}}D_{\boldsymbol{n}}^{\boldsymbol{p}}(w_{\boldsymbol{p},\boldsymbol{n}}) - n^{-2}\hat{K}_{\mathbf{G},\boldsymbol{n}}^{C,\boldsymbol{p}}\right)_{\boldsymbol{ij}} = \left(\frac{w_{\boldsymbol{j}+\mathbf{1},\boldsymbol{p},\boldsymbol{n}}}{W_{\boldsymbol{p}}(\boldsymbol{\xi}_{\boldsymbol{i}+\mathbf{1},\boldsymbol{p},\boldsymbol{n}})} - 1\right)(n^{-2}\hat{K}_{\mathbf{G},\boldsymbol{n}}^{C,\boldsymbol{p}})_{\boldsymbol{ij}}. \tag{B13}$$

Using (74) to (76), (50), (8), we see that (B13) is zero if $\|\boldsymbol{i}-\boldsymbol{j}\|_\infty > \|\boldsymbol{p}\|_\infty$; this proves (a2). Using (74) to (76), (4), (51), and the boundedness of the functions $\kappa_{\mathbf{G},st}$, we conclude that the spectral norm (and so the entries) of $n^{-2}\hat{K}_{\mathbf{G},\boldsymbol{n}}^{C,\boldsymbol{p}}$ are bounded by some constant $C$ independent of $n$. Hence, by (45), (A4), the modulus of (B13) can be bounded as follows for $\|\boldsymbol{i}-\boldsymbol{j}\|_\infty \leq \|\boldsymbol{p}\|_\infty$:

$$\left|\frac{w_{\boldsymbol{j}+\mathbf{1},\boldsymbol{p},\boldsymbol{n}}}{W_{\boldsymbol{p}}(\boldsymbol{\xi}_{\boldsymbol{i}+\mathbf{1},\boldsymbol{p},\boldsymbol{n}})} - 1\right||(n^{-2}\hat{K}_{\mathbf{G},\boldsymbol{n}}^{C,\boldsymbol{p}})_{\boldsymbol{ij}}| \leq C|w_{\boldsymbol{j}+\mathbf{1},\boldsymbol{p},\boldsymbol{n}} - W_{\boldsymbol{p}}(\boldsymbol{\xi}_{\boldsymbol{i}+\mathbf{1},\boldsymbol{p},\boldsymbol{n}})| \leq C\left[|w_{\boldsymbol{j}+\mathbf{1},\boldsymbol{p},\boldsymbol{n}} - W_{\boldsymbol{p}}(\boldsymbol{\xi}_{\boldsymbol{j}+\mathbf{1},\boldsymbol{p},\boldsymbol{n}})| + \omega_{W_{\boldsymbol{p}}}\left(\frac{\|\boldsymbol{p}\|_\infty}{\min(\boldsymbol{n})}\right)\right].$$

In view of (43) and the continuity of $W_{\boldsymbol{p}}$, the above inequality proves (b2) and concludes the proof. ■